

University of Kentucky

UKnowledge

Theses and Dissertations--Molecular and
Cellular Biochemistry

Molecular and Cellular Biochemistry


2024

THE EFFECTS OF SECRETION REGULATORS, α -SYNUCLEIN AND CYSTEINE STRING PROTEIN- α , IN THROMBOSIS AND HEMOSTASIS

Alexis N. Smith

University of Kentucky, iamalexis95@gmail.com

Author ORCID Identifier:

 <https://orcid.org/0000-0001-8160-9210>

Digital Object Identifier: <https://doi.org/10.13023/etd.2024.52>

[Right click to open a feedback form in a new tab to let us know how this document benefits you.](#)

Recommended Citation

Smith, Alexis N., "THE EFFECTS OF SECRETION REGULATORS, α -SYNUCLEIN AND CYSTEINE STRING PROTEIN- α , IN THROMBOSIS AND HEMOSTASIS" (2024). *Theses and Dissertations--Molecular and Cellular Biochemistry*. 72.

https://uknowledge.uky.edu/biochem_etds/72

This Doctoral Dissertation is brought to you for free and open access by the Molecular and Cellular Biochemistry at UKnowledge. It has been accepted for inclusion in Theses and Dissertations--Molecular and Cellular Biochemistry by an authorized administrator of UKnowledge. For more information, please contact UKnowledge@lsv.uky.edu.

STUDENT AGREEMENT:

I represent that my thesis or dissertation and abstract are my original work. Proper attribution has been given to all outside sources. I understand that I am solely responsible for obtaining any needed copyright permissions. I have obtained needed written permission statement(s) from the owner(s) of each third-party copyrighted matter to be included in my work, allowing electronic distribution (if such use is not permitted by the fair use doctrine) which will be submitted to UKnowledge as Additional File.

I hereby grant to The University of Kentucky and its agents the irrevocable, non-exclusive, and royalty-free license to archive and make accessible my work in whole or in part in all forms of media, now or hereafter known. I agree that the document mentioned above may be made available immediately for worldwide access unless an embargo applies.

I retain all other ownership rights to the copyright of my work. I also retain the right to use in future works (such as articles or books) all or part of my work. I understand that I am free to register the copyright to my work.

REVIEW, APPROVAL AND ACCEPTANCE

The document mentioned above has been reviewed and accepted by the student's advisor, on behalf of the advisory committee, and by the Director of Graduate Studies (DGS), on behalf of the program; we verify that this is the final, approved version of the student's thesis including all changes required by the advisory committee. The undersigned agree to abide by the statements above.

Alexis N. Smith, Student

Dr. Sidney W. Whiteheart, Major Professor

Dr. Trevor Creamer, Director of Graduate Studies

THE EFFECTS OF SECRETION REGULATORS, α -SYNUCLEIN AND CYSTEINE
STRING PROTEIN- α , IN THROMBOSIS AND HEMOSTASIS

DISSERTATION

A dissertation submitted in partial fulfillment of the
requirements for the degree of Doctor of Philosophy in the
College of Medicine at the University of Kentucky

By

Alexis Nicole Smith
Lexington, Kentucky

Director: Dr. Sidney W. Whiteheart, Professor of Molecular and Cellular Biochemistry
Lexington, Kentucky

2024

Copyright © Alexis Nicole Smith 2024
<https://orcid.org/0000-0001-8160-9210>

ABSTRACT OF DISSERTATION

THE EFFECTS OF THE SECRETION REGULATORS, α -SYNUCLEIN AND CYSTEINE STRING PROTEIN- α , IN THROMBOSIS AND HEMOSTASIS

Platelets play many critical roles in the vasculature ensuring proper hemostasis and maintaining vascular integrity. They can mediate these different processes via the release of different cargo molecules from granules. Cargo release from the granules is mediated by a family of proteins called Soluble NSF Attachment Protein Receptors (SNAREs). This process is complex and is regulated by several protein-protein interactions that are not completely characterized. SNARE chaperones have been identified for the t-SNAREs such as Munc18b/STXBP2 for Syntaxin-11, but none have been identified for the VAMPs and SNAP proteins. Proteins of interest as potential chaperones for VAMPs and SNAP proteins are respectively, α -synuclein and its interacting partner Cysteine String Protein- α (CSP α).

To address the roles of both α -synuclein and CSP α in secretion and hemostasis, we examined the platelet and hemostatic phenotype of α -synuclein^{-/-} mice and CSP α ^{-/-} mice using several *in vitro* assays and *in vivo* models. Measurements of granule secretion show that α -synuclein^{-/-} mice only have a mild activation-dependent dense granule secretion defect with minimal effects on α and lysosomal granule release. Consistent with the mild secretion phenotype α -synuclein^{-/-} mice did not have defective thrombus formation in the tail bleeding, FeCl₃ carotid injury or jugular vein puncture models. CSP α ^{-/-} mice, on the other hand, have defective granule secretion from both α and dense granules with minimum effects on lysosomal granule release. Consistent with the significant secretion defect, CSP α ^{-/-} mice had a significant tail bleeding defect and attenuated thrombus formation under flow. Loss of CSP α reduced GPVI levels and reduced α _{IIb} β ₃ activation especially in response to GPVI-specific agonists. Neither loss of α -synuclein nor CSP α affected proteins in the platelet secretory machinery. Immunofluorescence co-localization studies showed that both α -synuclein and CSP α co-stained with markers for both α and lysosomal granules. Subcellular fractionation studies showed that α -synuclein is mostly cytosolic while CSP α is membrane associated but is not found in lipid rafts.

The data presented in this dissertation identified two new regulatory elements in the platelet secretory machinery, α -synuclein and CSP α . α -Synuclein has a limited role while data for CSP α shows that is essential. Thus, my work gives insight into

how platelet secretion is regulated and will help us better understand what the proper threshold of platelet function is for proper thrombosis and hemostasis.

KEYWORDS: Platelets, SNAREs, α -synuclein, Cysteine String Protein- α (CSP α), Hemostasis and Thrombosis, Granule Exocytosis

Alexis Nicole Smith

(Name of Student)

03/15/2024

Date

THE EFFECTS OF SECRETION REGULATORS, α -SYNUCLEIN AND
CYSTEINE STRING PROTEIN- α , IN THROMBOSIS AND HEMOSTASIS

By
Alexis Nicole Smith

Dr. Sidney W. Whiteheart

Director of Dissertation

Dr. Trevor Creamer

Director of Graduate Studies

03/15/2024

Date

To my favorite angel, dad, Danny L. Smith

ACKNOWLEDGMENTS

First, I would like to acknowledge and express my gratitude to my fantastic mentor Dr. Sidney W. Whiteheart. Wally has truly been supportive of me during my scientific training and has pushed me to be the scientist I am today. His guidance and willingness to always help and listen to me whether it was to help me plan out an experiment or troubleshooting the same experiment for the millionth time has been invaluable. He always remained patient with me and believed in me even when I did not. He has helped me be more confident not only in myself but as a scientist as well. I will also forever be grateful for his support, especially during the COVID pandemic and when my dad passed. He allowed me to have the time and support I needed during the most trying time in my life to get to a better mental space and I will always appreciate that.

Next, I would like to thank each of my committee members: Dr. Jeremy Wood, Dr. Matthew Gentry, and Dr. Brett Spear. Each one of you have been extremely supportive of me and helpful with my projects. I also would like to thank my outside examiner Dr. Kenneth Fields for his time and contributions to my dissertation.

I would like to thank all the past and current members of the Whiteheart lab for their support during this journey. Past members: Dr. Jinchao Zhang, Dr. Meenakshi Banerjee, Dr. Harry Chanzu, and Linda Omali. Current members: Dr. Smita Joshi, Dr. Daniëlle Coenen, Dr. Shayan Mohammadmoradi, Dr. Shravani Prakhya, Dr. Joshua Lykins, Hammodah Alfar, Chi Peng, and Elizabeth Driehaus. They have always been there for me whether it is helping with a presentation or just taking a break to chat in the lab or going out for a random trivia night. I am also grateful for all the fun and wonderful things we did at conferences. I will cherish those memories as well, especially going out of the

country for the first time to London. I have been grateful for all of it and the friendships that we have I will always cherish. I am especially grateful for Smita Joshi; she took me under her wing when I first came to do rotations in the lab and has really been supportive of me ever since whether I needed help with an experiment or just an ear to listen too. She has been so supportive, and I honestly would not be here without her mentorship as well. I would also like to thank Ming Zhang as well she has been so helpful providing the mice I need for experiments and helping me out with my CSP α ^{-/-} strain because they have been pretty difficult to work with, but we made it work and I couldn't have done it without her. Special thanks to our department chair and DGS, Dr. Trevor Creamer, for always being supportive of me. I would like to thank Tonya, Rachel, Brenda, and Jonathan for always helping me out and making sure the department ran smoothly. Finally, I would also like to thank the Saha Cardiovascular Research Center for their support over the years and the wonderful opportunities to present my research.

Last, I want to acknowledge my family and friends. I want to thank my parents, Danny and Natalie Smith, for supporting me, especially moving 7.5 hours from home away. It was tough, but they were always supportive of me and my aspirations, and I know my late dad would be happy to see where I am today. To my siblings, Jayla and Donté Smith, thanks for always supporting me and listening to my rants about school and everything in between. To my grandma, Jewella Washington, thanks for always being there for me. To my best friend, Lynecia Christion, thanks for being supportive of my journey since our Ole Miss days. To my family and friends, thanks so much for always being supportive of me and being my biggest supporters during this journey. To my new friends and family, I made in Kentucky I will forever cherish you all and I am so grateful

for all your support during my journey. I want to give special thanks to Brittany Little; she has always been my little piece of Mississippi while being here in Kentucky, and I will forever be grateful for our friendship. There are so many more people I have not included here, and they all deserve my thanks. Thanks so much and I am forever grateful for every one of you!

I want to also thank all the angels I have gained during my PhD journey. Each one of you had a significant role in my life; my dad Danny Smith, my great-grandmother Aola Washington, my great aunt Rosie Washington, and so many more. I will forever cherish all of you and your memories. And I hope I am making you proud!

TABLE OF CONTENTS

ACKNOWLEDGMENTS	iii
LIST OF TABLES	ix
LIST OF FIGURES	x
LIST OF ABBREVIATIONS.....	xi
CHAPTER 1. INTRODUCTION	1
1.1 <i>Overview Platelet Biology and Structure</i>	1
1.2 <i>Platelet Granule Biogenesis</i>	3
1.2.1 Dense Granule Biogenesis and Defects	3
1.2.2 Alpha Granule Biogenesis and Defects	5
1.3 <i>Signaling</i>	6
1.3.1 GPIb-IX-V Complex.....	8
1.3.2 GPVI	8
1.3.3 $\alpha_2\beta_1$	9
1.3.4 Platelet ADP Receptors (P2Y ₁ , P2Y ₁₂ , and P2X ₁)	9
1.3.5 Thromboxane (TXA ₂).....	10
1.3.6 PAR Receptors.....	10
1.3.7 $\alpha_{IIb}\beta_3$	11
1.4 <i>Mechanisms of Platelet Secretion</i>	11
1.4.1 V-SNARES	13
1.4.2 T-SNARES	14
1.4.3 Post-translational Modifications: Acylation in Platelets.....	15
1.5 <i>SNARE Regulators</i>	17
1.5.1 SNARE Chaperones.....	17
1.5.1.1 Munc18b	17
1.5.1.2 STXBP5/Tomosyn 1	18
1.5.2 Tethering/Docking Factors	18
1.5.2.1 Rab27	18
1.5.2.2 Munc13-4.....	19
1.5.2.3 NSF and SNAPs.....	19
1.6 <i>Mouse Models of Hemostasis and Thrombosis</i>	20
1.6.1 Murine Tail-Bleeding Model	20
1.6.2 Murine FeCl ₃ Carotid Artery Injury Model	21
1.6.3 Murine Jugular Vein Puncture Model.....	22

1.6.4	<i>Ex Vivo</i> Bioflux Microfluidics Model.....	23
1.7	<i>α-Synuclein</i>	24
1.8	<i>Cysteine String Protein-α</i>	27
1.9	<i>Dissertation Overview</i>	32
CHAPTER 2. MATERIALS AND METHODS.....		37
2.1	<i>Materials</i>	37
2.1.1	Reagents.....	37
2.1.2	Antibodies.....	37
2.2	<i>Methods</i>	39
2.2.1	Murine Strains and Genotyping.....	39
2.2.2	Genomic DNA isolation from murine tail tip.....	40
2.2.3	Platelet Preparation from Mouse Blood.....	40
2.2.4	Platelet Preparation from Human Platelet Unit	41
2.2.5	Hematology Analysis.....	42
2.2.6	Granule Secretion Measurements	42
2.2.7	ATP Release Assay.....	44
2.2.8	Lumi-Aggregometry	45
2.2.9	Flow Cytometry	45
2.2.10	Western Blotting and Quantification	46
2.2.11	Hemostasis/Thrombosis Models.....	47
2.2.12	Subcellular Fractionation of Platelets	48
2.2.13	Spreading Assay.....	49
2.2.14	Sucrose-Density Gradient Fractionation (Lipid Rafts).....	50
2.2.15	Immunoprecipitation (IP)-Acyl-Biotinyl-Exchange (ABE)	50
2.2.16	Immunofluorescence Microscopy.....	51
2.2.17	Epifluorescence Microscopy.....	53
2.2.18	Data Processing.....	53
2.2.19	Study Approval	53
CHAPTER 3. ALPHA-SYNUCLEIN IS THE MAJOR PLATELET ISOFORM BUT IS DISEPENSABLE FOR ACTIVATION, SECRETION, AND THROMBOSIS.....		58
3.1	<i>Introduction</i>	58
3.2	<i>Results</i>	60
3.2.1	Hematological profile of α -synuclein ^{-/-} mice.....	60
3.2.2	Co-localization of α -synuclein with α and lysosomal granules	61
3.2.3	α -Synuclein ^{-/-} platelets have a mild secretion defect	62
3.2.4	α -Synuclein ^{-/-} platelets have no aggregation or spreading defect	63
3.2.5	Deletion of α -synuclein does not affect thrombosis in vivo	64
3.2.6	Loss of α -synuclein did not affect the platelet secretory machinery	64

3.3 Discussion.....	65
CHAPTER 4. UNCOVERING THE ROLE OF CYSTEINE STRING PROTEIN-ALPHA IN PLATELET SECRETION	83
4.1 Introduction.....	83
4.2 Results.....	86
4.2.1 CSP α ^{-/-} mouse hematology	86
4.2.2 Loss of CSP α does not affect the platelet secretion machinery levels.....	87
4.2.3 CSP α ^{-/-} platelets have defective dense and α -granule secretion.....	87
4.2.4 Deletion of CSP α results in severely defective thrombosis.....	88
4.2.5 Sub-platelet Distribution of CSP α	89
4.3 Discussion.....	90
CHAPTER 5. DISCUSSION.....	108
5.1 Overview	108
5.2 α -Synuclein's Limited Role in Platelet Secretion	110
5.3 Identification of CSP α 's Essential Role in Platelet Secretion	114
5.4 CSP α and α -Synuclein's Potential Role in Platelet Signaling.....	118
5.5 CSP α 's Potential Role in Hematopoiesis.....	120
5.6 Summary	122
REFERENCES	123
VITA.....	140

LIST OF TABLES

Table 3.1 Hematological parameters for α -Synuclein ^{-/-} mice	68
Table 4.1 Hematological parameters for CSP α ^{-/-} mice	94

LIST OF FIGURES

Figure 1.1 SNARE-mediated granule-plasma membrane fusion	34
Figure 1.2 SNARE chaperone function of Munc18b.....	35
Figure 1.3 Hypothesized roles of α -synuclein and CSP α in granule-plasma membrane fusion.....	36
Figure 2.1 Schematic of tail-bleeding assay	54
Figure 2.2 Schematic of FeCl ₃ carotid artery injury model.....	55
Figure 2.3 Schematic of jugular vein puncture model.....	56
Figure 2.4 Schematic of <i>ex-vivo</i> Bioflux microfluidics model.....	57
Figure 3.1 α -Synuclein is present on both lysosomes and α -granules	70
Figure 3.2 Control slides for immunofluorescence experiments	71
Figure 3.3 α -Synuclein ^{-/-} platelets have near normal platelet receptor levels and activation	72
Figure 3.4 α -Synuclein ^{-/-} platelets have normal receptor levels.....	73
Figure 3.5 α -Synuclein ^{-/-} platelets have a mild serotonin secretion defect.....	75
Figure 3.6 α -Synuclein ^{-/-} platelets have normal granule cargo levels.....	76
Figure 3.7 α -Synuclein ^{-/-} platelets have normal aggregation and ATP secretion	78
Figure 3.8 α -Synuclein ^{-/-} platelets do not have a spreading defect	79
Figure 3.9 α -Synuclein ^{-/-} mice have normal hemostasis and thrombosis	81
Figure 3.10 Platelet secretory machinery protein levels in α -synuclein ^{-/-} platelets are normal	82
Figure 4.1 Platelet secretory machinery protein levels in CSP α ^{-/-} platelets are normal ...	95
Figure 4.2 SNARE machinery protein levels in CSP α ^{-/-} brain are defective	96
Figure 4.3 CSP α ^{-/-} platelets have defective α -granule secretion and a negative effect on integrin activation	97
Figure 4.4 CSP α ^{-/-} platelets do not have a spreading defect	98
Figure 4.5 CSP α ^{-/-} platelets have defective GPVI levels, but no defect in PECAM levels	99
Figure 4.6 CSP α ^{-/-} platelets have defective dense granule secretion	100
Figure 4.7 CSP α ^{-/-} mice have a severe bleeding defect	101
Figure 4.8 CSP α ^{-/-} mice have defective thrombosis under flow at low-shear rates.....	103
Figure 4.9 CSP α is membrane associated and is present on both lysosomes and α -granules	105
Figure 4.10 Control slides for immunofluorescence experiments	106
Figure 4.11 CSP α is not found in lipid rafts	107

LIST OF ABBREVIATIONS

Abbreviation	Definition
ACD	Acid Citrate Dextrose
ADP	Adenosine Diphosphate
AMP	Adenosine Monophosphate
ANCL	Adult-Onset Neuronal Ceroid Lipofuscinosis
AP-3	Adaptor Protein-3
APT	Acyl Protein Thioesterase
ARC	Arthrogryposis, Renal Dysfunction, Cholestasis
ATP	Adenosine Triphosphate
ATPase	Adenosine Triphosphatase
BLOC	Biogenesis of Lysosome-Related Organelles Complex
BSA	Bovine Serum Albumin
cAMP	Cyclic Adenosine Monophosphate
cGMP	Cyclic Guanine Monophosphate
CHS	Chediak-Higashi Syndrome
CO ₂	Carbon Dioxide
COX	Cyclooxygenase
CSP	Cysteine String Protein
CSP α	Cysteine String Protein- α
CSP β	Cysteine String Protein- β
CSP γ	Cysteine String Protein- γ
DLB	Dementia with Lewy Bodies
DNA	Deoxyribonucleic Acid
DVT	Deep Vein Thrombosis
EDTA	Ethylenediaminetetraacetic Acid
EGF	Epidermal Growth Factor
EGTA	Ethylene Glycol Tetraacetic Acid
ELISA	Enzyme Linked Immunosorbent Assay
FACS	Fluorescence Activated Cell Sorting
FeCl ₃	Iron (III) Chloride
FHL	Familial Hemophagocytic Lymphohistiocytosis
FITC	Fluorescein
FSC	Forward Scatter
GPI	Glycosyl Phosphatidylinositol
GPS	Gray Platelet Syndrome
GPVI	Glycoprotein VI
GS	Griscelli syndrome

GWAS	Genome Wide Associated Studies
HET	Heterozygous
HPS	Hermansky-Pudlak Syndrome
HUVEC	Human Umbilical Endothelial Cell
ITAM	Immunoreceptor Tyrosine Based Activated Motif
KO	Knockout
LAMP	Lysosome Associated Membrane Protein
LRO	Lysosomal-Related Organelle
LRRK2	Leucine Rich Repeat Kinase 2
LYST	Lysosomal Trafficking Regulator
MCH	Mean Corpuscular Hemoglobin
MCHC	Mean Corpuscular Hemoglobin Concentration
MCV	Mean Cell Volume
MPV	Mean Platelet Volume
MRP4	Multidrug Resistance Associated Protein 4
MSA	Multiple System Atrophy
MVB	Multivesicular Body
NAC	Non-Amyloid Component
NBEAL2	Neurobeachin-Like-2
NEM	N-Ethylmaleimide
NGS	Normal Goat Serum
NK	Natural Killer Cell
NO	Nitric Oxide
PAT	Palmitoyl Acyl Transferase
PBS	Phosphate Buffered Saline
PCR	Polymerase Chain Reaction
PD	Parkinson Disease
PDGF	Platelet-Derived Growth Factor
PDVF	Polyvinylidene Difluoride
PE	Phycoerythrin
PECAM-1	Platelet Endothelial Cell Adhesion Molecule-1
PFA	Paraformaldehyde
PF4	Platelet Factor 4
PGI2	Prostacyclin I2
PINK1	Parkin PTEN-induced Putative Kinase 1
PIP2	Phosphatidylinositol 4,5-Bisphosphate
PKA	Protein Kinase A
PKG	Protein Kinase G
PLC	Phospholipase C

PNP-GlcNAC	p-Nitrophenyl N-acetyl- β -Glucosamine
PPT1	Palmitoyl Acyl Transferase
PRP	Platelet Rich Plasma
RabGGTase	Rab GeranylGeranyl Transferase
RANTES	Regulated Upon Activation, Normal T Cell Expressed, and Secreted
RBC	Red Blood Cell
RT	Room Temperature
SDS-PAGE	Sodium Dodecyl-Sulfate Polyacrylamide Gel Electrophoresis
SM	Sec/Munc18
SNAP	Soluble NSF Attachment Protein
SNAP-23	Synaptosomal-Associated Protein 23
SNAP-25	Synaptosomal-Associated Protein 25
SNARE	Soluble NSF Attachment Protein Receptor
SSC	Side Scatter
STXBP5	Syntaxin Binding Protein 5
TCA	Trichloroacetic Acid
TGN	Trans-Golgi Network
TXA _x	Thromboxane Receptor
VAMP	Vesicle Associated Membrane Protein
VPS	Vacuolar Protein Sorting
VMAT2	Vesicular Monoamine Transporter 2
VNUT	Vesicular Nucleotide Transporter
VWF	von-Willebrand Factor
WBC	White Blood Cell
WT	Wild-Type
3D-SIM	3-Dimensional Structured Illumination Microscopy

CHAPTER 1. INTRODUCTION

1.1 Overview Platelet Biology and Structure

Platelets are small, anucleate cell fragments that primarily maintain vascular hemostasis, but they have additional roles in wound healing, inflammation, immune cell recruitment, angiogenesis, and metastasis [1-4]. Platelets are small typically around 1-3 μm in diameter. In humans, the typical lifespan of a platelet is roughly 8-10 days while in mice it is 4-5 days [5-8]. Platelets are produced by their precursor cells, megakaryocytes, in the bone marrow and lungs. Megakaryocytes produce and assemble platelets by undergoing endomitosis. Through this process, megakaryocytes increase their ploidy and cytoplasmic volume allowing them to synthesize the proteins, organelles, and granules platelets need for proper function [9]. Once mature, megakaryocytes migrate from the osteoblastic niche to the vascular niche where they extend 10-20 proplatelet extensions into the blood vessels where they can release the platelets into the bloodstream [8, 10-12]. The process of megakaryocyte maturation and platelet production takes around 5 days in humans and 2-3 days in mice, and each megakaryocyte can produce 1,000-3,000 platelets [13].

Platelets lifespan and function are tightly regulated. Platelets are typically discoid in shape in their resting state but upon activation by an agonist via their receptors their intracellular Ca^{2+} levels increase causing their cytoskeletal to rearrange causing platelets to spread and protrude filopodia and lamellipodia to increase platelet surface area. This causes their granules to condense and either fuse together or fuse directly to the plasma membrane to release their cargo to stimulate thrombus formation and platelet recruitment [14, 15]. Platelets have three main granules alpha, dense, and lysosomal granules whose

contents are used to modulate the vascular microenvironment. Alpha granules are the most abundant and largest granules in platelets. There are approximately 50-80 granules per platelet, and they range in size from 200-500 nm. Alpha granule biogenesis is not well-understood in megakaryocytes, but they originate from the Trans-Golgi network (TGN) and mature in multivesicular bodies (MVBs) [16-22]. They contain over >300 proteins that are either synthesized *de novo* or plasma proteins that are endocytosed into megakaryocytes which are then sorted and packaged by MVBs into respective alpha granules [16, 17, 19, 22]. Alpha granules contain numerous proteins with different functions that contribute to primary and secondary hemostasis, including membrane proteins (P-selectin and $\alpha_{IIb}\beta_3$), chemokines (PF₄ and RANTES), adhesion proteins (fibronectin and von Willebrand factor (vWF)), growth factors (epidermal growth factor (EGF) and platelet-derived growth factor (PDGF)), and coagulation factors (Factor V and fibrinogen) [16, 17, 19, 23]. Some of these proteins are synthesized in megakaryocytes such as P-selectin, PF₄, and vWF while other proteins are endocytosed like fibrinogen, $\alpha_{IIb}\beta_3$, and Factor V [16, 19, 23]. To examine secretion from alpha granules, P-selectin membrane expression can be examined by flow cytometry and the release of different cargo molecules like PF₄ and vWF can be measured. Dense granules are the second most abundant granules in platelets with 3-8 granules per platelet and around 150 nm in size. Dense granule biogenesis is also not well-understood, but they are believed to be derived from the endosomal system instead of the TGN and mature in MVBs as well [16, 21, 24]. They are highly acidic and contain small molecules, including ADP, ATP, Ca²⁺, serotonin, and polyphosphates that contribute to primary hemostasis and platelet recruitment. Dense granules acidic pH, which is approximately 5.4, is maintained by an H⁺ ATPase proton pump [18, 25, 26]. Most of the bioactive amines

and adenine nucleotides in dense granules are transported inside by pumps. The vesicular nucleotide transporter (VNUT) is believed to be responsible for ADP and ATP uptake [27]. Uptake of serotonin from the platelet cytosol into dense granules is mediated by vesicular monoamine transporter 2 (VMAT2) [18, 28]. Multidrug resistance-associated protein 4 (MRP4) helps uptake cAMP into the dense granules [29-31]. Dense granule secretion can be evaluated by examining ADP/ATP release using luciferase-based luminescence techniques, exogenous release of [³H] serotonin, or by measuring membrane expression of CD63 and LAMP-2. Lysosomal granules are the least abundant in platelets with around 1-3 lysosomes per platelet. Their function overall in platelets is not well-understood, but they are believed to play a role in clot remodeling [16, 19, 32]. They contain acidic hydrolases like β -hexosaminidase and β -galactosidase and membrane proteins LAMP-1, LAMP-2, and CD63. Lysosomal granule secretion can be assessed by β -hexosaminidase release. Outside of the various functions of these granules, platelets do contain other organelles like the mitochondria, Golgi apparatus, dense tubular system, and peroxisomes that also contribute to overall platelet function as well.

1.2 Platelet Granule Biogenesis

1.2.1 Dense Granule Biogenesis and Defects

Dense granules belong to a family of organelles classified as lysosome-related organelles (LROs). Numerous LROs are in this family, including as melanosomes in melanocytes, cytolytic granules in T cells, Weibel-Palade bodies in endothelial cells, and basophilic granules in mast cells. They are classified as LROs because they are derived

from the endosomal system, have some lysosomal proteins, and they are acidic in nature once during their life cycle [24, 33-35]. Dysfunction in the LROs, in particular dense granules, has been associated with numerous biogenetic disorders such as Hermansky-Pudlak syndrome (HPS) and Chediak-Higashi syndrome (CHS) [24, 34, 36].

The biogenesis of dense granules is not well-understood except that they are derived from the endosomal system and mature in MVBs [16, 21, 24]. It was not until the characterization of some of the dense granule biogenetic disorders like HPS and CHS that we started to gain insights into how dense granules are formed in megakaryocytes. HPS is a group of disorders associated with oculocutaneous albinism, visual impairment, and excessive bleeding [24, 34, 36]. The excessive bleeding is because HPS patients have no or diminished numbers of dense granules. Studies have found mutations in ten genes in humans with HPS, and the disease has also been found in mice furthering the understanding of HPS and LRO biogenesis with over 15 different mouse models [34]. The genes involved in HPS all encode different protein complexes: adaptor protein-3 (AP-3) and the Biogenesis of Lysosome-related Organelles Complex (BLOC)-1, -2, and -3. Studies from mice have found additional mutations in two subunits of BLOC-1, VPS33A, Rab geranylgeranyl transferase (RabGGTase), and plasma membrane cysteine/glutamate transporter SLC7A11 [21, 24, 34]. These genes, when mutated, disrupt their respective protein complexes resulting in the mistrafficking of membrane proteins and cargo, causing dense granules to not be formed correctly or at all.

Chediak-Higashi syndrome (CHS) is like HPS in that patients suffer from oculocutaneous albinism and bleeding, but CHS patients also suffer from neurological impairments and dysregulation of their immune system. CHS is linked to one gene,

LYST/CHS1, and mutations lead to enlargement of LROs, inhibiting their ability to secrete [37-40]. The exact function of the LYST protein is unclear, but studies suggest it plays a role in trafficking and LROs maturation [37, 40].

Outside of the dense granule biogenetic disorders that disrupt dense granule formation, there are a series of diseases that impair secretion from the dense granules. The most well-known diseases are Familial Hemophagocytic Lymphohistiocytosis Types 3-5 (FHL Types 3-5). These life-threatening diseases characterized by defects in cytotoxic T-cells and natural killer (NK) cells. These patients also suffer from severe bleeding and bruising [34, 41-43]. They are all associated with mutations that disrupt platelet granule secretion: FHL Type 3 is associated with the Munc13-4/Unc13D gene, FHL Type 4 is associated with the Syntaxin-11 gene, and FHL Type 5 is associated with the Munc18b gene [44-47]. Studies from our lab and others have shown that patients and mice with these disrupted genes have a severe reduction in dense granule secretion as well as reduced secretion from the other granules [44-48]. The reduction in dense granule secretion severely impacts hemostatic function which leads to the severe bleeding phenotypes seen in both the patients and the mice. These diseases show that not all gene mutations affect dense granule biogenesis some can affect the overall function.

1.2.2 Alpha Granule Biogenesis and Defects

The biogenesis of alpha granule is not well-understood, but we know that they are derived from the TGN and mature in MVBs [16-22]. It was not until the characterization of the α -granule storage pool disorders arthrogyrosis, renal dysfunction, and cholestasis syndrome (ARC syndrome) and gray platelet syndrome (GPS) that we had insights into the

α -granule development [16, 20, 21, 34, 49-52]. ARC syndrome patients suffer from arthrogyrosis, kidney tubule acidosis, cholestasis, and severe bleeding. They also suffer from reduced lifespan, often dying before one year of age. This syndrome was found to be caused by mutations in either VPS33B or its partner VPS16B [21, 34, 35, 51]. These mutations result in decreased trafficking which affects α -granule maturation causing little to no α -granules to be present in these patients. These mutations also disrupt the incorporation of both synthesized and endocytosed cargo into the α -granules that are present [53]. Patients with GPS suffer from macrothrombocytopenia, splenomegaly, myelofibrosis, and mild to moderate bleeding. This syndrome is associated with mutations in the gene NBEAL2. Its exact role is not completely understood, but patients with this syndrome suffer from empty α -granules suggesting that it is involved in the trafficking of cargo into α -granules [49, 51, 52, 54-56]. None of these syndromes affected the development of dense granules which suggests that α -granules and dense granules mature via different pathways.

1.3 Signaling

Platelets play a crucial role in maintaining vascular hemostasis. They do this by the multitude of receptors on their surface which can, upon vascular injury, adhere to the injury and initiate thrombus formation and recruit other platelets to the site as well. Outside of their role in hemostasis, platelets have receptors that have additional roles in inflammation, angiogenesis, and metastasis [1-4]. During the process of thrombus formation, a multitude of receptors on the platelet membrane that includes the integrins ($\alpha_{IIb}\beta_3$, $\alpha_2\beta_1$, $\alpha_5\beta_1$, $\alpha_6\beta_1$, $\alpha_v\beta_3$), the leucine-rich repeat receptors (GPIb-IV-V complex, Toll-like receptors), G-

protein coupled receptors (PAR-1, PAR-3, and PAR-4 thrombin receptors, P2Y₁ and P2Y₁₂ ADP receptors, thromboxane (TXA_x) receptors), the immunoglobulin superfamily proteins (GPVI, FCγRIIA), C-type lectin receptors (P-selectin), tyrosine kinase receptors (thrombopoietin receptors, Gas-6, ephrins, Eph kinases), and many more receptors [57]. These receptors interact and crosstalk to play various roles to ensure proper thrombus formation.

To ensure that neither spontaneous nor uncontrolled thrombus formation occurs in the vasculature, platelets are regulated by several extrinsic and intrinsic inhibitory regulators. The most important of these being nitric oxide (NO) and prostacyclin (PGI₂), both of which are produced by endothelial cells to limit platelet activation when no damage is present [57-59]. NO prevents platelet activation by diffusing into platelets and binding to the enzyme guanylyl cyclase, leading to the increase production of cGMP via PKG activation, prevents intracellular Ca²⁺ levels from increasing. PGI₂ mediates its effects by binding to the PGI₂ receptor on platelets which increases cAMP level leading to PKA activation; this also prevents an increase in intracellular Ca²⁺ levels [29, 58, 60]. Outside of these two main regulators it has been shown that CD39 and PECAM-1 also inhibit platelet activation [57]. CD39 is a receptor on endothelial cells and reduces the levels of ATP and ADP by hydrolyzing them into AMP which limits platelet activation [61, 62]. PECAM-1 is a receptor on platelets that undergoes phosphorylation when platelets are activated by thrombin and other agonists leading to a decrease in platelet aggregation [63]. These receptors and molecules work in combination to prevent occlusive thrombi from forming.

Thrombus formation by platelets can be initiated by a variety of agonists, including thrombin, convulxin, collagen, fibrinogen, collagen-related peptide (CRP), ADP/ATP, and U46619. They can be classified as strong agonists like thrombin and convulxin or weak agonists such as ADP/ATP and collagen depending on the duration and quantity used to generate a response in platelets [64]. Thrombus formation *in vivo* is typically initiated when an injury occurs in three steps: 1. “Initiation” is the phase when platelets adhere to the exposed subendothelial matrix proteins vWF and collagen and become activated. 2. “Extension” is the phase when additional platelets are recruited and activated by the production of secondary agonists like thromboxane (TXA₂), ADP, and thrombin. 3. “Stabilization” is the phase where the thrombus is consolidated to prevent it from disaggregating [57]. In this thesis, I will highlight the main receptors and their ligands involved in thrombus formation.

1.3.1 GPIb-IX-V Complex

This receptor is the second most common in platelets with 25,000-50,000 copies per platelet. It is important for initial platelet adhesion at the site of injury because it mediates interactions with immobilized vWF at high-shear rates allowing platelets to slow and form bonds with collagen through the collagen receptors for more stable adhesion [57, 65-67]. GPIb-IX-V is can also bind and interact with other ligands such as thrombin, collagen, and P-selectin.

1.3.2 GPVI

This receptor is best known for its interaction with collagen and allowing stable platelet adhesion to the site of injury [57, 68]. It is a part of the immunoglobulin superfamily

proteins, and it forms a complex with FcR γ which bears an immunoreceptor tyrosine-based activation motif (ITAM) which acts as the signal transducing subunit of the receptor. Upon activation, GPVI dimerizes which leads to the phosphorylation of FcR γ by the Src kinases. This phosphorylation activates the Syk kinases which leads to the activation and phosphorylation of PLC γ 2. Activation of PLC γ 2 hydrolyzes phosphatidylinositol 4,5-biphosphate (PIP₂) and raises intracellular Ca²⁺ levels to activate platelets [59, 65, 69]. This promotes production of the secondary agonists such as TXA₂ and ADP and promotes integrin activation. GPVI is also able to interact with other agonists, including CRP and convulxin and numerous studies have examined platelet function using them [64, 70, 71].

1.3.3 $\alpha_2\beta_1$

This integrin receptor plays a role in platelet adhesion by interacting with collagen. It is believed that GPVI binding with collagen first initiates the inside-out signaling needed for $\alpha_2\beta_1$ to change its conformation and increase its affinity to interact with collagen further stabilizing platelet adhesion [57, 72, 73]. This receptor works in synergy with GPVI to ensure proper platelet adhesion and activation.

1.3.4 Platelet ADP Receptors (P2Y₁, P2Y₁₂, and P2X₁)

These are classified as G-protein coupled receptors. The receptors P2Y₁ and P2Y₁₂ are responsible for amplifying platelet activation and aggregation by interacting with the ADP that is released from both platelets and RBCs [74-76]. P2X₁ is an ATP-driven calcium channel that can, under high-shear, amplify the platelets response to collagen and contribute to platelet aggregation [77, 78]. These receptors play an important role in contributing to platelet activation and aggregation at the site of injury.

1.3.5 Thromboxane (TXA₂)

This G-protein coupled receptor also contributes to further amplifying platelet activation and aggregation. During platelet activation TXA₂ is synthesized by the enzymes cyclooxygenase (COX) and TXA₂ synthase. Once synthesized it can act in either an autocrine or paracrine fashion to recruit and further activate platelets [57, 79, 80]. An analog of TXA₂, U46619, can be used to activate the receptor and has been used in numerous studies to investigate how the TXA₂ receptor contributes to platelet function [81].

1.3.6 PAR Receptors

These G-protein coupled receptors are commonly known as the thrombin receptors. PAR-1 and PAR-4 are in humans and PAR-3 and PAR-4 are in mice. Thrombin is the most potent agonist and is produced during vascular injury on the surface of activated platelets. Thrombin is generated by the prothrombinase complex (FXa in complex with FVa) which activates FII to stimulate thrombin generation [57, 82-84]. Thrombin, by itself, is strong enough agonist to stimulate platelet activation. Thrombin can activate the PAR receptors by cleaving the N-terminal sequence which exposes a new N-terminus that can act as a peptide to activate the receptor [85]. In humans, PAR-1 mediates activation at low thrombin concentrations while at high thrombin concentrations PAR-4 is used [86, 87]. In mice, studies showed that PAR-4 is the main thrombin receptor needed for thrombin activation [87-89]. G-protein coupled receptor signaling is different from ITAM signaling. In G-protein coupled receptor signaling, PLC β is used to increase intracellular Ca²⁺ levels

to activate platelets [59, 65]. These receptors serve to amplify platelet activation and aggregation.

1.3.7 $\alpha_{IIb}\beta_3$

This integrin is platelet specific and is the most abundant receptor on platelets with 50,000-80,000 copies per platelet. It plays an essential role in thrombus stabilization. It is activated by the binding of all the different agonists to the different receptors on platelets such as collagen binding to GPVI and vWF binding to GPIb-IX-V complex which mediates inside-out signaling. Inside-out signaling causes $\alpha_{IIb}\beta_3$ to change its conformation from its low-affinity state to its high-affinity state where it can bind to fibrinogen, vWF, and other adhesion proteins. The binding of these different ligands in particular fibrinogen activates outside-in signaling which signals to the platelets to stabilize and bridge the platelets together in the thrombus to prevent disaggregation [57, 65, 90-93].

1.4 Mechanisms of Platelet Secretion

Platelets modulate the vascular microenvironment via the release of their granule contents in a process called granule-plasma membrane fusion or exocytosis. The numerous cargo molecules secreted from the granules have been shown to not only function in thrombosis and hemostasis, but also in numerous other processes such as e.g., inflammation, antimicrobial responses, and metastasis [1-4]. Platelets release these molecules upon activation by an agonist which causes an increase in intracellular Ca^{2+} levels leading to the fusion of the granules to the plasma membrane to release their cargo. Various cargo molecules from the different granules have different roles. Dense granules contain molecules such as ADP, ATP, and serotonin that recruit platelets and further

amplify platelet activation. Alpha granules contain the most diverse cargo with molecules like vWF and fibrinogen that contribute to clot stabilization. Lysosomal granules contain acidic hydrolases including β -hexosaminidase and β -galactosidase that are believed to contribute to clot remodeling. Studies have shown that the release kinetics from these granules have no thematic pattern and agonist strength has the most influence [64]. Dense granule secretion is the fastest and the most essential for primary hemostasis because defects in its secretion are linked to bleeding diatheses such as FHL Type (3-5). Alpha granule secretion is next with the most kinetically diverse release; defects in its release are also linked to bleeding diatheses but not to the same degree as defective dense granule secretion. Lysosomal granules have the slowest release and require the most stimulation. Their roles in platelet function are not well-understood, but their function has been shown to be reduced in some bleeding diatheses. Secretion from the granules is regulated by a group of proteins called Soluble N-ethylmaleimide sensitive factor Attachment protein Receptor (SNARE) proteins that mediate granule-plasma membrane fusion. These proteins and processes are highly conserved in eukaryotes and have been studied in numerous other secretory cells, including neurons, chromaffin cells, and neutrophils [18, 94-98]. SNAREs are classified based on their subcellular localization and a charged amino acid in their central region. (v/R, Arg) SNAREs are on the granules and (t/Q, Gln) SNAREs are on the plasma membrane (Figure 1.1) [95, 99]. All SNARE proteins contain 1-2 amphipathic, heptad-repeat cytosolic domains called the SNARE motif, which consists of ~60-70 amino acids. The v-SNAREs and t-SNAREs interact through these SNARE domains to form a transmembrane complex that mediates granule-plasma membrane fusion. This transmembrane complex consists of four SNARE domains: one domain from

the (v/R) SNARE proteins, one domain from the Syntaxin (Q_a) SNARE proteins, and two domains from the SNAP (Q_{bc}) SNARE proteins that come together into four-helical bundle to mediate membrane fusion [95, 98]. Previous studies from our lab and others have established the main proteins that are involved in platelet SNARE-complex assembly as shown in (Figure 1.1), but current studies are now trying to understand how the process is regulated to better understand how platelets contribute to thrombosis and hemostasis.

1.4.1 V-SNARES

The presence and characterization of the different roles of SNARE proteins in platelets have been shown in numerous studies from our lab and others [100-103]. Platelets contain multiple v-SNARE proteins: VAMP-2, -3, -4, -5, -7, -8 and Ykt6. VAMP-7 and -8 are established as the most abundant in humans while VAMP-2, -7, -8 are the most abundant in mice. VAMP-2 is the only isoform that is present in mice and not in humans, and its deletion in mice is embryonic lethal [104]. Global VAMP3^{-/-} mouse studies show that VAMP-3 has a role in endocytosis/trafficking but the platelets have no defect in secretion and thrombosis [105, 106]. VAMP-4 and -5 levels are significantly lower compared to the rest of the VAMP proteins and have not yet been studied [102]. Global VAMP-7^{-/-} mice only have a mild secretion effect and no significant defect in thrombosis [107-109]. Global VAMP-8^{-/-} mouse studies show that secretion is affected from all three granules and that thrombus formation is reduced. These studies show the importance of VAMP-8 in platelet secretion and have established it as the dominant v-SNARE in platelet function [110, 111]. Signifying its importance, VAMP-8 has been linked to increased cardiovascular risks in several Genome Wide Association Studies (GWAS) [112-114].

Current studies are being done in our lab to investigate Ykt6's role in platelet secretion and thrombosis. Deletion of the VAMP proteins has also been performed in combination with other VAMP proteins to better understand how they contribute individually or in combination to platelet secretion and thrombosis. Global VAMP3^{-/-}8^{-/-} mice are embryonic lethal (Whiteheart, unpublished). The deletion of VAMP-2 in mice must be platelet-specific since its deletion is embryonic lethal. VAMP2^{Δ3Δ} platelet-specific knockout mice have no defect in platelet secretion [115]. Global VAMP3^{-/-}7^{-/-} mice and platelet-specific and global VAMP2^{Δ3Δ}7^{-/-} mice have defective alpha and lysosomal granule secretion, but no defect in dense granule secretion and thrombosis [109]. Platelet-specific and global VAMP2^{Δ3Δ}8^{-/-} mice have significant defects in secretion from all three granules and defective thrombus formation [115]. Unpublished studies (Joshi *et. al*, in preparation) in global VAMP7^{-/-}8^{-/-} mice and platelet-specific and global VAMP2^{Δ3Δ}7^{-/-}8^{-/-} mice show that secretion is drastically affected from all three granules and thrombus formation is significantly affected. These studies show that only when VAMP-8 is knocked out is when dense granule secretion becomes further defective, supporting its role as the dominant v-SNARE in platelets. Studies also show the overlapping functions of the VAMP proteins in platelet secretion and that only when dense granule secretion is affected will defects in thrombus formation be observed [109, 115].

1.4.2 T-SNARES

Platelets contain two sets of (t/Q, Glu) SNARE proteins, Syntaxin proteins and SNAP proteins. These include Syntaxin 2, 4, 6, 7, 8, 11, 12, 16, 17, and 18 and SNAP-23, -25, and -29 [100-102]. Syntaxin-11 has been established as the main syntaxin protein

important for platelet secretion. Its function was established in a study done with Familial Hemophagocytic Lymphohistiocytosis type 4 (FHL4) patients that have no Syntaxin-11. It was shown that secretion was defective from all three granules in these patients resulting in a severe bleeding diathesis [45]. SNAP-23 was found to be essential in platelet secretion in previous studies in our lab using inhibitory antibodies. Consistent with this, a recent study using platelet specific SNAP23^Δ mice further confirmed its importance because secretion from all three granules was severely reduced as well as thrombus formation [116-119]. It has been shown that VAMP-8, SNAP-23, and Syntaxin-11 all co-immunoprecipitated together in a SNARE complex, and they are all present together in lipid raft fractions after platelet activation [45, 120]. Both Syntaxin-11 and SNAP-23 lack classical transmembrane domains, but both contain cysteine-rich regions that are acylated [121-123]. Acylation of SNAP-23 and Syntaxin-11 has been shown to be important for platelet secretion and function [120, 124].

1.4.3 Post-translational Modifications: Acylation in Platelets

Acylation has been identified as one of the critical post-translational modifications needed for proper platelet function. There are several ways proteins can be modified by lipids: 1. N-myristylation, in which a C₁₄ saturated fatty acid can be attached cotranslationally to glycine residues, 2. Glycosyl phosphatidylinositol (GPI), whereby GPI is attached to the C-terminus of the protein, 3. S-prenylation, in which where attachment of a farnesyl (C₁₅) or geranylgeranyl (C₂₀) is irreversibly attached to a cysteine in the transmembrane sequence motif CAAX, and 4. S-acylation, whereby a C₁₆ fatty acid group is attached to a cysteine residue by a thioester bond [125]. S-acylation is reversible and

does not require a transmembrane sequence motif; it is also the most common way to attach acyl groups to proteins [125, 126]. The addition of an acyl group increases the hydrophobicity of the protein and allows it to associate with lipid rafts to mediate protein-protein interactions. The reversibility of this modification has been identified as a regulatory mechanism as seen in studies examining Ras localization and in platelets [127, 128]. The enzymes involved in protein acylation have been identified in platelets and are comprised of palmitoyl acyl transferases (PATs) and the acyl protein thioesterases (APTs) that attach or remove acyl groups, respectively, from proteins. There are numerous PATs and APTs in platelets, but the exact ones involved in platelet acylation have not been identified, possibly because they seem to be able to compensate for each other when inhibited [125, 126].

Numerous acylated proteins have been identified in platelets with diverse roles in DNA repair, signaling, metabolism, immunity, and transport [129]. This led to the key identification of the main t-SNAREs, SNAP-23, and Syntaxin-11, which are important for secretion but do not have classical transmembrane domains instead they have cysteine rich regions [121, 123]. Previous studies done in our lab by Zhang *et al.* determined that the cysteine rich regions in SNAP-23 and Syntaxin-11 are reversibly acetylated and that acyl turnover was important for their function. It was also shown that VAMP-8 along with SNAP-23 and Syntaxin-11 localized to lipid rafts after platelet activation. The exact functional role of lipid rafts is unclear, but its disruption leads to defects in platelet secretion, suggesting functional importance in platelets [124].

The study of acylated proteins identified numerous other acetylated proteins in the SNARE complex machinery, including Syntaxin-2, -8, -10, -12, and VAMP-3, -4, -5, -7

[129]. This also led to the identification of one protein of interest Cysteine String Protein- α (CSP α). This protein contains a cysteine-string rich region similar to SNAP-23 and Syntaxin-11 [130-133]. It has not been determined whether all 11 of CSP α cysteine residues are acetylated, but acetylation has been determined to be important for its role in neurons in synaptic vesicle fusion [131, 133, 134]. In humans, CSP α dysfunction has recently been linked to a new disease termed adult-onset neuronal ceroid lipofuscinosis (ANCL). This disease is not only linked to dysfunction in CSP α , but it is also linked to dysfunction of the APT, palmitoyl protein thioesterase 1 (PPT1) [135-137]. PPT1 plays a role in the lysosomal degradation of acylated proteins by removing their acyl groups before degradation. The hypothesis is that the accumulation of CSP α aggregates in ANCL patients disrupts the function of PPT1, leading to the accumulation of various proteins that can no longer be degraded by lysosomes and thus causing the pathogenesis of the disease [135].

Acylation is important for platelet function. Since the degree of CSP α acylation has not been determined, studies to determine its degree of acylation and if its function is important for platelet function would be important. Biochemical assays and *in vitro* experiments were performed to figure this out in this dissertation (Chapter 4).

1.5 SNARE Regulators

1.5.1 SNARE Chaperones

1.5.1.1 Munc18b

Munc18b belongs to the Sec/Mun18 (SM) family of proteins that have been established as crucial syntaxin chaperones for exocytosis (Figure 1.2) [96, 138-140]. In

addition to Munc18b, platelets also contain the isoforms Munc18a and Munc18c. Munc18b is the most abundant isoform [102]. Studies have established that Munc18b is the most crucial isoform for platelet secretion while Munc18c, when partially deleted or completely deleted in platelet-specific knockout mice, was found to have a minimal role in platelet secretion [138, 141]. The importance of Munc18b in platelet secretion was established in patients that have Familial Hemophagocytic Lymphocytosis Type 5 (FHL Type 5). These patients suffer from severe bleeding and secretion defects from all three granules [44]. Also, Munc18b deficiency in these patients also resulted in the loss of Syntaxin-11 [45]. This further established Munc18b's role as a Syntaxin-11 chaperone in platelet secretion, as shown in (Figure 1.2).

1.5.1.2 STXBP5/Tomosyn 1

STXBP5/Tomosyn belongs to the family of WD-40 repeat containing proteins that are associated with exocytosis and cytoskeletal proteins. It was initially discovered in neurons and found to interact with Syntaxin-1 and was found to negatively affect neuronal exocytosis [142, 143]. Its discovery in platelets identified it as a key player in platelet secretion [100-102]. STXBP5 interacts with the main t-SNAREs (SNAP23 and Syntaxin-11) and localizes to lipid rafts. STXBP5^{-/-} mice have defective secretion from all three granules and severe hemostatic defects [144, 145]. STXBP5 is associated with increased cardiovascular risks in several GWAS studies [146-148].

1.5.2 Tethering/Docking Factors

1.5.2.1 Rab27

Rab27 proteins belong to the Rab GTPase family that are critical regulators of endocytic and exocytotic pathways [149]. Platelets contain two Rab27 isoforms, Rab27a and Rab27b [102]. Both proteins are known to interact with the effector protein Munc13-4 [150-152]. Defects in Rab27a are associated with Griscelli syndrome, but these patients have no known bleeding defects [34, 153]. Studies investigating the functional roles of Rab27a and Rab27b in platelets determined that Rab27b was important for dense granule biogenesis and secretion [154]. Rab27b^{-/-} mice had reduced dense granule numbers and severely impaired secretion, whereas the Rab27a^{-/-} mice had no granule secretion defects.

1.5.2.2 Munc13-4

Munc13-4 belongs to the family of Munc13 proteins which also include Munc13-1, Munc13-2, and Munc13-3. Munc13-4 is ubiquitously expressed, but it is found highly expressed in hematopoietic cells while the others are expressed solely in the brain [155, 156]. *In vitro* studies determined that Munc13-4 was important for the docking of the granules during the last steps of membrane fusion [48]. Mouse studies with Unc13d^{Jinx} mice also confirmed the importance of Munc13-4 because secretion was severely reduced from the dense granules, although there were only mild impacts to alpha and lysosomal granule secretion [47]. Defects in Munc13-4 are associated with FHL Type 3 but there are no known bleeding disorders in these patients; but studies done with Unc13d^{Jinx} mice suggest they should have bleeding defects as well [34, 43].

1.5.2.3 NSF and SNAPs

The disassembly of SNARE complexes for recycling requires the two proteins AAA⁺ ATPase N-ethylmaleimide sensitive fusion protein (NSF) and Soluble NSF Attachment

Protein (SNAP). Studies established that both proteins were present in platelets and essential for granule secretion [103, 157]. It has also been shown that the interaction of SNAP proteins with the SNARE complex is essential for stimulating the ATPase activity of NSF to disassemble SNARE complexes [158-162]. S-nitrosylation has also been shown to be important in regulating the function of NSF [163]. Disassembly of the SNARE complexes after membrane fusion is essential to ensure that the SNARE proteins are ready and “primed” for the next membrane fusion event [95, 98, 161].

1.6 Mouse Models of Hemostasis and Thrombosis

1.6.1 Murine Tail-Bleeding Model

The tail-bleeding assay is a widely used model that evaluates hemostatic function in mice. This assay is commonly used to determine the role of different coagulation factors and platelet function and secretion in maintaining the hemostatic balance [164, 165]. In this assay, a scalpel is used to transect the tail either at a predetermined length (1-5 mm) or at a specific circumference. The mouse’s tail is immediately placed in 37 °C saline and observed until bleeding ceases. Average bleeding times for WT mice is 150-300 seconds. Prolonged bleeding times or consistent rebleeding suggests that the hemostatic balance is disrupted and that platelets cannot effectively form a hemostatic plug to stop bleeding [164, 165]. This has been shown in several secretion deficient mouse strains, for example, both the platelet-specific and global VAMP2 $\Delta 3\Delta 8^{-/-}$ mice and the Unc13d^{Jinx} mice have severe bleeding defects in tail bleeding assay [47, 115]. This assay overall allows researchers to assess the contributions of coagulation factors or platelet function to determine what is

essential for maintaining the hemostatic balance to help with the development of anti-thrombotic therapeutics.

1.6.2 Murine FeCl₃ Carotid Artery Injury Model

The ferric-chloride carotid artery injury model is widely used to investigate the mechanisms of arterial thrombosis. In this model, vascular injury is induced by applying a filter paper soaked in a FeCl₃ solution which can range concentration from 2.5% to 20% for a predetermined time (1-5 min) on the carotid artery. After the oxidative injury is induced, time to occlusion is measured by using a Doppler flow probe to measure blood flow until it reaches a reading of 0 mL/min for 30-60 seconds, which is considered when a stable occlusive thrombus has formed. However, there are differing interpretations of how clot formation is induced in the FeCl₃ carotid injury model. Initially, clot formation was thought to be induced by exposure of the subendothelial, extracellular matrix (ECM) proteins like collagen, which would cause platelet activation leading to thrombus formation [166]. Alternatively, recent literature suggests that the subendothelial ECM is not exposed and that clot formation may instead be induced by the migration of FeCl₃ through the endothelium wall leading to the aggregation of RBCs, which precipitates platelet aggregation [167-169]. This is further complicated by studies using GPVI^{-/-} mice (a known collagen receptor and platelet activator). In some models there is no phenotype while in others the occlusion time is prolonged [167]. The difference in results is believed to be due to differences in the vessels that were injured or the FeCl₃ concentration used. Overall, this model is used to better understand the mechanisms of arterial thrombosis and investigate how platelet function and secretion can contribute. Data from this model also contributes

to better understanding how atherothrombotic disorders develop and help with the development of strategies to manage them.

1.6.3 Murine Jugular Vein Puncture Model

The recently developed jugular vein puncture model serves as a valuable tool for assessing thrombosis in the context of common injuries, such as puncture wounds from sharp metal objects [170, 171]. This injury model is used to evaluate how platelets mediate thrombus formation when an injury occurs to the adventitia leading to acute blood loss. In this model, vascular injury is induced by puncturing the jugular vein using a 30-gauge needle. After the injury is induced, bleeding is observed until it ceases. Clot formation after this injury is believed to be induced by the exposure of tissue factor from the injury which leads to platelet activation and recruitment [170, 171]. Distinguishing itself from the ferric-chloride carotid artery injury model, this approach focuses on the venous side of circulation, where clots are more red-blood cell centric due to reduced blood pressure. Beyond assessing platelet behavior during acute blood loss, this model also provides insights into the structure of thrombi. Recent data in the literature suggests that the accumulation of platelets in thrombi follows a “Cap and Build” paradigm compared to the original “Core and Shell” paradigm because images show that the platelets form a loose outer shell over the injury without filling the hole [170, 172]. Findings from this model contribute to a deeper understanding of platelet-mediated thrombus formation during acute blood loss, offering potential insights into the development of therapeutic strategies.

1.6.4 *Ex Vivo* Bioflux Microfluidics Model

The *ex vivo* Bioflux microfluidics model is a tool used to assess clot formation at either arterial or venous flow rates to assess the roles of platelet function and secretion when exposed to ECM agonists such as collagen or fibrinogen. This model also can be used to assess clot formation in response to a variety of anticoagulants, inhibitors, or drugs [173, 174]. One benefit of this system is the minimum amount of sample you can use to run an experiment. In this assay either whole blood or washed platelets are used. Whole blood is typically used to mimic what occurs during thrombus formation *in vivo* because RBCs contribute to platelet margination [173]. In this system, hirudinized whole blood is flowed over immobilized collagen at either 35 or 10 dyn/cm² for a certain time period to mimic either arterial or venous blood flow, respectively [175]. Hirudin is added to the whole blood to minimize activation via thrombin since it is a strong platelet agonist. This ensures that any defects seen in clot formation are because of the respective ECM agonist used. After flowing the whole blood for the respective time period, one can visualize and assess clot formation from representative images. These images are scored on several different parameters such as surface area coverage, morphology, contraction, and multilayer formation. The scoring of these different parameters gives insight into whether clot formation is deficient depending on the conditions that were used. Data from this model gives insights into how platelet function and secretion contribute to thrombus formation in different contexts.

1.7 α -Synuclein

α -Synuclein (SNCA) is the most abundant neuronal protein and is highly enriched in presynaptic nerve terminals. It is a member of the synuclein family and was first identified in *T. californica* (pacific electric ray) using antibodies against cholinergic synaptic vesicles [176]. It was given the name synuclein because of its presynaptic localization “syn” and “nuclein” because it was found on the nuclear envelope as well. However, no studies have confirmed the localization of synuclein on nuclear envelopes and this conclusion may have been due to antibody contamination [177]. Its vertebrate homolog was later identified in a rat cDNA library [178]. Later studies then led to the identification of two other members of the synuclein family, β -synuclein and γ -synuclein. β -synuclein and γ -synuclein are expressed in the brain, but γ -synuclein has less specificity and is primarily expressed in the peripheral nervous system [179-182]. α -Synuclein has been found to be present outside of the brain in tissues such as, skeletal muscle, heart, lymphocytes, vascular endothelial cells, and platelets [102, 183-185]. Only the α -synuclein isoform is present in platelets [100-102, 186]. Synucleins are restricted to vertebrates because they have not been found present in yeast, *D. melanogaster* (fruit flies), or *C. elegans* (nematode worms) [187]. This suggests that maybe synucleins are not required for neuron and other cellular functions, but extensive work done in the field argues that they have an essential function because disruption of α -synuclein function leads to Parkinson disease and many other neurodegenerative diseases [188-191]. However, α -synuclein’s molecular function is still unknown.

α -Synuclein is a small, acidic soluble protein (14 kDa) with three domains, including the N-terminal lipid-binding α -helix domain, the central non-A β component

(NAC) domain, and the acidic C-terminal domain. Its N-terminal domain consists of seven series of 11-residue repeats with each repeat containing a highly conserved KTKGEV sequence which is also found in the apolipoproteins that α -synuclein resembled [180, 192]. This domain is responsible for membrane binding and upon binding can form either a single, elongated α -helix or a broken α -helix conformation depending on membrane curvature [193]. The NAC domain is hydrophobic and is prone to aggregation. The C-terminal domain is highly unstructured and modulates protein-protein interactions. Studies show that the C-terminal domain is subject to post-translational modifications that may be important in regulating α -synuclein's function and preventing aggregation [194-196]. Numerous studies suggest that α -synuclein functions as a chaperone modulating SNARE-complex assembly (Figure 1.3) [197-207]. *In vitro* work in HEK293 cells showed that full-length α -synuclein was able to promote SNARE-complex assembly in a dose-dependent manner, and it was also shown that α -synuclein co-immunoprecipitates with the main members of the neuronal SNARE-complex assembly; SNAP-25, syntaxin-1, and VAMP-2 [198]. However, it was found that α -synuclein only has a direct interaction with VAMP-2 and that the C-terminus domain of α -synuclein modulates the interaction by binding to the N-terminus of VAMP-2 [198]. When examining its function *in vivo* in α -synuclein^{-/-} mice it does not appear to have as significant of a role because the mice are phenotypically normal, and no structural changes are apparent in their brain except for reduced dopamine levels [208-210]. Only when all three of the synucleins are knocked out in $\alpha\beta\gamma$ ^{-/-} mice is there neurological impairments as the mice age [211, 212]. Of particular interest is that α -synuclein is able to rescue SNARE-complex assembly in $\alpha\beta\gamma$ ^{-/-} mice in a dose-dependent manner [198]. This suggests that α -synuclein levels may be important later in life for

neuron function. A study done in the laboratory of Dr. Thomsa Südhof, suggests that α -synuclein functions as a chaperone because they were able to show that transgenic expression of α -synuclein rescued the neurodegenerative phenotype seen in Cysteine String Protein- $\alpha^{-/-}$ mice by restoring SNARE-complex assembly. It was able to restore SNARE-complex assembly without restoring SNAP-25 levels suggesting that α -synuclein and CSP α work together either upstream or downstream of one another in SNARE-complex assembly [199]. These and other studies confirmed the role of α -synuclein in SNARE-complex assembly and suggest that α -synuclein has roles in fusion pore opening and docking [200, 202-206]. Studies of α -synuclein function in other non-neuronal cells such as endothelial cells and platelets have been done, but its physiological function in these cells is still unclear [186, 213-216].

α -Synuclein (SNCA) is well known as being a major component of Lewy bodies, protein aggregates in the brain, which is a neuropathological feature of Parkinson disease (PD) and many other neurodegenerative diseases such as Alzheimer, Dementia with Lewy Bodies (DLB), and Multiple System Atrophy (MSA). These Lewy bodies lead to the death of dopaminergic neurons in the *substantia nigra pars compacta*, causing a severe reduction in dopamine levels and leads to most of the motor-based symptoms PD patients suffer from, such as bradykinesia, tremors, rigidity, and difficulty walking [191, 217-219]. Bleeding diatheses have been reported in PD patients, and they are more prone to cerebral microbleeds if they have PD in conjunction with dementia [220-224]. This increase in microbleeds in PD patients with dementia is because of the development of cerebral amyloid angiopathy that leads to vessel weakening [225]. The disease usually presents around 55-65 years of age and death is usually caused by the inability to swallow which

leads to aspiration pneumonia. It is a slow, progressive disease so it often does not get diagnosed until the motor symptoms are present, making it difficult to treat. Thus, finding valid disease biomarkers is important. There are current studies investigating α -synuclein levels in the blood and cerebrospinal fluid to potentially detect PD earlier in life [226-228]. Most cases of PD are idiopathic, but there are familial cases of the disease caused by either duplication or triplication of the SNCA gene or by missense mutations in the SNCA gene: E46K, H50Q, G51D, A53T, A53E, A53V, and A30P [191, 219, 229, 230]. PD can also be caused by mutations in other genes such as Leucine rich repeat kinase 2 (LRRK2), vascular protein sorting 35 (VPS35), Parkin, PTEN-induced putative kinase 1 (PINK1), and Daisuke-Junko-1 (DJ1) [219, 229, 231-237]. These mutations disrupt α -synuclein function by either changing its association with membranes or by making it more prone to aggregation because all the mutations occur in the N-terminal binding domain. Studies suggest α -synuclein aggregation could lead to impairment of SNARE function, disrupting dopamine release, or it could cause mistrafficking and lead to lysosomal dysfunction which could be the cause of the death of dopaminergic neurons [208, 235, 238-240]. However, I will not be focusing on the mutations found in SNCA. Further studies need to be done to get a clear understanding of α -synuclein's function and elucidate why its dysfunction leads to so many neurodegenerative diseases.

1.8 Cysteine String Protein- α

Cysteine String Protein- α (CSP α) is well-known as a presynaptic vesicle protein and chaperone in the CSP protein family (Figure 1.3). It was first identified in *D. melanogaster* by using brain-specific monoclonal antibodies [241]. After its discovery in

fruit flies, the first vertebrate homolog was discovered in *T. californica* (pacific electric ray) and in subsequent years it was found in many mammalian species including mice and humans [130, 242, 243]. The presence of CSP proteins is exclusive to species that have a nervous system including fruit flies and nematode worms, because the protein has not been found present in unicellular eukaryotes, specifically yeast, which have been used to characterize many of the presynaptic proteins [130, 244-246]. Genomic sequencing has shown that mammalian species express three different CSP proteins (α , β , and γ) while fruit flies and *C. elegans* have a single CSP protein which can be alternatively spliced in fruit flies [130, 247-249]. CSP α has been found to be present in both neuronal and non-neuronal cells that specialized in exocytosis, such as PC12 cells, pancreatic β cells, platelets, and many more [100, 129, 245, 250, 251]. CSP β and CSP γ were first believed to be testis-specific, but there is now evidence showing that they are present in the brain and other tissues as well [130, 252-254]. There have also been studies examining the function of CSP β and CSP γ , respectively, in both CSP $\beta^{-/-}$ and CSP $\gamma^{-/-}$ mice, but their exact molecular function is unclear [130, 254]. On the other hand, there has been extensive work done examining the role of CSP α .

CSP α /DNACJ5/CLN4 is a part of the DNAJ/Hsp40 family of co-chaperones. The structure of CSP α consists of an N-terminal “J” domain, conserved linker region, a central cysteine rich region, and a variable C-terminal domain. Its “J” domain is a unique feature of all proteins in the DNAJ/Hsp40 family, and it is classified as a Type III protein because of its “J” domain location within the protein sequence [255]. The “J” domain region contains an HPD motif that is central for its ability to bind to Hsp70/Hsc70 proteins to activate their ATPase activity [255-258]. The 11 consecutive cysteine residues in the

central cysteine rich region are the reason behind the naming of CSP. Most of the cysteine residues are believed to be acetylated, but it has not yet been established whether all of them are [130, 132-134]. This region has been shown to be essential for membrane attachment and intracellular signaling. The C-terminal domain has been shown to play a role in exocytosis and modulating protein interactions [259]. Biochemical studies determined that CSP α functions like other typical “J” domain proteins because of its ability to bind Hsc70 and enhance its ATPase activity [256-258]. Later studies showed that CSP α functions in a chaperone complex with Hsc70 and small glutamine-rich tetratricopeptide repeat protein (SGT) [260, 261]. Extensive genetic studies in CSP mutant fruit flies conducted at the same time showed that the deletion of CSP had a semi-lethal phenotype and a temperature-sensitive paralysis phenotype with severe neurodegeneration and synapse dysfunction [249, 262]. Only 4% of fruit flies survived to adulthood and of those that survived they only lived 4-5 days at 22 °C while at 27 °C survival was less than a day. The genetic studies done in fruit flies suggested that CSP proteins play a role in exocytosis which was later confirmed in studies done with CSP $\alpha^{-/-}$ mice [199, 261, 263-265]. CSP $\alpha^{-/-}$ mice exhibited the same progressive neurodegenerative and lethal phenotype seen in fruit flies [265]. CSP $\alpha^{-/-}$ mice are phenotypically normal until approximately 2-3 weeks of age and that is when they start rapidly losing weight and presenting neurological symptoms such as muscle weakness and sensorimotor defects. Their survival rate is typically around 90 days. The neurological defects in CSP $\alpha^{-/-}$ mice were determined to be caused by the loss of functional SNAP-25, leading to its degradation or accumulation and inhibiting neuronal SNARE-complex assembly [263]. CSP α 's co-chaperone activity is required for the proper folding of SNAP-25 to facilitate SNARE-complex assembly in neurons [261]. One

significant aspect of those studies was the unique ability of α -synuclein to rescue the lethality of the $CSP\alpha^{-/-}$ mice without increasing SNAP-25 levels suggesting that these two proteins are linked functionally [199, 261, 263]. This was further shown because deletion of α -synuclein or any of the other synuclein proteins in the $CSP\alpha^{-/-}$ mice further exacerbated the neurodegenerative phenotype. Furthermore, another study showed that $CSP\alpha$ overexpression in 1-120h α syn mice, these mice express the truncated α -synuclein form prone to aggregation, can reduce α -synuclein aggregation and rescue dopamine release [266]. These studies confirmed the role of $CSP\alpha$ as a co-chaperone in neuronal exocytosis, but further studies are needed to ensure that $CSP\beta$ and $CSP\gamma$ are not also playing a role. Studies have not been completed in non-neuronal cells such as pancreatic β cells, adrenal chromaffin cells or platelets that express $CSP\alpha$ in the $CSP\alpha^{-/-}$ mice to characterize their function and to determine if the deletion of $CSP\alpha$ also affects their function. Pancreatic β cells and adrenal chromaffin cells have been characterized in *in vitro* studies and $CSP\alpha$ was shown to have roles in exocytosis in those cells [251, 267, 268]. *In vivo* studies would help determine whether $CSP\alpha$ has different roles in other cells that may not have SNAP-25 or any other proteins it interacts with.

$CSP\alpha/DNACJ5/CLN4$ has been recently linked to several neurodegenerative diseases, but it is perhaps best for its pathology in adult-onset neuronal ceroid lipofuscinosis (ANCL), also known as Kufs' or Parry disease [136, 137, 269-272]. ANCL is characterized by progressive neuronal dysfunction, premature neuronal death, and the accumulation of lipofuscin. It is classified as a neurodegenerative lysosomal disorder because of the accumulation of misfolded and proteolysis-resistant proteins that make up the lipofuscin deposits in neurons. Symptoms of the disease include seizures, movement

disorders, cognitive deterioration, and progressive dementia [137, 270]. Bleeding diatheses have not been reported in these patients, but they could be similar to Familial hemophagocytic lymphohistiocytosis patients, in which bleeding histories were not reported because it was not consistent or obvious [34, 44, 45]. This disease usually presents around late 20s or early 30s and leads to early premature death in patients. ANCL has been genetically linked to two mutations, L115R and L116 Δ , and a recent study has found a new mutation that results in a C124_C133 duplication [135, 136, 269, 272-276]. All three of these mutations occur in the central cysteine rich region in CSP α which is important for membrane binding and intracellular targeting. Studies suggest that the mutations in this region reduce CSP α palmitoylation, making it more prone to aggregate and disrupts its attachment to membranes, causing it to mislocalize [135, 274, 275]. This mislocalization is believed to reduce CSP α 's co-chaperone activity with SNAP-25. These mutations cause both a partial loss and gain of function because CSP α mislocalization increases its chaperone activity elsewhere in the cell [135]. In ANCL, there are other proteins affected by the deletion of CSP α ; the most notable of these was palmitoyl protein thioesterase 1 (PPT1) [135, 137, 277]. These two proteins are linked, and CSP α has been shown to be a substrate of PPT1. Studies in ANCL have shown that PPT1 levels are increased, but its enzymatic activity is significantly reduced [135, 136, 270, 277]. The reduction in PPT1 enzymatic activity has been shown to affect the palmitoylation of lysosomal and synaptic proteins [278]. An interesting hypothesis in the Henderson paper is that the accumulation of CSP α aggregates leads to defective trafficking to the synapse, which leads to PPT1 upregulation, through the activation of the TFEB transcription factor, to depalmitoylate CSP α but instead leads to the accumulation of PPT1 and its mislocalization. This results in

the accumulation of proteins that would normally be degraded by lysosomes [135]. The increase in PPT1 levels were not observed in $CSP\alpha^{-/-}$ mice, but SNAP-25 levels are reduced in ANCL patients [270, 279]. Further studies are needed to determine what exactly leads to the pathogenesis of ANCL, but $CSP\alpha$ has been determined to be the central protein involved.

1.9 Dissertation Overview

Platelets are essential for maintaining the vascular microenvironment and their dysfunction can be life-threatening causing a wide range of bleeding diatheses and occlusive cardiovascular events [51, 280]. Current anti-thrombotic therapeutics, while effective, often lead to severe bleeding defects underlining the need for better therapeutics. The work in this dissertation focuses on better understanding the process of platelet secretion and the molecular mechanisms that regulate the process. This process is complex and not completely characterized. Regulatory proteins such as Munc18b, a chaperone for Syntaxin-11, have been shown to be crucial for platelet granule secretion because its dysfunction leads to FHL Type 5 [44]. However, regulatory proteins for VAMP/SNAP-23/25 proteins have not been identified. Recent studies have identified proteins of interest that could be possible chaperones for the VAMPs and SNAP-23/25 proteins; candidates include α -synuclein and its interacting protein $CSP\alpha$. Their dysfunction is associated with several neurodegenerative diseases while their molecular functions remain unknown. We chose to use platelets as a model to gain insights into their molecular roles in both platelets and neurons. We hope to be able to quantify and discern the molecular roles of these proteins in platelets to help contribute to the development of better anti-thrombotic

therapeutics as well as better understand why when these proteins are dysfunctional, they cause severe neurodegenerative diseases. In (Figure 1.3), we have a depiction hypothesizing their potential roles in platelet SNARE-complex assembly. The first part of the dissertation investigates the role of α -synuclein in platelet secretion and function while the second part of the dissertation analyzes the critical role of CSP α . The work presented here will provide insight into how platelet secretion is regulated, and the proper threshold needed for thrombosis and hemostasis.

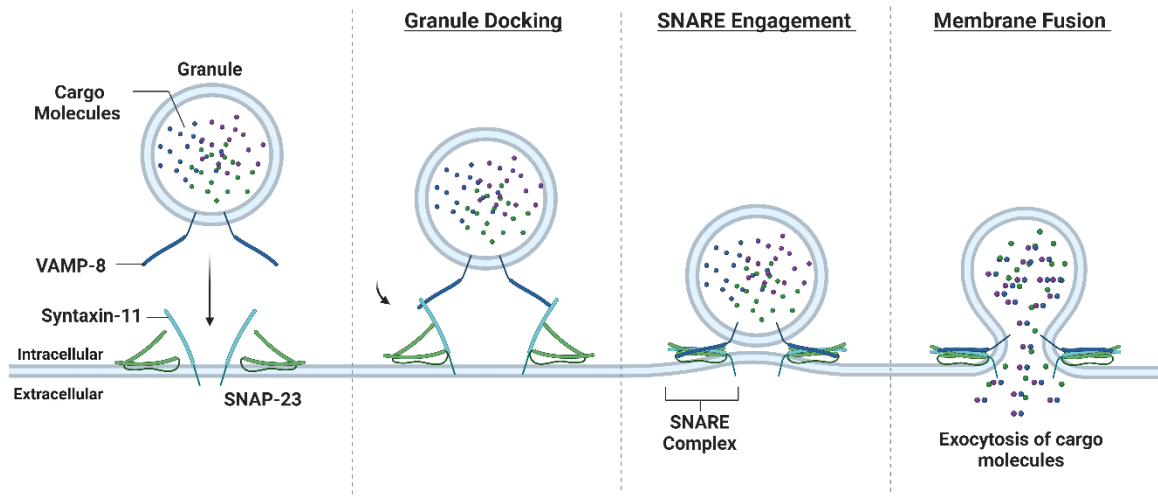


Figure 1.1 SNARE-mediated granule-plasma membrane fusion

SNARE-mediated membrane fusion occurs in a series of steps as shown above that leads to the release of cargo molecules from the granules. The machinery depicted are the main SNARE proteins involved in granule-plasma membrane fusion. The v-SNARE, VAMP-8, is located on the granule membrane while the t-SNAREs, Syntaxin-11 and SNAP-23, are located on the plasma membrane. These proteins come together and form a transmembrane complex that mediates granule-plasma membrane fusion for cargo release.

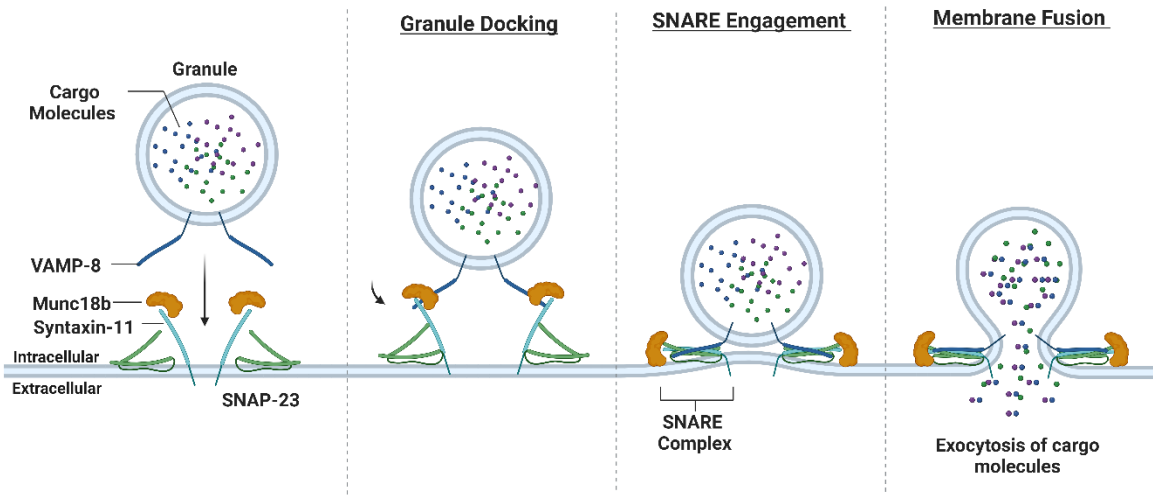


Figure 1.2 SNARE chaperone function of Munc18b

SNARE-mediated membrane fusion is a highly complex process that is regulated by a variety of proteins and post-translational modifications. One of the most well-known chaperones in platelet SNARE-complex assembly is the protein, Munc18b. Munc18b functions as a t-SNARE chaperone for Syntaxin-11 ensuring that it is correctly folded for proper SNARE-complex assembly to occur.

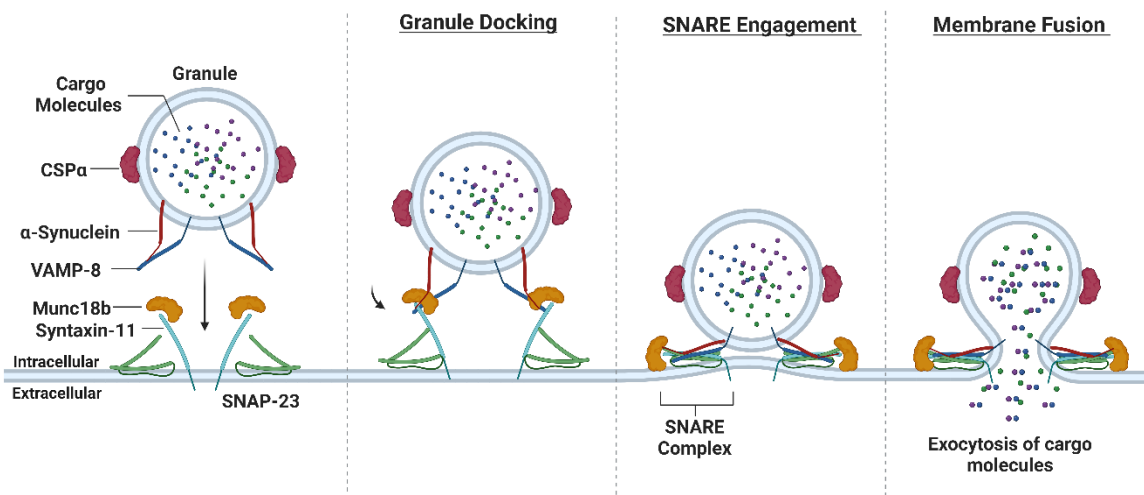


Figure 1.3 Hypothesized roles of α -synuclein and CSP α in granule-plasma membrane fusion

SNARE-mediated membrane fusion is a highly complex process that is regulated by a variety of proteins and post-translational modifications. In this depiction, we have hypothesized the potential roles of α -synuclein and CSP α in platelet SNARE-complex assembly. α -Synuclein's hypothesized role in platelet SNARE-complex assembly is to interact with the VAMP proteins on the granule membrane while CSP α is hypothesized to interact with the SNAP proteins on the plasma membrane to ensure proper SNARE-complex assembly.

CHAPTER 2. MATERIALS AND METHODS

2.1 Materials

2.1.1 Reagents

Apyrase, hirudin, human fibrinogen, biotin, ATP, N-Ethylmaleimide (NEM), Tris (2-carboxyethyl) phosphine hydrochloride, and proteinase K were from Sigma (St. Louis, MO). Thrombin, ADP, collagen, and CHRONO-LUME reagents were from Chronolog (Havertown, PA). Convulxin and prostaglandin I₂ (PGI₂) were from Cayman (Ann Arbor, MI). U46619 was from Enzo Life Sciences (Farmingdale, NY). CRP (collagen-related peptide) was a gift from Versiti Blood Research Institute (Milwaukee, WI). Normal Goat Serum (NGS), BCA protein assay kit, hydroxylamine HCl, and Pierce ECL plus western blotting substrate were from ThermoFisher Scientific (Waltham, MA). Biotin-BMCC was from ProteoChem (Hurricane, UT). Streptavidin-Agarose beads were from Agilent Technologies (Santa Clara, CA). CellTiter-Glo luminescent cell viability assay (G7570) was from Promega (Madison, WI). Acid citrate dextrose (ACD) blood collection tubes (364606) were purchased from BD Diagnostics (Sparks, MD). Other reagents used were no less than least laboratory grade.

2.1.2 Antibodies

Mouse monoclonal FITC-CD62P (RB40.34; 553744), rat anti-mouse PE-LAMP-1 (1D4B; 558661), and rat anti-mouse PE-CD63 antibodies were from BD Biosciences (San Jose, CA). Rat-anti mouse FITC-CD41/CD61 (Leo.F2; M025-1) antibody and rat anti-mouse PE-Jon/A (JON/A; M023-2) antibodies were from Emfret Analytics (Eibelstadt, Germany). Rabbit anti- α -synuclein (2642S) antibody and rabbit anti-GAPDH (8884)

antibody were from Cell Signaling Technology (Danvers, MA). GDI mouse monoclonal (4E1G1; 66434-1-Ig) and Syntaxin-4 rabbit polyclonal (14988-1-AP) antibodies were from Proteintech (Rosemont, IL). Rabbit anti-cysteine string protein- α (AB1576) antibody was from Millipore Sigma (Burlington, MA). SNAP-25 mouse monoclonal (SP12; sc-20038) was from Santa Cruz Biotechnology (Dallas, TX). Mouse anti-VAMP-2 (SP10; NBP1-19332) antibody and rabbit anti-VAMP-3/Cellubrevin (NB300-510) antibodies were from Novus Biologicals (Centennial, CO). Rabbit anti-VAMP-7/Ti-VAMP (158.2; 232 011) antibody was from Synaptic Systems (Göttingen, Germany). Rabbit anti-beta actin (PA1-16889) antibody was from ThermoFisher Scientific (Waltham, MA). Rabbit anti-Munc18b, anti-syntaxin-11, anti-SNAP-23, and polyclonal VAMP-8 antibodies were generated by our laboratory [110]. Rabbit anti-VMAT2 antibody was a gift from Dr. Martin Chow (University of Kentucky, USA). The alkaline phosphatase conjugated goat anti-mouse IgG (A3562) and goat anti-rabbit-IgG (A3687) antibodies were from Sigma (St. Louis, MO). ECL horseradish peroxidase (HRP) conjugated anti-rabbit IgG (NA934V) antibody was from Amersham Biosciences (Slough, Buckinghamshire, UK). Rat anti-mouse P Selectin/CD62P (MAB737) antibody was from ThermoFisher Scientific (Waltham, MA), and rat anti-mouse LAMP-1 (1D4B) antibody was from Developmental Studies Hybridoma Bank (Iowa City, IA). The secondary antibodies used in the immunofluorescence experiments were Alexa 488 goat anti-rat-IgG (A11006) and Alexa 568 goat anti-rabbit-IgG (A11008) from Life Technologies (Carlsbad, CA).

2.2 Methods

2.2.1 Murine Strains and Genotyping

The following mice were used for the experiments described in this thesis.

C57BL/6 (WT) mice were purchased from Jackson Laboratory and bred in our animal vivarium.

Global α -Synuclein^{-/-} mice (B6; 129X1-Scna^{tm1Rosl}/J; Stock # 003692) were purchased from Jackson Laboratory and were bred using heterozygous crosses. The genotyping primers and conditions were as follows:

Primers and Genotyping Conditions:

- Forward α -Synuclein Neo Primer: 5' AGGCGATAGAAGGCGATGCG 3'
- Reserve α -Synuclein Neo Primer: 5' CAAGACCGACCTGTCCGGTG 3'
- Forward JAX WT Primer: 5' GCGACGTGAAGGAGCCAGGGA 3'
- Reverse JAX WT Primer: 5' CAGCGAAAGGAAAGCCGAGTGATGTACT 3'

The PCR reaction conditions were 94 °C for 10 min, followed by 30 cycles of 94 °C for 1 min, 56 °C for 45 sec, 72 °C for 1 min, and finally 72 °C for 10 min. The PCR reactions yielded a 630 bp DNA product indicative of the α -Synuclein mutant gene and 320 bp DNA product indicative of the WT gene.

Global Cysteine String Protein- α ^{-/-} mice (B6; 129S6-Dnajc5^{tm1Sud}/J; Stock # 006392) were purchased from Jackson Laboratory and were bred using heterozygous crosses. The genotyping primers and conditions were as follows:

Primers and Genotyping Conditions:

- Wild-type Forward Primer: 5' CAAGAATGCAACCTCAGATGAC 3'
- Common Primer: 5' CTTTAAAGTGTGTTTACTTTTTGGTG 3'
- Mutant Forward Primer: 5' GAGCGCGCGCGGCGGAGTTGTTGAC 3'

The PCR reaction conditions were 94 °C for 7 min, followed by 35 cycles of 94 °C for 45 sec, 55 °C for 30 sec, 72 °C for 45 sec, and finally 72 °C for 10 min. The PCR reactions yielded a 150 bp DNA product indicative of the CSP mutant gene and 336 bp DNA product indicative of the WT gene.

2.2.2 Genomic DNA isolation from murine tail tip

Mouse tail tips (3-5 mm) cut from 3–4-week-old pups or harvested during the tail-bleeding assay (3 mm) were digested overnight in 400 µL of tail lysis buffer (50 µM Tris/HCl, pH 7.5, 100 µM EDTA, 100 µM NaCl, and 1% SDS) containing 20 µL of 10 mg/mL proteinase K at 55 °C. After digestion, the solution was mixed with 200 µL of saturated NaCl and centrifuged at 16,430 x g for 30 min at 4 °C. The supernatant containing genomic DNA was then collected and mixed with 1 mL of 100% ethanol. The samples incubated at RT for 10 min and the genomic DNA was recovered by centrifugation at 16,430 x g for 10 min. The DNA pellets were then washed with 1 mL of 70% ethanol, dried in a speed-vac centrifuge for 20 min, and resuspended in 75 µL of sterile ddH₂O.

2.2.3 Platelet Preparation from Mouse Blood

Mice were euthanized by CO₂ inhalation. The thoracic region was then exposed, and blood was collected from the right atrium by a 1 mL syringe attached to a 26 G needle filled with approximately 120 µL of 3.8% sodium citrate with apyrase (0.2 U/mL) and prostaglandin I₂ (PGI₂; 1 µg/mL). After collection, the blood samples were diluted with

either 1:1 1X filtered PBS or 0.9% filtered saline, apyrase (0.2 U/mL), and PGI₂ (1 mg/mL) and incubate for 5 min at RT. The samples were then centrifuged using a Beckman Coulter Avanti J-15R centrifuge (Beckman Coulter, Inc. Brea, California) at 950 RPM at RT. Platelet Rich Plasma (PRP) was collected and apyrase and PGI₂ were added as well for a 5 min incubation at RT. The PRP was then centrifuged at 1,750 RPM to pellet the platelets. The platelet pellet was resuspended in HEPES Tyrode Buffer pH 6.5 (20 mM HEPES/KOH, 128 mM NaCl, 2.8 mM KCl, 1 mM MgCl₂, 0.4 mM NaH₂PO₄, 12 mM NaHCO₃, 5 mM D-Glucose) with 0.2 U/mL apyrase, 1 mg/mL PGI₂, and 1 mM EGTA and centrifuged at 1,750 RPM RT to recover the platelets. The pellet was resuspended in HEPES Tyrode Buffer at pH 7.4. Platelet concentration was calculated using a Z2 Counter (Beckman Coulter, Inc. Brea, California). Platelet counts were measured in triplicates and the final count was the average. Platelets were then diluted to the concentration needed for each experiment.

2.2.4 Platelet Preparation from Human Platelet Unit

Platelet units from the Kentucky Blood Bank were isolated and adjusted to the concentration needed for each experiment as described [120]. Platelets were transferred to 50 mL conical tubes and centrifuged at 250 x g for 20 min at RT to separate white blood cells from platelet rich plasma (PRP). The PRP was collected and 0.2 U/mL apyrase and 1 mg/mL PGI₂ were added as well for a 10 min incubation at RT. The PRP was then centrifuged at 900 x g for 10 min to pellet the platelets. The platelet pellet was then resuspended in HEPES Tyrode Buffer pH 6.5 with apyrase, PGI₂, and centrifuged at 850 x g at RT to recover the platelets. The pellet was then resuspended in HEPES Tyrode Buffer

at pH 7.4. Platelet concentration was calculated using a Z2 Counter (Beckham Coulter, Inc. Brea, California).

2.2.5 Hematology Analysis

Blood was collected from the right ventricle using a 1 mL syringe attached to a 26 G needle with 3.8% sodium citrate, apyrase, and PGI₂ as described above from control WT, HET, and KO littermates. A 50 μ L aliquot of blood was analyzed using an IDEXX ProCytex DX Hematology Analyzer (IDEXX Laboratories, Westbrook, ME). Statistical analyses were done using GraphPad Prism v 10.0.2 (San Diego, CA).

2.2.6 Granule Secretion Measurements

Mouse platelets were collected and isolated as above and incubated with 0.4 μ Ci/mL [³H] serotonin (Perkin-Elmer Cetus Life Sciences, Boston, MA) for 30 min at 37 °C. Final platelet concentrations were adjusted to 2.5×10^8 /mL and CaCl₂ was added to a final concentration of 1 mM. Platelets incubated for 5 min and 50 μ L of the suspension was aliquoted into 1.5 mL Eppendorf tubes for assay. Platelets were either stimulated with various thrombin concentrations (0.005, 0.01, 0.05, 0.1, or 0.5 U/mL) or for different time points (15, 30, 45, 60, 90, 120, and 300 sec). Hirudin (2X the concentration of thrombin) was used to stop the reactions. Samples were then placed on ice. All samples were centrifuged at 16,200 x g for 2 min in a microfuge. The supernatants were removed, placed in another tube, and the pellets were lysed with 60 μ L of lysis buffer (1% Triton X-100 in 1X PBS, pH 7.4) for 45 min on ice.

Dense Granule Secretion

To measure dense granule secretion, the release of [³H] serotonin was measured. Supernatant (25 µL) or pellet samples were added to 3 mL of scintillation cocktail (Econo-safe™, Research Products International Corp, Mt. Prospect, IL) and a Tri-Carb 2100TR liquid scintillation analyzer (Beckham, Fullerton, CA) was used to measure radioactivity. Release was calculated as percent release = [(amount in supernatant)/(amount in supernatant + amount in pellet)] * 100.

Alpha Granule Secretion

To measure alpha granule secretion, Platelet Factor 4 (PF4) was measured. A commercial sandwich ELISA assay was executed per the manufacturer's instructions (R&D). Clear ELISA plates (Costar, #3369, Fisher Scientific) were coated overnight with capture antibody against mouse PF4 (2 µg/mL) at RT. The next day, plates were washed and blocked with blocking buffer (0.05% Tween 20/1% BSA/5% Sucrose in 1X PBS) for 1 hr. After washing, diluted supernatant and pellets (reagent diluent recipe) were added and incubated at RT for 2 hrs. Recombinant mouse PF4 was plated in a serial dilution to make a standard curve, with a maximum concentration of 2 ng/mL. After washing, the biotinylated detection antibody was added to the plate at RT for 2 hrs. After washing, the plate was coated with streptavidin-conjugated horseradish peroxidase at RT in the dark for 30 min. After washing, the plate was coated with TMB Substrate (Pierce, #34021, Thermo Scientific) to detect the signal. 2M H₂SO₄ was used to stop the reaction. Release was calculated as percent release = [(amount in supernatant)/(amount in supernatant + amount in pellet)] * 100.

Lysosomal Granule Secretion

To measure lysosomal secretion, a colorimetric assay was used to measure β -hexosaminidase activity using a PNP-GlcNAc substrate. In a 96-well ELISA plate, 100 μ L of citrate-phosphate buffer (53.4 mM citric acid, 93.2 mM Na₂HPO₄, pH 4.5) containing 10 mM *p*-Nitrophenyl-N-acetyl- β -D-glucosaminide was added and either 6 μ L of supernatant or 3 μ L of pellet sample were added to each well. These samples incubated at 37 °C for 18 hrs and the reactions were stopped with 100 μ L of 1 M NaOH. Using a Biotek Elx808 plate reader (Biotek Instruments Inc, Winooski, VT), the optical density of each well was measured at 405 nm. Release was calculated as percent release = [(amount in supernatant)/(amount in supernatant + amount in pellet)] * 100.

2.2.7 ATP Release Assay

To measure ATP release from dense granules, a modified protocol was used [281]. Platelet rich plasma (PRP) was isolated and adjusted to a concentration of 1×10^8 /mL and CaCl₂ was added to a final concentration of 0.7 mM. Platelets incubated for 5 min and 100 μ L of the PRP were plated into a 96-well white, opaque polystyrene plate (Pierce, #15042, Thermo Scientific). Then 50 μ L of the CellTiter-Glo substrate (made in 1X PBS) were added to the wells to detect ATP release. After the addition of the CellTiter-Glo substrate, the platelets were either held in a resting state (no agonist) or stimulated with thrombin or convulxin. ATP was plated in a serial dilution to make a standard curve, with a maximum concentration of 1 μ M ATP. After activation, using a Biotek Synergy H1 plate reader (Biotek Instruments Inc, Winooski, VT) the luminescence of each well was measured over a 10 min period at 37 °C for 2 min increments to determine the amount of ATP release from platelets.

2.2.8 Lumi-Aggregometry

Washed platelets were prepared as described above. ATP release and aggregation were measured using a Chrono-Log Model 700 Lumi-aggregometer (Havertown, PA). Mouse platelets (250 μL of $3 \times 10^8/\text{mL}$) were placed in a siliconized glass cuvette (Chrono-Log) with a metal stirring bar (Chrono-Log) spinning at 1,200 RPM for 3 min at 37 °C. When ATP release was being measured, 10 μL of Chrono-Lume reagent was also added (Chrono-Log). Agonists (thrombin or collagen as indicated) were added to initiate platelet activation as indicated. The aggregation traces were monitored by turbidity and ATP release was measured by luminescence using AGGRO/Link8 software (Chrono-Log) as described [282].

2.2.9 Flow Cytometry

Washed mouse platelets (20 μL of $5 \times 10^7/\text{mL}$) were either held in a resting state (no agonist) or stimulated with various concentrations of thrombin, convulxin, CRP, U46619 for 2 min at RT. Platelets then were incubated with 2.5 μL of FITC-conjugated or PE-conjugated antibodies for 20 min at 37 °C. The samples were diluted 10-fold with HEPES Tyrode buffer pH 6.5 to stop the reaction and transferred to polystyrene FalconTM tubes (BD Biosciences, San Jose, CA). Fluorescent intensity was measured using BD FACSymphonyTM flow cytometer (BD Biosciences, San Jose, CA). The platelet populations were detected by adjusting the voltages for forward light scattering (FSC) and side light scattering (SSC). Fluorescent intensity was optimized by adjusting the voltage for excitation of green (FITC) and yellow (PE) channels. Platelet fluorescent intensities were analyzed using FlowJoTM software v10.8.0 (BD Biosciences, San Jose, CA). Fifty

thousand events were analyzed for each sample, and fluorescent intensities plotted as a histogram with statistical values as described [175].

2.2.10 Western Blotting and Quantification

Platelets

Mouse platelets were prepared as described above and the concentration of platelets was adjusted to 5×10^7 platelets per well. Platelet proteins were separated by sodium dodecyl sulfate-polyacrylamide gel electrophoresis (SDS-PAGE) and then were transferred onto Immobilon-P polyvinylidene fluoride (PVDF) membranes (Millipore Corp., Bedford, MA) for 1 hr at 100 V. The PVDF membrane was blocked and placed in primary antibody (diluted in blocking buffer) overnight at 4 °C. The proteins were detected with alkaline phosphatase-conjugated secondary antibodies (diluted in blocking buffer) for 1 hr at RT using vista-ECF substrate (Amersham Biosciences). The proteins were visualized with a Typhoon FLA 9500 scanner v1.1 (GE Healthcare, Chicago, IL) using excitation at 488 nm, measuring emission at 532 nm, and quantified using ImageQuantTL software (v5.2, GE Healthcare). The proteins were also visualized using a Bio-Rad ChemiDoc (Hercules, CA) using Alexa 488 and quantified using Bio-Rad ImageLab software v6.1.

Brain

Mice were euthanized by CO₂ inhalation. The brain was removed by removing the skull of the mouse. After removal, the brain was sliced finely and then homogenized using a Dounce homogenizer using 2 mL cold 1X PBS. The amount of protein in the homogenate was then quantified using a BCA protein assay and adjusted to 50 µg/µL. Brain proteins

were then separated by SDS-PAGE like the platelets described above and visualized using the same methodology as well.

2.2.11 Hemostasis/Thrombosis Models

Tail Bleeding Assay

Mice (6-8 weeks old) were anesthetized using ketamine hydrochloride 75 mg/kg i.p. As shown in (Figure 2.1), the tails were transected 3 mm from the tip and immediately placed into a 15 mL conical tube filled with 37 °C normal saline. The time from the transection until cessation of bleeding was recorded. After initial cessation of bleeding, the mice were observed for an additional minute to exclude re-bleeding. Bleeding in mice that was over 10 min was manually stopped.

FeCl₃ Carotid Injury Model

This FeCl₃-induced carotid injury model was performed as described in a paper recently published from our lab [283]. Mice (8-12 weeks old) were anesthetized using Avertin (tribromoethanol; 0.2 g/kg, i.p.). After 10-15 min, the toe-pinch reflex was used to monitor anesthesia state. As shown in (Figure 2.2), the left carotid artery was exposed using blunt dissection under a dissecting microscope. A miniature Doppler flow probe (0.5VB, Transonic Systems Inc., Ithaca, NY) was placed under the carotid artery to monitor blood flow. It was adjusted to maximize blood flow. After baseline readings, the carotid artery was dried, and thrombus formation was induced by placing a round filter paper (1 mm diameter) saturated with 7.5% FeCl₃ solution (1 µL) made in 1X PBS on top of the carotid artery for 3 min. The filter paper was removed, and the area was washed with normal saline and the time from the removal of the filter paper until cessation of blood flow was recorded. The recording was stopped after 30 min if blood flow did not stop.

Jugular Vein Puncture Model

Mice (8-12 weeks old) were anesthetized using Avertin (tribromoethanol; 0.2 g/kg, i.p.). As shown in (Figure 2.3), the left external jugular vein was exposed using blunt dissection under a dissecting microscope. Thrombus formation was induced by puncturing the vein with a 30 G needle. Normal saline was then pumped into the area to remove extravasating blood and help determine cessation of blood flow. Time from injury to the cessation of blood flow was recorded.

Bioflux Microfluidics System

The Bioflux microfluidics experiments were performed as described [175]. Blood was collected as described above from an individual mouse. As shown in (Figure 2.4), a 100 μ L aliquot of whole blood was taken and incubated with 4 U/mL hirudin, 1 mM CaCl_2 , and 0.5 $\mu\text{g/mL}$ DiOC₆. After incubation, the blood was perfused over immobilized collagen (40 $\mu\text{g/mL}$) in a Bioflux microfluidic flow chamber (Fluxion Biosciences, Oakland, CA) at either a shear rate of 35 or 10 dyn/cm^2 . Representative images were taken after post-perfusion washing with PBS/0.5% BSA with a Nikon Eclipse Ti2 inverted microscope at 40X magnification. Images were processed using Fiji ImageJ software and scored based on surface area coverage, morphology, contraction, and multilayer formation.

2.2.12 Subcellular Fractionation of Platelets

This experiment was performed as described in [120]. Washed human platelets were collected and isolated as described above. Final platelet concentration was adjusted to $1 \times 10^9/\text{mL}$ and resuspended in HEPES Tyrode Buffer pH 7.4 with protease inhibitors and 4 mM Na_3VO_4 . Platelets were either held in a resting state or stimulated for 10 minutes with 0.1 U/mL thrombin. After stimulation, the platelets were disrupted by five freeze-

thaw cycles. After the freeze-thaw cycles, plasma membrane proteins were obtained by centrifugation at 100,000 x g for 1 hr at 4 °C. The supernatant (cytosol) was retained while the pellet underwent treatment with 1% Triton X-100 on ice for 45 min. Triton X-100 soluble and insoluble were separated by centrifugation at 100,000 x g for 1 hr at 4 °C. Trichloroacetic acid (TCA) preparation was used to concentrate each fraction and then subjected to SDS-PAGE and western blotting analysis.

2.2.13 Spreading Assay

Human fibrinogen coated slides were prepared by incubating human fibrinogen (50 µg/mL) in filtered 0.9% saline onto Nunc Lab–Tek II 16 well chamber slide (ThermoFisher Scientific) overnight at 4 °C. The slides were washed twice with 1X PBS and then incubated with 1% BSA (denatured at 55 °C for 30 min) for at least 1 hr. Washed mouse platelets were isolated as described and incubated with CellMask Green plasma membrane stain (ThermoFisher Scientific) for 30 min at 37 °C. Final platelet concentration was adjusted to 1×10^8 /mL and 1 mM CaCl₂ and platelet poor plasma (1:100) was supplemented before aliquoting the platelets on the slide. The slides were then placed into a 37 °C incubator for the respective time points (30, 60, 90, and 120 min). After each time point, the spread platelets were fixed using 4% paraformaldehyde (in 1X PBS) and incubated overnight at 4 °C. The next day, the slides were washed twice with 1X PBS and the plastic sealing was removed. The coverslip (24 X 60 mm) was mounted using VectaShield Antifade Mounting Medium (Vector Laboratories Newark, CA). The coverslip was sealed with nail polish and samples were visualized using a Nikon Eclipse E600 microscope using Axiovision software SE64Rel. 4.8.3. Images were processed using Zeiss Zen 3.5 (ZEN lite) software 3.5.093.00002.

2.2.14 Sucrose-Density Gradient Fractionation (Lipid Rafts)

This experiment was performed as described in [120]. Human platelets were isolated and adjusted to 1×10^9 /mL in HEPES Tyrode Buffer pH 7.4. The platelets were then lysed with 2X lysis buffer (50 mM MES (pH 6.5), 300 mM NaCl, 2% CHAPS (3-[(3-Cholamidopropyl) dimethylammonio]-1-propanesulfonate), protease inhibitors, and 4 mM Na_3VO_4). The lysate mixture was then mixed with 80% sucrose to make a 40% sucrose-lysate mixture. This mixture was then put into ultracentrifuge tubes (12 mL; 14 X 89 mm Beckman Coulter) and then 30% sucrose, and 5% sucrose were put sequentially on top of the 40% sucrose-lysate mixture. The tubes were then centrifuged at $200,000 \times g$ at 4°C for 18 hrs. After centrifugation, the samples were collected in 1 mL fractions by peristaltic pump (Minipuls 3; Gilson). Each fraction was concentrated by trichloroacetic acid (TCA) precipitation and then subjected to western blotting.

2.2.15 Immunoprecipitation (IP)-Acyl-Biotinyl-Exchange (ABE)

Human platelets were isolated and adjusted to 1×10^9 /mL in HEPES Tyrode Buffer pH 7.4. The platelets were then pelleted at $850 \times g$ for 8 minutes. The pelleted platelets were then lysed with 2 mL of lysis buffer (4% SDS, 50 mM Tris HCl pH 7.4, and 5 mM EDTA). 20 mM TCEP (tris(2-carboxyethyl) phosphine) is then added to the lysate mixture for 1 hr at 37°C . After the incubation with TCEP, 100 mM NEM (N-Ethylmaleimide) is added for 2.5 hr at 37°C . To isolate the proteins, chloroform-methanol precipitation is used in a (1:4:2:3) ratio with the lysate mixture. After the chloroform-methanol precipitation the pellet was dried at 40°C for 20 min. The dried pellet was resuspended in the 2 mL of the lysis buffer. To biotinylate the sample, 1.33 mM of BMMC-Biotin is added to the lysate mixture along with 1 M HA (Hydroxylamine HCl) to remove palmitate from the cysteines

for 1 hr at RT. A lysate mixture without 1 M HA was used as a negative control. After this chloroform-methanol precipitation was used to isolate the proteins from the lysis buffer. The pellet was dried at 40 °C for 20 min. The dried pellet was then resuspended in 500 µL of buffer (1% SDS, 50 mM Tris HCl pH 7.4, and 5 mM EDTA). To get rid of unbiotinylated proteins, the protein mixture was incubated in streptavidin-agarose beads for 1 hr mixing at RT. To elute the proteins from the beads, 25 mM biotin was added at 95 °C for 5 minutes. If no proteins are coming off the beads an additional 25 mM biotin can be added to wash and elute the remaining proteins. Then 5X SDS buffer was added for 95 °C for 5 minutes. The elution mixture from the beads were subjected to western blotting.

2.2.16 Immunofluorescence Microscopy

The immunofluorescence experiments were performed as described [284]. Coverslips (18x18 mm) were soaked in concentrated nitric acid overnight at RT. On the second day, the coverslips were thoroughly washed with ddH₂O and transferred onto parafilm in a petri dish. A thin layer of Poly-D-lysine (300 µL of 0.1 mg/mL) was placed on the coverslips, and incubated overnight at 4 °C. On the third day, the Poly-D-lysine was removed. Washed platelets were prepared as described above and the concentration of platelets was adjusted to 1x10⁹/mL. They were fixed in suspension for 30 min at RT with paraformaldehyde (2% final; PFA). After fixation, the fixed platelets were added onto the coverslips and incubated overnight at 4 °C. On the fourth day, the unbound platelets were removed, and they were washed once with 1X PBS and post-fixed for 10 min with 2% PFA in 1X PBS. The coverslips were then placed in a 6-well plate and were reduced with 0.1% NaBH₄ for 10 min while shaking at low speed on a rotary mixer (Stovall Life Sciences Inc. NC, USA). After reduction, the coverslips were washed for 5 min 3X with 1X PBS while

shaking at low speed on a rotary mixer (Stovall Life Sciences Inc. NC, USA). The platelets were then permeabilized with 0.2% Triton X-100 in 1X PBS for 15 min. The solution was replaced with a blocking buffer (10% NGS/0.05% Triton X-100 in 1X PBS). After blocking for 90 min, remove the blocking buffer and add the primary antibodies diluted in antibody buffer (5% NGS/0.05% Triton X-100 in 1X PBS) and incubate overnight at 4 °C. On the final day, the primary antibody buffer was removed, and coverslips were washed for 15 min 5X with wash buffer (1% NGS/0.05% Triton X-100 in 1X PBS) at RT. After washing, the coverslips were incubated with secondary antibodies conjugated with fluorophores (1:1000) in antibody buffer (5% NGS/0.05% Triton X-100 in 1X PBS) for 1 hr at RT covered, while shaking. After incubation, the secondary antibody was removed, and the coverslips were washed for 15 min 5X with wash buffer. They were then washed for 5 min with 1 X PBS and post-fixed with 2% PFA for 10 min (no shaking). They were then washed again for 5 min 3X with 1X PBS while shaking. The coverslips were mounted on slides (25 X 75 mm) using Molecular Probes™ Prolong™ Diamond Antifade Mounting media (P46965, Life Technologies, Carlsbad, CA) and cured in the dark for at least 48 hr before imaging. The slides were visualized and imaged using a Nikon Super-Resolution Inverted Microscope S (Schroeder) using software v4.51.01. The microscope was equipped with Stochastic Optical Reconstruction and Structured Illumination Microscopy modalities and fitted with an Apo SR 100X/1.49 NA oil objective (Nikon Ti-E N-STORM/N-SIM) from Nikon Americas Inc. (Melville, New York). Images were processed using NIS-Elements v5.02 N-SIM/STORM software from Nikon Americas Inc., and Adobe Illustrator v26.5.1.

2.2.17 Epifluorescence Microscopy

Mouse platelets were prepared as described above and a 20 μ L aliquot of platelet rich plasma (PRP) was taken and incubated with 1 μ M mepacrine for 30 minutes at RT. After incubation, the PRP was placed on slides (25 X 75 mm) and covered with coverslips (18 x 18 mm) and sealed together. The slides were visualized and imaged using a Nikon Eclipse E600 microscope using Axiovision software SE64Rel. 4.8.3. Images were processed using Zeiss Zen 3.5 (ZEN lite) software 3.5.093.00002.

2.2.18 Data Processing

GraphPad Prism v10.0.2 was used to generate secretion assay plots, thrombosis models survival curves, flow cytometry, aggregation, merged intensity plots, and western blot quantifications. Statistical analyses were computed by GraphPad Prism v10.0.2. In all studies, the p values are as indicated and values less than 0.05 were considered significant.

2.2.19 Study Approval

All animal work was approved by the Institutional Animal Care and Use Committee at the University of Kentucky.

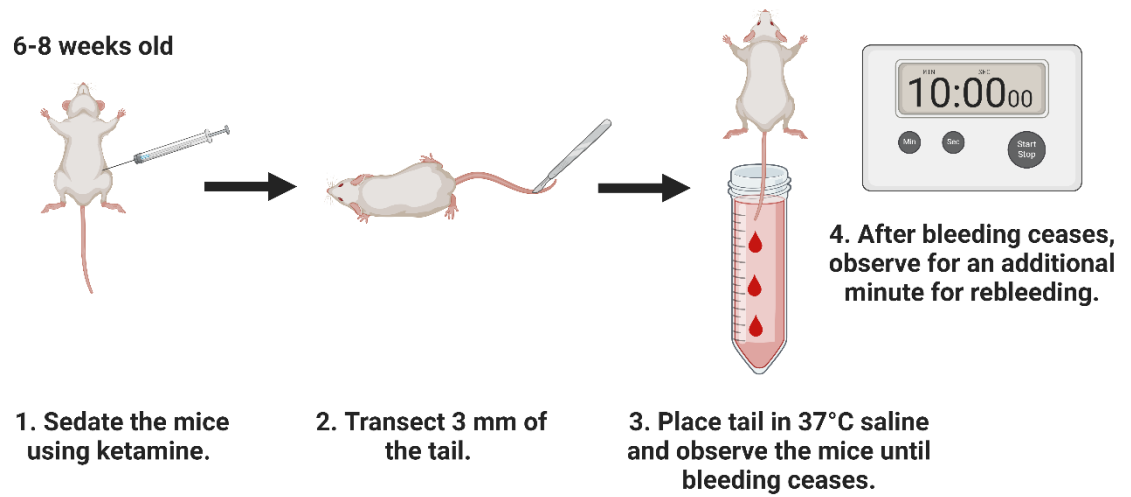


Figure 2.1 Schematic of tail-bleeding assay

In this schematic, we are detailing how the tail bleeding assay was performed. While the mice are sedated, 3 mm of their tail was transected and immediately placed in 37 °C normal saline. The time from transection until bleeding ceased was recorded. After initial cessation of bleeding, the mice were observed for an additional minute for re-bleeding.

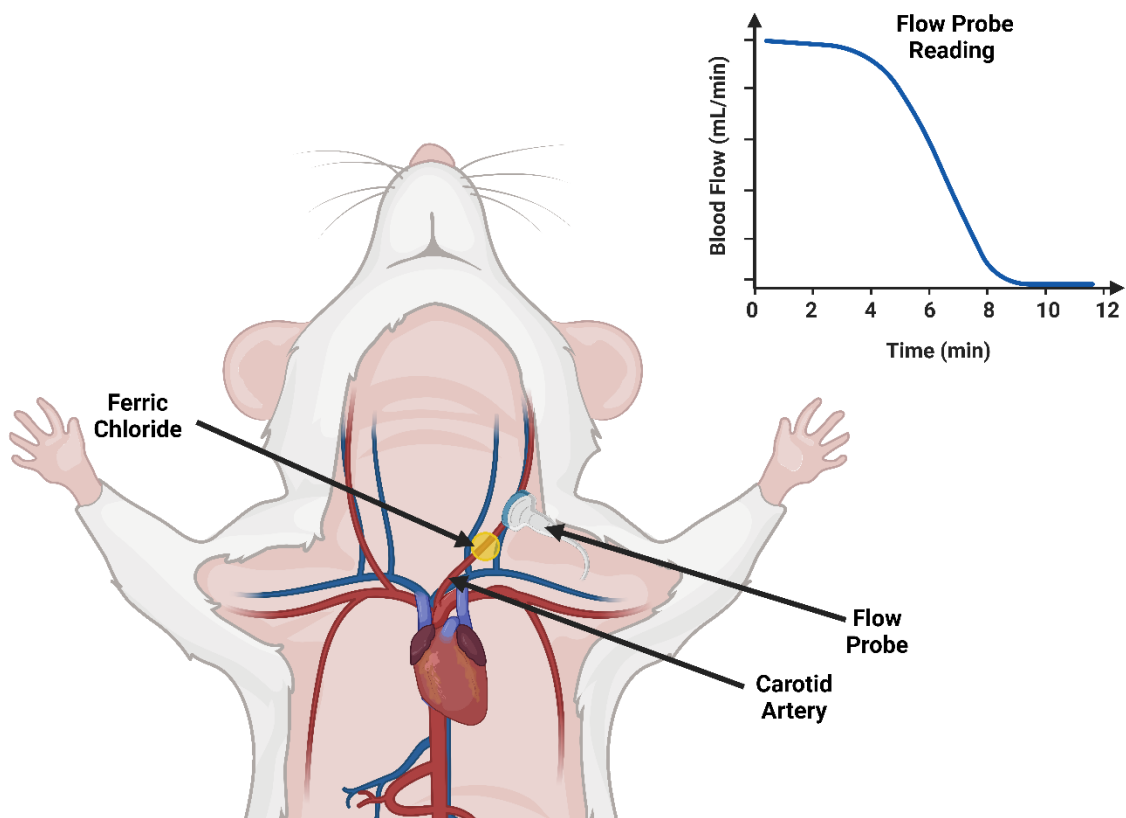


Figure 2.2 Schematic of FeCl₃ carotid artery injury model

In this schematic, we are detailing how the FeCl₃ carotid artery injury model was performed. Once the mouse was sedated a dissecting microscope was used to expose the carotid artery using blunt dissection. The miniature Doppler flow probe was then placed under the carotid artery and adjusted to measure maximum blood flow. After baseline readings, the carotid artery was dried and thrombus formation was induced by placing a filter paper (1 mm diameter) saturated with 7.5% FeCl₃ solution on top of the carotid artery for three minutes. After three minutes, the filter paper was removed and the area was washed with normal saline. The time from removal of filter paper to the formation of an occlusive thrombus was observed as highlighted by the graph.

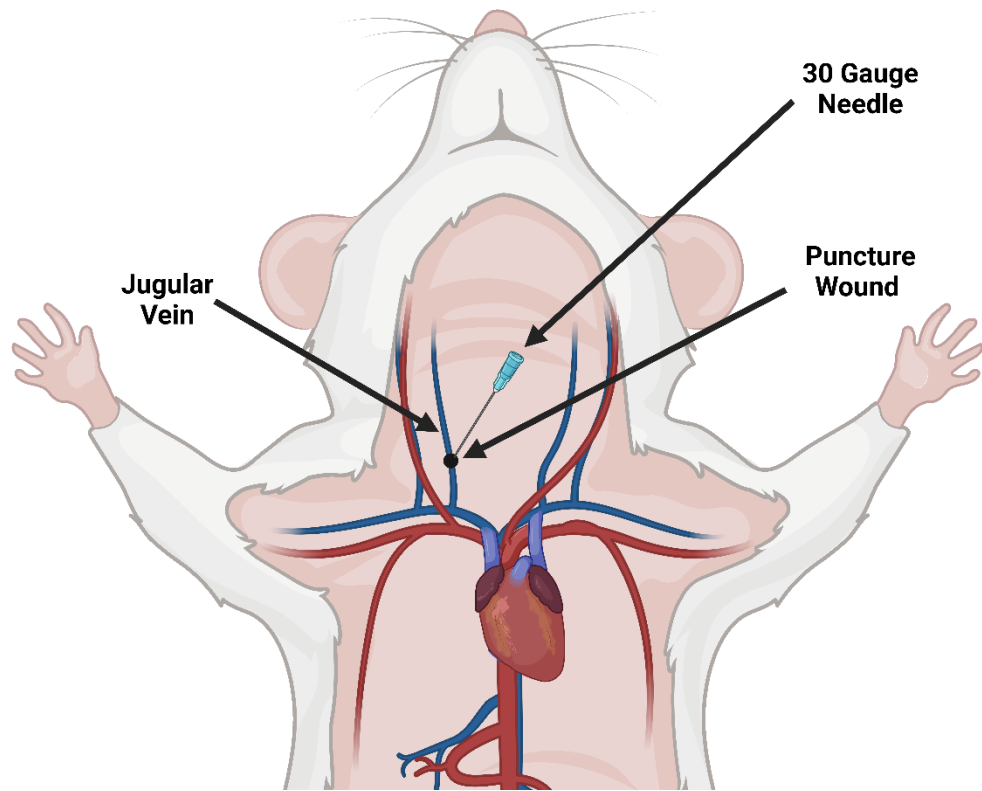


Figure 2.3 Schematic of jugular vein puncture model

In this schematic, we are detailing how the jugular vein puncture model was performed. Once the mouse was sedated a dissecting microscope was used to expose the jugular vein using blunt dissection. Once the jugular vein was exposed, vessel injury was induced by puncturing the jugular vein with a 30 G needle. The time from injury until bleeding cessation was recorded.

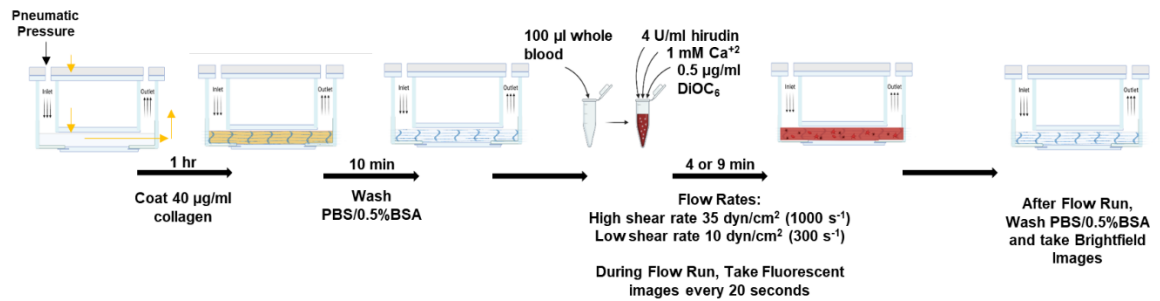


Figure 2.4 Schematic of *ex-vivo* Bioflux microfluidics model

In this schematic, we are detailing how the Bioflux microfluidics experiment were performed. The Bioflux microfluidic chamber was coated with collagen for 1 hr and then washed with PBS/0.5% BSA for 10 minutes. After washing, a 100 μL aliquot of whole blood was taken and incubated with 4 U/mL hirudin, 1 mM CaCl_2 , and 0.5 $\mu\text{g/mL}$ DiOC₆. After incubation, the blood was perfused over immobilized collagen (40 $\mu\text{g/mL}$) in the Bioflux microfluidic flow chamber at either a shear rate of 35 or 10 dyn/cm^2 . Representative images were taken after post-perfusion washing with PBS/0.5% BSA.

CHAPTER 3. ALPHA-SYNUCLEIN IS THE MAJOR PLATELET ISOFORM BUT IS DISEPENSABLE FOR ACTIVATION, SECRETION, AND THROMBOSIS

3.1 Introduction

Platelets play many roles in the vasculature ensuring hemostasis and maintaining vascular integrity. These processes are supported by the various cargo molecules released from the three types of granules in platelets: α , dense, and lysosomes [102, 115]. Granule cargo release is mediated by a family of membrane proteins called Soluble N-ethylmaleimide sensitive factor Attachment Protein Receptors (SNAREs). SNAREs are classified based on their subcellular localization and a charged amino acid at their SNARE domain's center: (v/R, Arg) SNAREs located on the vesicles and (t/Q, Gln) SNAREs located on target membranes [98, 99]. These proteins (v-SNAREs and t-SNAREs) form a transmembrane complex that spans the two bilayers to mediate granule-membrane fusion for cargo release [95, 161]. Data from our laboratory and others have shown that the v-SNARE, VAMP-8, and the t-SNAREs, SNAP-23 and Syntaxin-11, are the dominant v- and t-SNAREs, respectively, needed for platelet secretion [44, 102, 110, 117-119]. Several SNARE regulators have also been identified in platelets. Some, such as Munc13-4, SLP4, Rab27, Exocyst, *etc.*, appear to control granule-plasma membrane docking to improve the efficiency of release [47, 102, 140, 161, 285]. Others, such as Munc18b and STXBP5, serve as chaperones that control when and where the SNAREs interact. Dysfunctions in these regulators have variable effects. Some are essential *i.e.*, Munc13-4, while the loss of others has only a modest effect on release, *i.e.*, Exocyst [47, 285]. Taken together, these data imply that platelet secretion is controlled by sequential protein-protein interactions culminating in membrane fusion and cargo release.

The chaperone mode of SNARE regulation is exemplified by Munc18b and its interaction with Syntaxin-11. Sec1/Munc18 (SM) proteins are needed for cognate syntaxin sorting and serve as a template for the formation of the transbilayer SNARE complex [140, 286]. Chaperones for other classes of SNAREs (*i.e.*, VAMPs and SNAP-23/25s) have been reported but not as definitively characterized. Proteins of interest as potential chaperones are the synucleins. This family, containing α -, β -, γ -synuclein, and synoretin are thought to promote SNARE-complex assembly and affect fusion pore opening and thus cargo egress [176, 196-207]. α -Synuclein is highly expressed in the brain and other tissues, such as heart, skeletal muscle, pancreas, and vascular endothelial cells [100, 101, 184, 287, 288]. Studies have shown that α -synuclein enhances fusion pore opening and docking, and that the N-terminal region is critical for these functions [202, 204, 219, 287]. It is the only isoform expressed in mouse platelets and its abundance (42,300 molecules/platelet) is similar to other elements of the platelet secretory machinery, such as Syntaxin-11 (12,200 molecules/platelet), Munc18b (18,700 molecules/platelet), SNAP-23 (27,500 molecules/platelet), and VAMP-8 (37,800 molecules/platelet) [100-102].

α -Synuclein is most well-known for its pathological role in neurodegenerative diseases, particularly Parkinson disease; but it is less clear how its dysfunction leads to these diseases [218, 219, 230, 287]. Most cases of Parkinson disease are idiopathic, but there are some rare familial cases caused by mutations in α -synuclein including A30P, A53T, E46K, H50Q, and G51D. Affected patients often have increased risks for cerebral microbleeds [220-224]. Studies show that cerebral microbleeds occur more often in Parkinson disease patients that have developed dementia than patients without dementia. This increased risk is associated with cerebral amyloid angiopathy, which affects vascular

integrity potentially leading to the development of microbleeds. Data are inconsistent regarding whether microbleeds occur more often in either the deep or lobar regions of the brain, but there is a clear association between microbleeds and cognitive decline. Whether this bleeding risk is due to vascular defects or hemostatic dysfunction is unclear. Since platelet function is important for controlling microvessel integrity, we sought to determine if α -synuclein contributes to platelet function, specifically in secretion and thrombosis [184, 215, 219, 288].

Although α -synuclein has been suggested to have a role in SNARE-complex assembly and fusion pore opening, its exact molecular role in these processes is unknown. Platelets are a good model to study the function of α -synuclein since it is abundant and the only isoform present [100, 101]. In this project, we analyze the role of α -synuclein using platelets from α -synuclein^{-/-} mice. We found that its deletion caused a modest defect in activation-dependent secretion. Consistent with this modest secretion defect, the α -synuclein^{-/-} mice had no significant bleeding diathesis in the three models tested. Our data suggest that α -synuclein does not play a central role in platelet secretion and is thus either not required for SNARE-complex assembly or is compensated for by another protein or pathway.

3.2 Results

3.2.1 Hematological profile of α -synuclein^{-/-} mice

To probe the role of α -synuclein in thrombosis and hemostasis, we used global α -synuclein^{-/-} mice from Jackson Laboratory and confirmed that α -synuclein was deleted from platelets via western blotting. Platelet biogenesis appeared unaffected since platelet

counts and sizes were similar in knockouts and WT littermate controls (Table 3.1). Although platelets were normal in the α -synuclein^{-/-} mice there was a statistically significant decrease in erythrocyte (RBC) volume 51.7±1.35 fL versus 48.7±1.22 fL (p value <0.0001). There was no significant difference between leukocyte or RBC counts. The differences in erythrocytes were not pursued in this manuscript. While the values in literature are inconclusive and differ, potentially due to the use of different hematological analyzers, there have been reports that α -synuclein is abundant in RBCs. The increase RBC size in α -synuclein^{-/-} mice could be due to some effect on hemoglobin or RBC biogenesis [289-291].

3.2.2 Co-localization of α -synuclein with α and lysosomal granules

To determine the localization of α -synuclein in platelets, we used 3-Dimensional Structured Illumination Microscopy (3D-SIM) to examine immunofluorescence staining (Figure 3.1 A and B). The staining pattern of α -synuclein suggests both a diffuse cytoplasmic and a punctate, potentially granular, distribution. To assess whether α -synuclein is on a granule, we performed colocalization studies with both P-selectin (membrane marker for α -granules) and LAMP-1 (membrane marker for lysosomes). In resting platelets, there was some overlap between LAMP-1 and α -synuclein though incomplete (Figure 3.1A; Pearson correlation coefficient: 0.345 and Mander's overlap: 0.675). Similarly, there was also some colocalization with P-selectin (Figure 3.1B; Pearson correlation coefficient: 0.408 and Mander's overlap: 0.680). Absence of non-specific antibody staining was confirmed in (3.2 A and B). Colocalization studies with endosomal markers (*i.e.*, Rabs) were not done, however, it is possible that α -synuclein could be present on those compartments based on the punctate staining pattern and the lack of complete

colocalization with standard granule markers. We further addressed whether loss of α -synuclein affected dense granules. Given that methods for imaging dense granules are limited, we evaluated dense granule numbers per platelets by vital staining with mepacrine [292]. The average numbers of mepacrine-positive structures were similar in wild-type (4.73 ± 1.74 /platelet; $n=40$ platelets) vs. α -synuclein^{-/-} (4.93 ± 1.86 /platelet; $n = 27$ platelets) platelets. Localization of α -synuclein in platelets was further assessed to determine the extent to which it associated with platelet membranes in either a resting or activated state (Figure 3.1C). Platelets were disrupted by freeze-thaw cycles and cytosolic and membrane fractions were generated by ultracentrifugation. In resting and activated platelets, α -synuclein is present mostly in the supernatant 70% (S₁) and 30% in the pelleted membranes treated with Triton X-100 (S_{TX}). The ratio of α -synuclein in the membrane fractions did not change upon activation with 0.1 U/mL thrombin for 10 min. These data correlate with the immunofluorescence staining (Figures 3.1 A and B) where we see a diffuse cytoplasmic staining of α -synuclein.

3.2.3 α -Synuclein^{-/-} platelets have a mild secretion defect

Surface exposure of P-selectin (α -granules), LAMP-1 (lysosomal granules), and $\alpha_{IIb}\beta_3$ integrin activation expression were assessed in α -synuclein^{-/-} platelets by flow cytometry (Figure 3.3). Platelets were stimulated with thrombin (Figure 3.3 A, E, I), convulxin (Figure 3.3 B, F, J), CRP (Figure 3.3 C, G) or U46619 (Figure 3.3 D, H) for 2 min at various concentrations. In response to 0.1 U/mL thrombin, P-selectin, Jon/A and LAMP-1 expression were unaffected (Figure 3.3 A, E, I). In response to both concentrations of convulxin (100 and 200 ng/mL), there was a slight reduction in P-selectin exposure (Figure 3.3B) and in Jon/A binding that did not reach statistical significance

(Figure 3.3F). There was no significant difference in LAMP-1 exposure (Figure 3.3J). In response to both concentrations of CRP (1 and 10 $\mu\text{g}/\text{mL}$) and U46619 (30 and 1000 nM), there were slight reductions in both P-selectin exposure and Jon/A binding but these did not reach statistical significance (Figure 3.3 C, D, G and H). We further addressed whether receptor levels were affected and there was no change in CD41/61, GPVI, or PECAM in the $\alpha\text{-synuclein}^{-/-}$ platelets (Figure 3.4). These data imply that $\alpha\text{-synuclein}$ plays a minor role in granule secretion. To further define the role of $\alpha\text{-synuclein}$ in granule secretion, we examined agonist- and time-dependent release of cargo from all three granules: dense, α , and lysosomes (Figure 3.5). Dense granule secretion from $\alpha\text{-synuclein}^{-/-}$ platelets, when stimulated for 2 min, with thrombin was slightly decreased $\sim 10\%$ at the various thrombin concentrations (Figure 3.5A). Alpha and lysosomal secretion were comparable to WT platelets (Figure 3.5 B and C). When $\alpha\text{-synuclein}^{-/-}$ platelets were stimulated with 0.1 U/mL thrombin at various time points there was no significant difference in secretion from the dense, α , or lysosomal granules (Figure 3.5 D, E, F). There were no defects in serotonin uptake (dense granule cargo), or the levels of PF4 (α -granule cargo) and β -hexosaminidase (lysosome cargo) in the $\alpha\text{-synuclein}^{-/-}$ platelets (Figure 3.6). These data suggest that $\alpha\text{-synuclein}$ plays only a minor role in platelet secretion and that it may play a subtle role in ITAM signaling pathways leading to integrin activation.

3.2.4 $\alpha\text{-Synuclein}^{-/-}$ platelets have no aggregation or spreading defect

Dense granule release is extremely sensitive and has the fastest release kinetics compared to the other granules. To confirm the slight defect from the secretion assay, we used lumi-aggregometry to analyze aggregation and ATP/ADP release in response to 0.05, 0.025, and 0.0125 U/mL thrombin, and 5 $\mu\text{g}/\mu\text{L}$ collagen. Aggregation was unaffected

(Figure 3.7 A-D). ATP/ADP release was minimally affected in α -synuclein^{-/-} platelets (Figure 3.7 E-H). We also evaluated whether the deletion of α -synuclein could affect spreading on fibrinogen-coated surfaces (Figure 3.8). α -Synuclein^{-/-} platelets spread at similar rates when compared to WT platelets at the respective time points (30, 60, 90, and 120 min). These data imply that the loss of α -synuclein has no significant effects on specific platelet activities.

3.2.5 Deletion of α -synuclein does not affect thrombosis in vivo

We next evaluated how the deletion of α -synuclein affected hemostasis and thrombosis using three injury models: tail-bleeding, FeCl₃-induced carotid injury, and jugular vein puncture (Figure 3.9). Tail-bleeding times for WT mice 313±219 sec (mean ± SD, n=22) and α -synuclein^{-/-} mice 331±227 sec (n=26; p=0.815) were comparable (Figure 3.9A). In the FeCl₃-induced carotid injury model, the average occlusion times were slightly faster for the α -synuclein^{-/-} mice 8.56±7.50 min (n=12) compared to WT mice 11.6±8.55 min (n=13; p=0.252) but it was not statistically significant (Figure 3.9B). In the jugular vein puncture model, the average bleeding times were also similar for both WT mice 77.8±15.0 sec (n=6) and α -synuclein^{-/-} mice 75.3±14.7 sec (n=6, p=0.909) (Figure 3.9C). These data suggest that the slight defect in granule secretion, noted above, is not significant enough to influence hemostasis and thrombosis.

3.2.6 Loss of α -synuclein did not affect the platelet secretory machinery

Semiquantitative western blotting was used to assess the levels of other proteins in the platelet secretory machinery (Figure 3.10). Expression of the v-SNAREs VAMP-2, VAMP-3, VAMP-7, and VAMP-8 were unaffected. The t-SNAREs Syntaxin-11 and SNAP-23 were also unaffected. We examined the t-SNARE chaperone, Munc18b, and

Cysteine String Protein- α (CSP α), which interacts with α -synuclein, and both were unaffected. Thus, the loss of α -synuclein had no effect on any of the platelet secretory machinery examined.

3.3 Discussion

In this chapter, we examined the platelet and hemostatic phenotype of animals lacking α -synuclein, since reports had suggested patients with Parkinson's disease might have a bleeding diathesis [220-224, 293]. We confirmed the deletion of the protein in platelets, but its deletion had no significant effects on the other SNARE proteins examined. Secretion from platelets lacking α -synuclein was modestly defective. Consistently, hemostasis was unaffected in the tail-bleeding model and thrombosis was unaffected when examined on both the arterial (FeCl₃ carotid artery injury model) and venous (jugular vein puncture model) vasculature. From our data, α -synuclein plays only a limited role in platelet secretion and hemostasis.

Previous studies suggested roles for α -synuclein in platelet activation and in endothelial cell release of von Willebrand Factor (vWF) [214, 215]. Addition of exogenous α -synuclein to platelets inhibited ionomycin- and thrombin-induced α -granule release but had no effect on dense granule or lysosome release [215]. This inhibition was dose dependent but not time or temperature dependent (working at 4, 25, and 37 °C). Mutant forms of α -synuclein, lacking N or C-terminal domains were without effect. In contrast to our data in Figure 3.1, exogenous α -synuclein was found associated with the platelet cytoskeleton and there was no staining of granules. In HUVEC cells exogenous α -synuclein and its overexpression inhibited release suggesting that α -synuclein was a

negative regulator of Weibel-Palade Bodie secretion [214]. In other studies, platelet function was examined in a multimerin 1/ α -synuclein double-deficient strain [213]. Platelet adhesion and thrombus formation were reduced and partially rescued when multimerin was added back. The authors did not fully determine if the defects were due to the loss of multimerin or α -synuclein; however, given the multiple roles of multimerin in promoting collagen and von Willebrand factor binding, it is difficult to discern whether α -synuclein has any independent role in platelets.

The molecular mechanisms of α -synuclein's physiologic function remain unclear. Several reports suggest it assists in SNARE-complex assembly, vesicle docking, fusion pore opening, or as a SNARE-chaperone [44, 176, 196-207]. Platelets offer a unique system to probe the role of α -synuclein since they have activation-dependent secretion from three different compartments and there are clear *in vitro* and *in vivo* outcomes (*e.g.*, bleeding, Figure 3.10) if secretion is defective. Additionally, platelets contain only one synuclein isoform so the likelihood of confounding compensatory activity from another isoform is limited [100, 101, 184]. Overall, our data suggest only a minimal role for α -synuclein; however, our experiments do have limitations. In neurons, α -synuclein acts as a chaperone for VAMP-2 and when deleted neuronal SNARE-complex assembly is reduced [198]. If α -synuclein is a v-SNARE chaperone, specific for a single VAMP, its importance may be masked by the fact that platelets contain at least 5 different VAMPs, which are functional in platelet secretion (VAMP-2, -3, -7, -8, Ykt6; Joshi et al in preparation) [102, 115]. Thus, a VAMP-specific role might be compensated for by a different VAMP that does not need its chaperone activity. It should be noted that loss of α -synuclein did not affect the levels of any of the VAMPs examined (Figure 3.10).

α -Synuclein is highly abundant in both the brain and platelets suggesting it plays a critical role, but its function is still unknown. Mutant forms of the protein have been linked to neurodegenerative diseases, *e.g.*, Parkinson disease, due in part to their ability to form potentially toxic aggregates. These patients have an increased risk of cerebral microbleeds and developing deep vein thrombosis (DVT) [220-224]. These risks also correlate with dementia. Together these symptoms and data might suggest a physiological role for α -synuclein in platelet function that is dysregulated by the mutant forms. Our data show that the complete loss of the protein does not cause significant platelet dysfunction. However, α -synuclein could play a role in endothelial cells and when mutated could cause a defect in vascular integrity that precipitates bleeding or DVT risks [214, 288]. Further analysis with patient samples will be needed to fully assess this possibility.

The importance of the different v-SNAREs to platelets has been assessed by manipulating them in various mouse strains and measuring how they contribute individually or in combination to platelet granule secretion [115]. In this study we have used the same approach to assess whether a purported v-SNARE regulator/chaperone, α -synuclein, is critical for platelet secretion and function. Overall, our data suggest that this protein is not essential for platelet secretion or function. Loss of α -synuclein did not affect hemostasis in three injury models and had only a modest effect of dense granule secretion. Thus, our data do not directly support a role for α -synuclein in platelets.

Table 3.1 Hematological parameters for α -Synuclein^{-/-} mice

Parameter	WT (C57Bl/6J)	α-Synuclein^{-/-}	p Value
Erythrocytes			
Erythrocytes (M/ μ L)	8.38 \pm 0.455	8.31 \pm 0.286	0.222
MCV (fL)	48.7 \pm 1.22	51.7 \pm 1.35	<0.0001
Hemoglobin (g/dL)	12.3 \pm 0.744	12.8 \pm 0.417	0.0290
MCH (pg)	14.6 \pm 0.354	15.4 \pm 0.275	<0.0001
MCHC (g/dL)	30.0 \pm 0.600	29.4 \pm 1.79	0.268
Reticulocytes (K/ μ L)	404 \pm 100	411 \pm 101	0.811
Platelets			
Platelets (K/ μ L)	722 \pm 152	774 \pm 153	0.555
MPV (fL)	6.61 \pm 1.16	6.70 \pm 1.02	0.608
Leukocytes			
WBC (K/ μ L)	9.68 \pm 2.69	8.53 \pm 1.91	0.217

Results are the means \pm SD and are compared by using the unpaired student *t* test (complete blood count: WT n=15 and α -synuclein^{-/-} n=13). Abbreviations: MCV: mean corpuscular volume, MCH: mean corpuscular hemoglobin, MCHC: mean corpuscular hemoglobin concentrations, MPV: mean platelet volume, WBC: white blood cells.

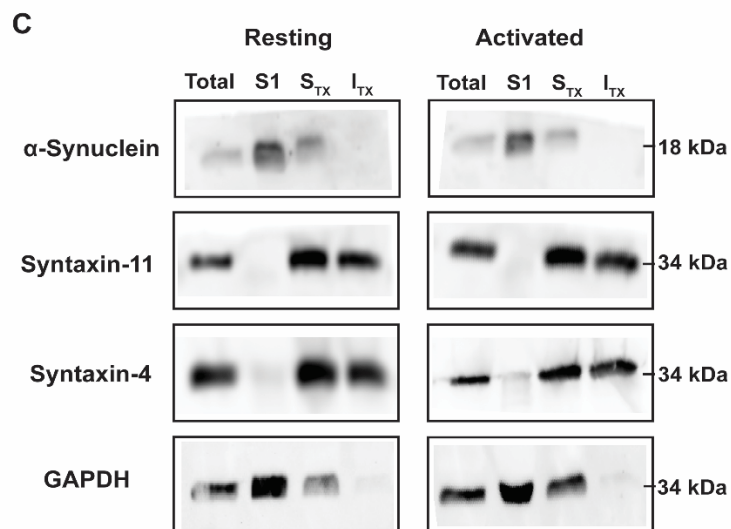
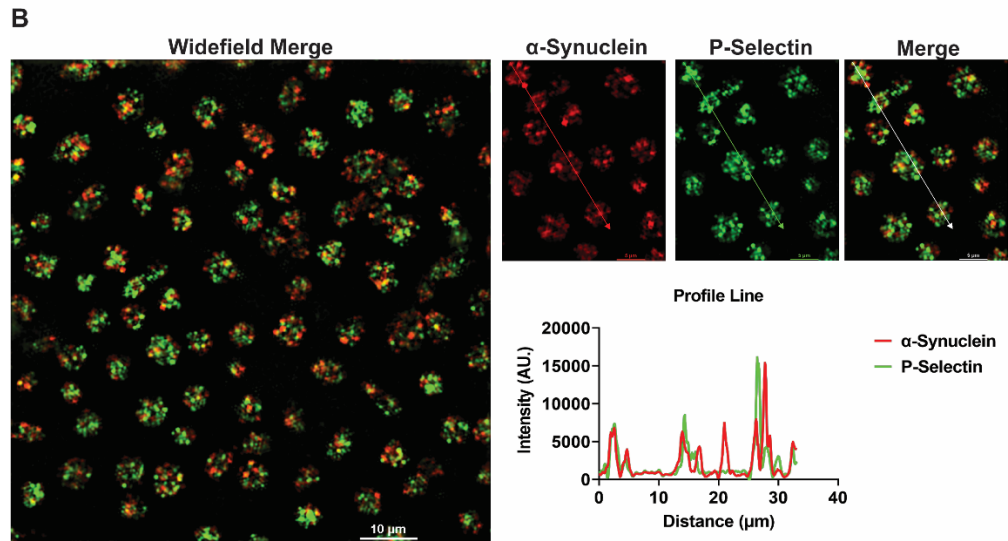
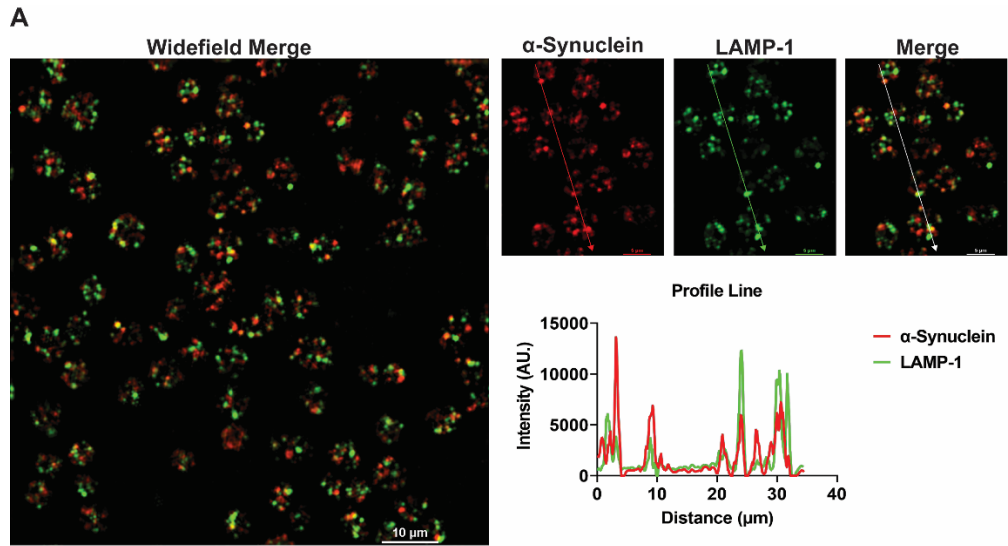


Figure 3.1 α -Synuclein is present on both lysosomes and α -granules

(A) WT platelets were immunostained for α -synuclein (red) and LAMP-1 (green) and imaged by using 3-Dimensional structured illumination microscopy (3D-SIM). The white lines in the merged images indicate where the profile line analyses were performed. Profile line analyses are shown below the images. (B) WT platelets were immunostained for α -synuclein (red) and P-selectin (green). Scale bar: 10 μ m for widefield merge images; 5 μ m for cropped images. (C) Samples were prepared from washed human platelets subjected to five thaw-freeze cycles and centrifuged to separate membrane and cytosol (S1) fractions. The pellet fraction was treated with 1% Triton X-100 to obtain Triton X-100 soluble (S_{TX}) and Triton X-insoluble (I_{TX}) fractions which were separated by ultracentrifugation. The fractions were analyzed by SDS-PAGE and probed by Western blotting with the indicated antibodies. All data are representative of 2 independent experiments.

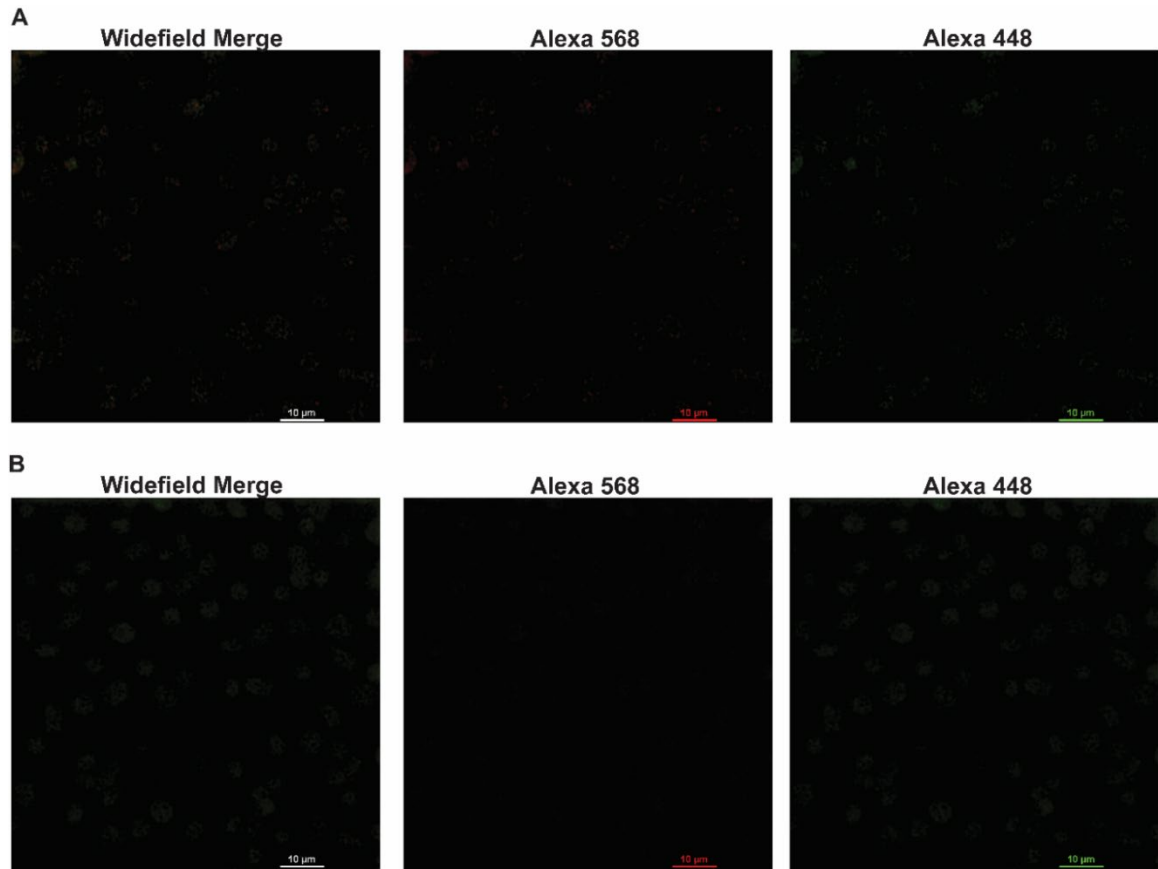


Figure 3.2 Control slides for immunofluorescence experiments

(A) WT platelets were immunostained for Alexa 568 goat anti-rabbit secondary antibody (red) and Alexa 488 goat anti-rat secondary antibody (green) with no primary antibodies and imaged by super-resolution microscopy. These are representative control images from the α -synuclein (red) and LAMP-1 (green) experiment. (B) WT platelets were immunostained for Alexa 568 goat anti-rabbit secondary antibody (red) and Alexa 488 goat anti-rat secondary antibody (green). These are representative control images from the α -synuclein (red) and P-selectin (green) experiment. Scale bar: 10 μ m.

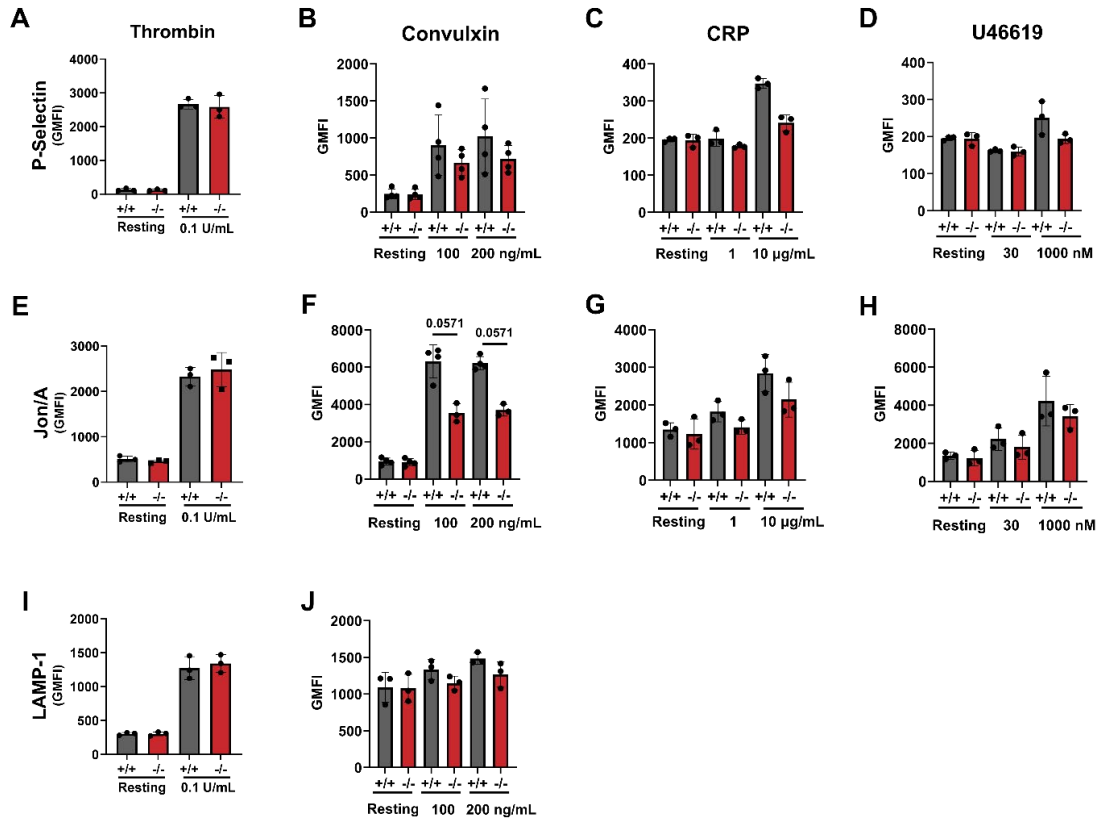


Figure 3.3 α -Synuclein^{-/-} platelets have near normal platelet receptor levels and activation

Washed platelets (5×10^7 /mL) from WT and α -synuclein^{-/-} mice were stimulated with 0.1 U/mL thrombin (A, E, I), convulxin (B, F, J), CRP (C, G), and U46619 (D, H) for two minutes and then incubated with FITC anti-P-selectin (A-D), PE-conjugated Jon/A (E-H), or PE-conjugated LAMP-1 (I-J) antibodies for 20 min at 37 °C. Fluorescent intensities were measured by flow cytometry. Shown are representative data and geometric mean fluorescent intensity (GMFI) (mean \pm standard error of the mean) of 3 independent experiments. Statistical analyses were performed using the unpaired Student *t* test.

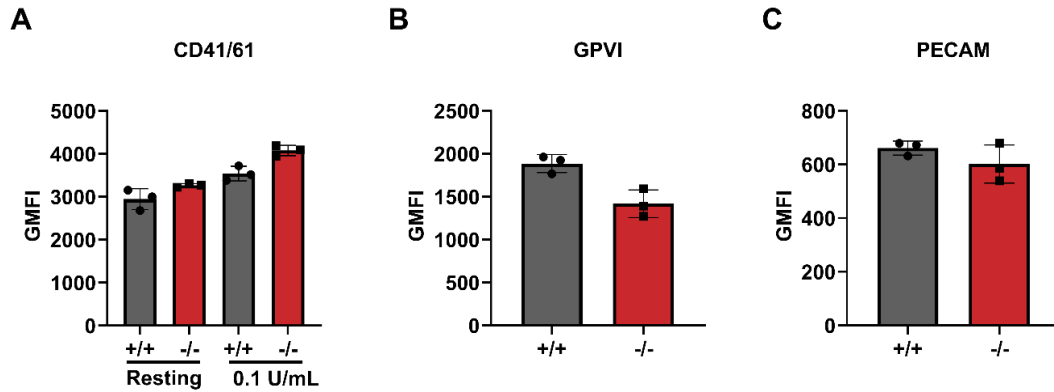


Figure 3.4 α -Synuclein^{-/-} platelets have normal receptor levels

Washed platelets ($5 \times 10^7/\text{mL}$) from WT and α -synuclein^{-/-} mice were resting or stimulated with 0.1 U/mL thrombin for two minutes and then incubated with FITC anti-CD41/61 (A), FITC-conjugated GPVI (B), or FITC-conjugated PECAM antibodies for 20 min at 37 °C. Fluorescent intensities were measured by flow cytometry. Shown are representative data and geometric mean fluorescent intensity (GMFI) (mean \pm standard error of the mean) of 3 independent experiments. Statistical analyses were performed using the unpaired Student *t* test.

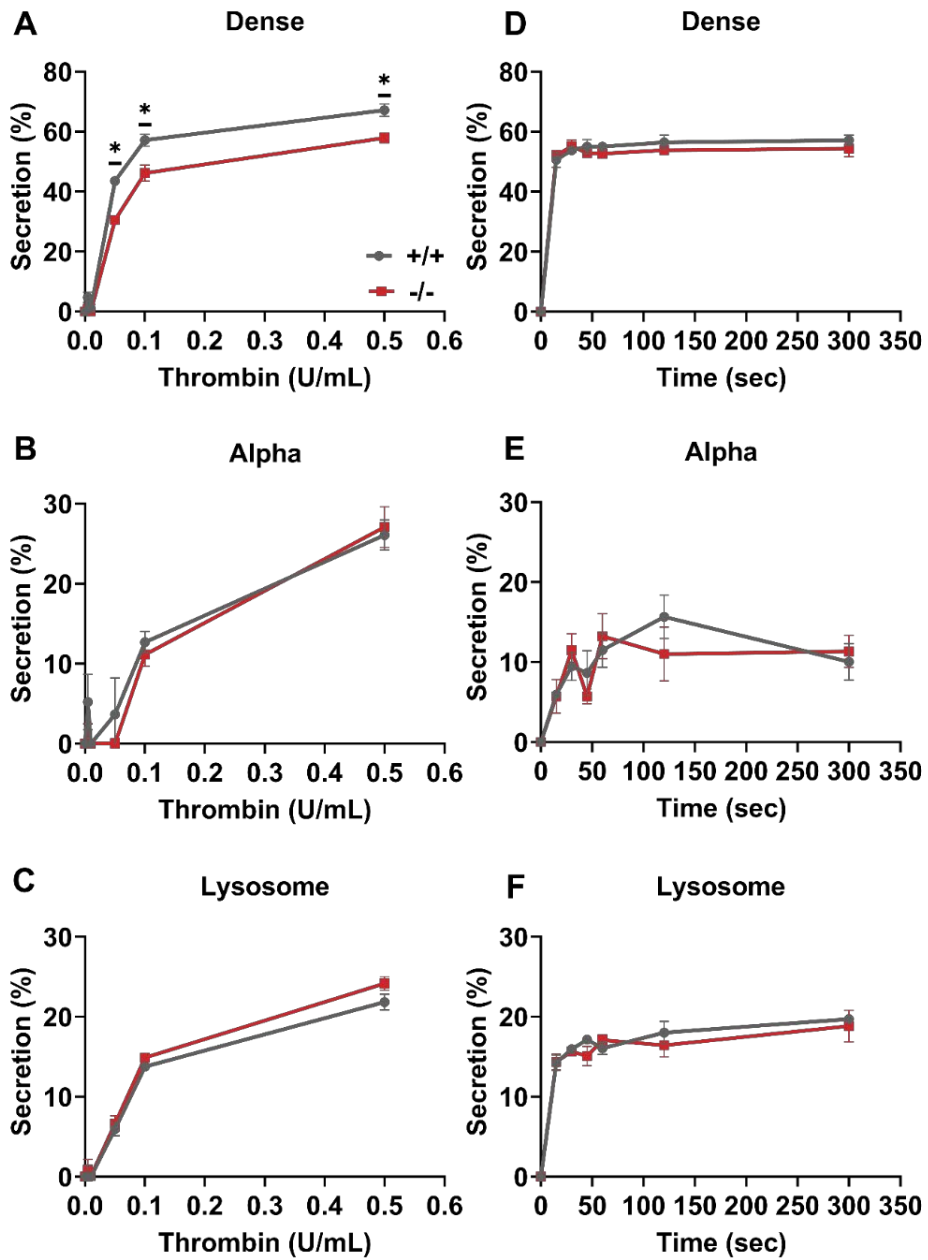


Figure 3.5 α -Synuclein^{-/-} platelets have a mild serotonin secretion defect

Washed platelets ($2.5 \times 10^8/\text{mL}$) were either stimulated with various thrombin concentrations or for different time points and secretion was measured from each granule type in WT and α -synuclein^{-/-} platelets. (A, D) Dense granule release, (B, E) α -granule release, and (C, F) lysosomal release. (A-C) For the thrombin dose-response experiment, platelets were stimulated for 2 min with the indicated concentrations of thrombin. (D-F) For the time-course experiments, platelets were stimulated with 0.1 U/mL thrombin for the indicated times. Data are mean \pm standard error of the mean of triplicate measurements and are representative of ≥ 4 independent experiments. Statistical analyses were performed using two-way ANOVA multiple comparisons.

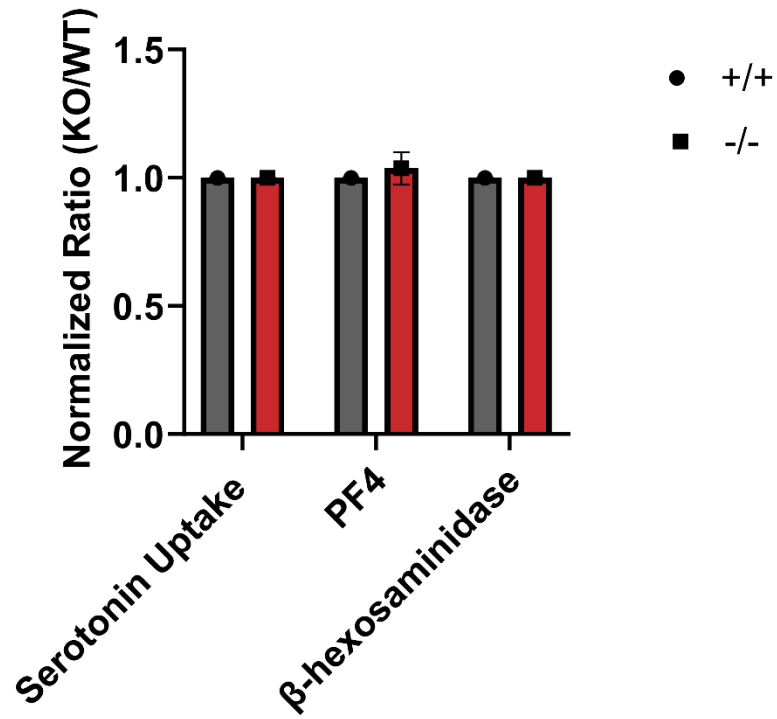


Figure 3.6 α -Synuclein^{-/-} platelets have normal granule cargo levels

Serotonin uptake, PF4, and β -hexosaminidase levels were measured from secretion kinetic experiments. Data are mean \pm standard error of the mean of triplicate measurements and are representative of 3 independent experiments. Statistical analyses were done using the averages of the technical replicates and performed using the Wilcoxon signed rank test.

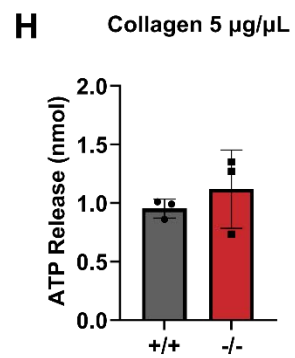
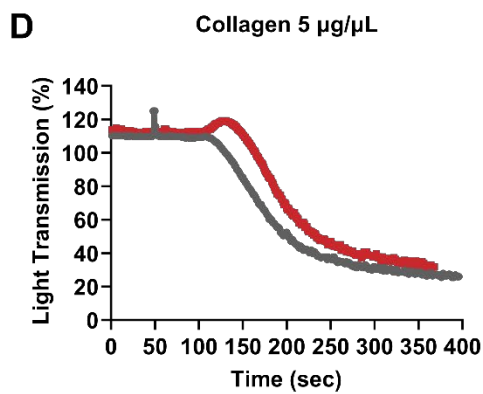
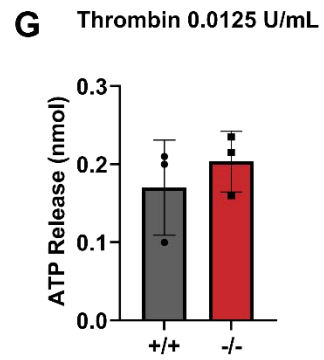
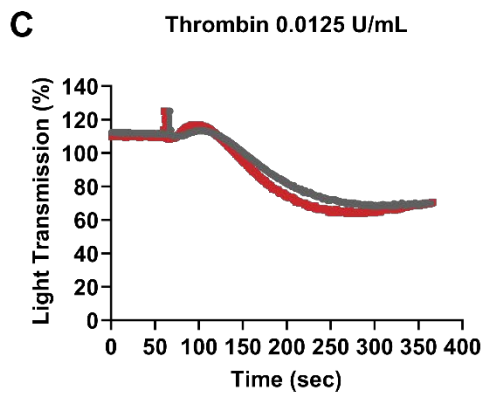
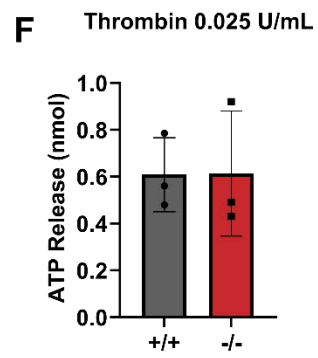
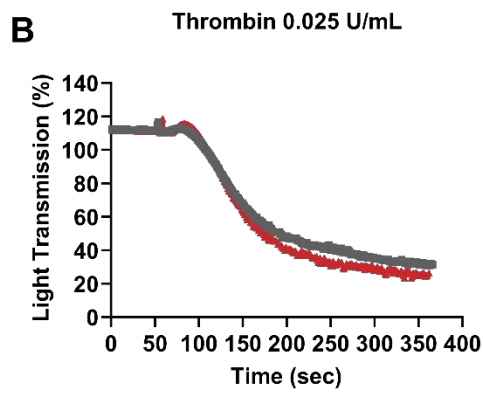
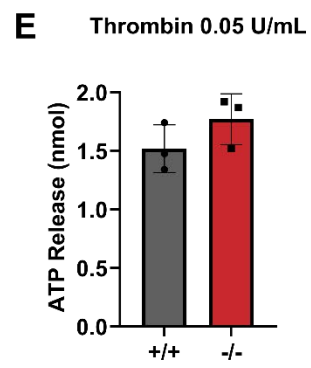
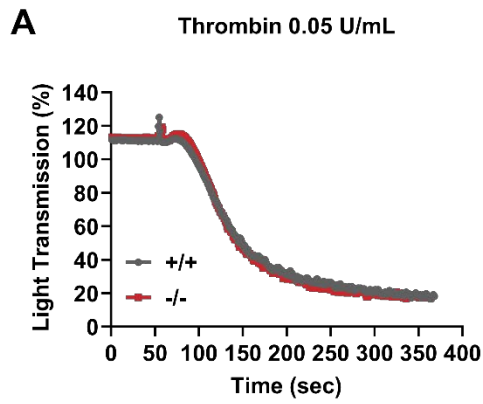


Figure 3.7 α -Synuclein^{-/-} platelets have normal aggregation and ATP secretion

Aggregation and ATP release were monitored simultaneously in a lumi-aggregometer. Washed platelets (3×10^8 /mL) from WT (gray traces) and α -synuclein^{-/-} (red traces) were stimulated with 0.05 U/mL thrombin (A), 0.025 U/mL thrombin (B), 0.0125 U/mL thrombin (C), or (D) 5 μ g/ μ L collagen. (E-H) ATP/ADP release was measured from the respective conditions and were graphed as mean \pm SD. Statistical analyses were performed using the unpaired Student *t* test.

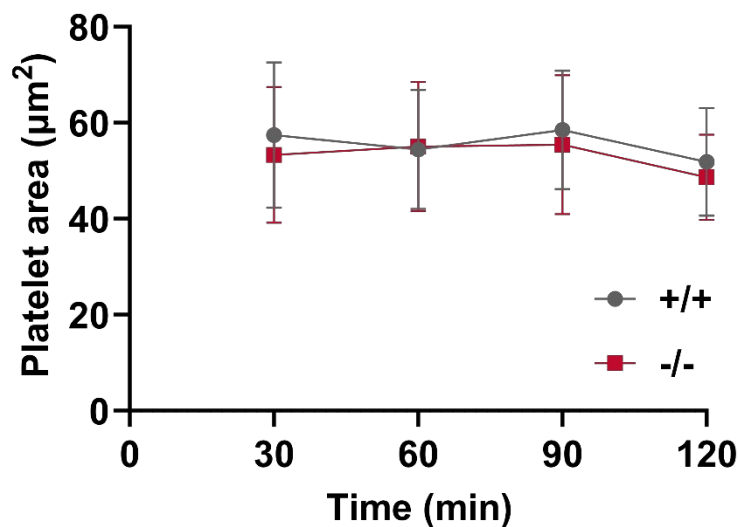


Figure 3.8 α -Synuclein^{-/-} platelets do not have a spreading defect

Washed platelets ($1 \times 10^8/\text{mL}$) from α -synuclein^{-/-} and WT mice were allowed to adhere and spread on fibrinogen-coated coverslips. At the respective timepoints, the platelets were fixed and imaged for analysis. For each time point, >50 platelets were measured for quantification. Data are mean \pm standard error. Statistical analyses were done using two-way ANOVA multiple comparisons.

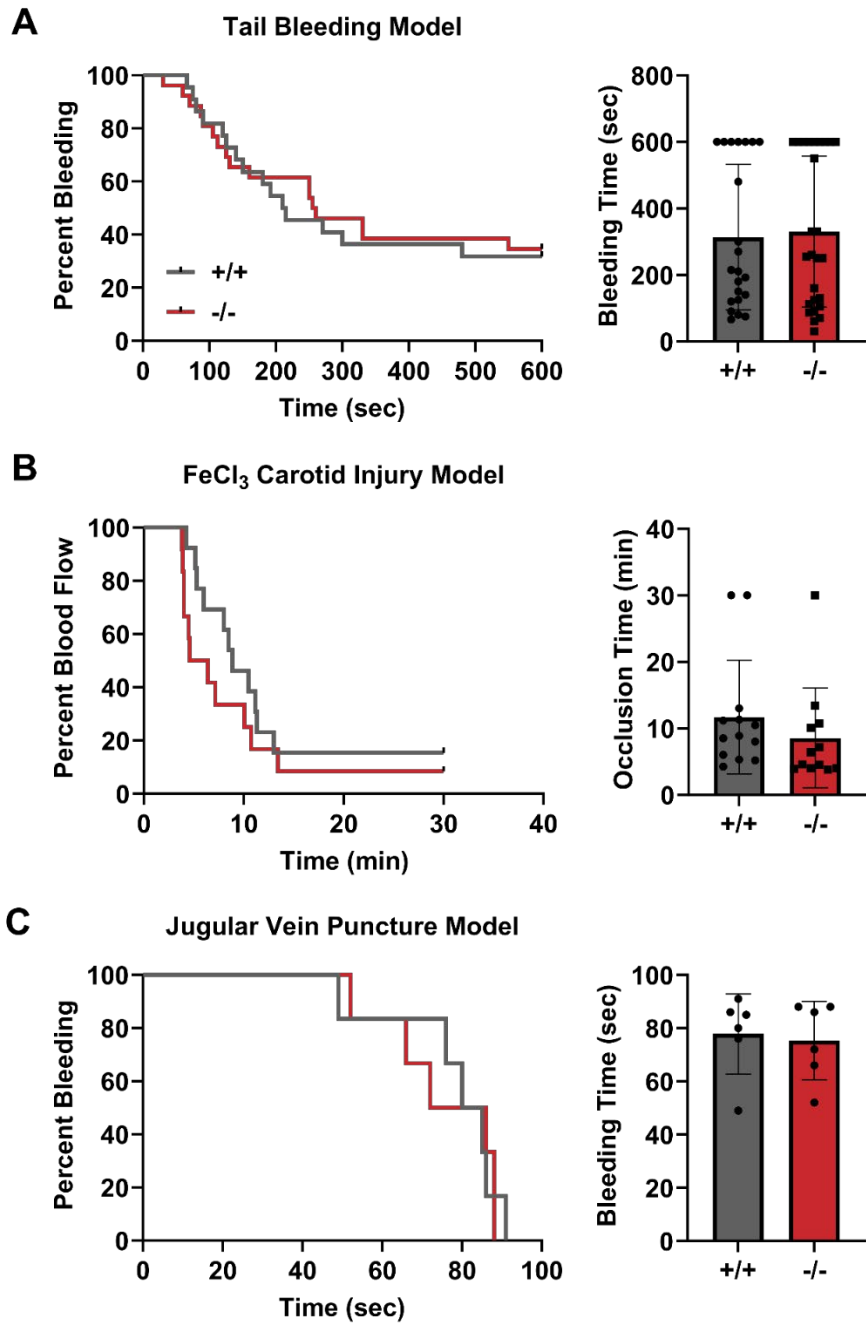


Figure 3.9 α -Synuclein^{-/-} mice have normal hemostasis and thrombosis

Surgeries were performed to analyze thrombus formation in different contexts. (A) Tail-bleeding (n=22 WT and n=26 α -Synuclein^{-/-} mice), (B) FeCl₃ model (n=13 WT and n=12 α -synuclein^{-/-} mice), and (C) Jugular model (n=6 WT and n=6 α -synuclein^{-/-} mice). Statistical analyses were done using the Kaplan-Meier method using the log-rank comparison test.

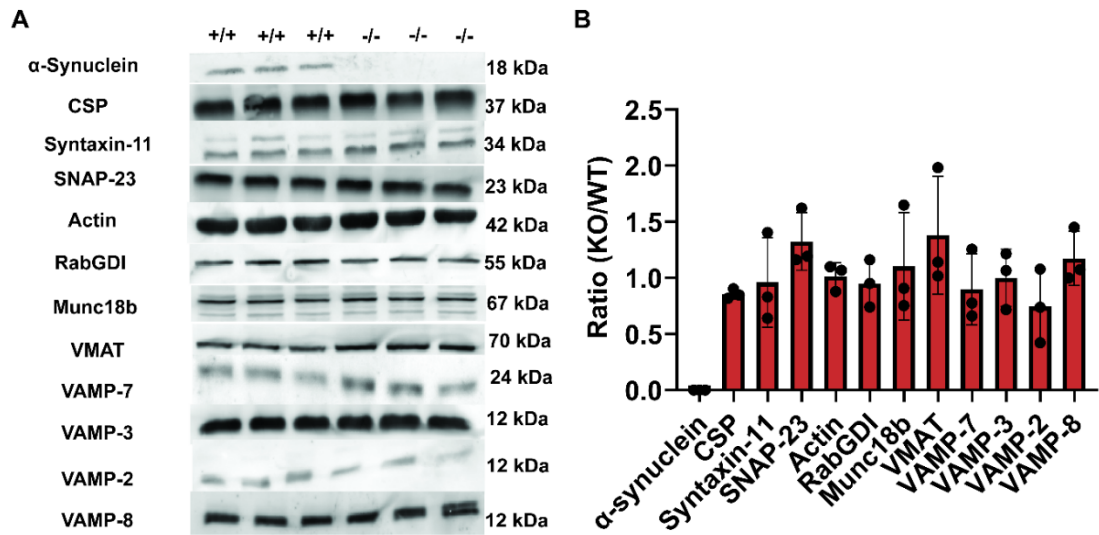


Figure 3.10 Platelet secretory machinery protein levels in α -synuclein^{-/-} platelets are normal

(A) Washed platelets (5×10^7 platelets per lane) were prepared from α -synuclein^{-/-} and WT mice ($n=3$), and the indicated proteins were probed by western blotting. Data are representative of the three independent experiments and 3 individual mice were used for biological replicates for both WT and α -synuclein^{-/-} mice. α -Synuclein, CSP α , SNAP-23, and VAMP-8 were normalized using Rab GDI a loading control. VMAT and VAMP-3 were normalized using Syntaxin-11 a loading control. Munc18b, VAMP-7, and VAMP-2 were normalized using Actin a loading control. (B) Quantification of protein levels was performed using ImageQuantTL, and data was plotted as the ratio of α -synuclein^{-/-} mice over WT mice. Statistical analyses were done using the averages of the technical replicates and performed using the paired Student *t* test.

CHAPTER 4. UNCOVERING THE ROLE OF CYSTEINE STRING PROTEIN-ALPHA IN PLATELET SECRETION

4.1 Introduction

Platelets are involved in numerous processes; however, their key role is in maintaining vascular hemostasis. Platelets secrete a wide variety of molecules to modulate the vascular microenvironment from their three main granules: dense, α , and lysosomes [17, 102]. Defects in cargo release from these granules result in a myriad of problems often resulting in bleeding diatheses or other pathologies [34, 35, 51]. Further, manipulation of platelet secretion, at least genetically, appears to lessen the formation of occlusive clots [109, 115]. Therefore, gaining insight into the mechanisms and regulation of platelet exocytosis is crucial for a more comprehensive understanding of how platelets contribute to thrombosis and hemostasis.

Platelets mediate granule cargo release using a family of proteins called Soluble N-ethylmaleimide sensitive factor Attachment Protein Receptors (SNAREs). SNAREs are categorized based on their subcellular localization and a charged amino acid at the central region of their SNARE domain: (v/R, Arg) SNAREs on the vesicles and (t/Q, Glu) SNAREs on the target membranes [94, 98, 99]. The SNAREs come together from opposing membranes and form a transmembrane complex to mediate membrane fusion and granule-cargo release. Findings from our laboratory and others have demonstrated the importance of the roles of VAMP-8, Syntaxin-11, and SNAP-23 in platelet exocytosis [44, 45, 115-117]. Understanding the regulation of platelet secretion is ongoing, with some proteins, including Munc18b and Munc13-4, shown to be essential while the loss of other proteins, like α -synuclein, has only had modest effects on cargo release [44, 47, 186]. The modest

effect of α -synuclein on platelet function has led us to investigate its interacting protein Cysteine String Protein- α (CSP α) because little is known about its effects on platelet exocytosis.

CSP α /DNACJ5/CLN4 is a member of the CSP family which contains CSP α , CSP β , and CSP γ . This protein family belongs to the DNAJ/Hsp40 family of co-chaperones [130, 255]. CSP α is highly expressed in the brain and other cells specialized for exocytosis such as lymphocytes while CSP β and CSP γ , originally thought to be testis specific, are present in many tissues as well [130, 252-254]. CSP α is known to form a chaperone complex with Hsc70 and small glutamine rich tetratricopeptide repeat protein (SGT) [96, 260, 261]. Studies have shown that CSP α is important for promoting SNARE-complex assembly by acting as a chaperone for, SNAP-25, because mice that lack CSP α have a shortened lifespan of ~60 days and experience progressive neurodegenerative symptoms [252, 261, 263-265, 294]. CSP α also appears to have a unique relationship with α -synuclein [199]. Studies in CSP α ^{-/-} mice showed that adding transgenic α -synuclein back into these mice rescued SNARE-complex assembly levels and prevent further neurodegeneration. However, CSP α overexpression in 1-120h α Syn mice reduced α -synuclein aggregation and rescued dopaminergic neuron release [266].

CSP α /DNACJ5/CLN4 is associated with adult-onset neuronal ceroid lipofuscinosis (ANCL), and linked to other neurodegenerative diseases, including Parkinson, Alzheimer, and Huntington disease [136, 137, 269-272]. It is not exactly clear how CSP α dysfunction leads to these diseases. ANCL is a part of the neuronal ceroid lipofuscinoses (NCL) disease family, which is the most prevalent neurodegenerative lysosomal storage disorder. The main characteristic of this family is ceroid accumulation and progressive neuron death.

ANCL is a genetically inherited disease that has been shown to be caused by mutations in CSP α (*i.e.*, L115R, L116 Δ , and C124_C133duplication) [136, 137, 269, 272-276]. Patients with ANCL present with a variety of neurologic symptoms, yet none have been reported to have bleeding diatheses. On a molecular level, when CSP α is deleted, there is a significant reduction in the t-(Q_{bc})-SNARE in mouse brain and SNARE complex formation is reduced [261, 263, 270]. However, its molecular mechanism remains unclear and its role in platelet function is untested.

Regarding platelet function, the role of CSP α in endo/lysosome function is of interest since platelet granules are lysosome- and endosome-related organelles. Platelet granule-related disease such as Hermansky-Pudlak (HPS), Chediak-Higashi (CHS), Griscelli (GS), and Gray Platelet (GPS) syndromes are due to disruptions in dense or α -granules [24, 34, 36, 38, 49, 51, 52, 55, 56, 153]. This, together with our recent data on the role of α -synuclein in platelets, led us to examine the role of CSP α in platelet function and hemostasis [186]. We found that the deletion of CSP α results in defects in both α and dense granule secretion. Consistent with the defects, CSP α ^{-/-} mice had a significant tail bleeding defect and a defective thrombus formation in a low-shear microfluidics chamber. In response to the GPVI specific agonist convulxin, CSP α ^{-/-} platelets had reduced α IIB β 3 activation and reduced resting GPVI levels. Colocalization studies in platelets determined that CSP α has a punctate granular distribution and is present on both α and lysosomal granules. Taken together, our data demonstrates an important role for CSP α in platelet secretion and thrombosis.

4.2 Results

4.2.1 CSP $\alpha^{-/-}$ mouse hematology

To examine the role of Cysteine String Protein- α (CSP α) in thrombosis and hemostasis, we used global CSP $\alpha^{-/-}$ mice. Platelet biogenesis was unaffected since platelet counts and sizes in CSP $\alpha^{+/-}$ and CSP $\alpha^{-/-}$ mice were similar to wild-type (Table 4.1). In contrast, erythrocytes and leukocyte populations were affected in the CSP $\alpha^{-/-}$ mice. There was a significant decrease in erythrocyte (RBC) volume in the CSP $\alpha^{-/-}$ mice 45.2 ± 2.68 fL vs. 50.8 ± 1.44 fL in the CSP $\alpha^{+/+}$ mice (p value 0.0118), which was also seen in CSP $\alpha^{+/-}$ mice (p value 0.0040). There was also an increased number of circulating reticulocytes in the CSP $\alpha^{-/-}$ mice 470 ± 110 K/ μ L vs. 335 ± 36.2 K/ μ L in the CSP $\alpha^{+/+}$ mice (p value 0.0230) suggesting that there may be a high RBC turnover rate. White blood cell counts were decreased in the CSP $\alpha^{-/-}$ mice 4.80 ± 1.90 K/ μ L vs. 10.7 ± 3.16 K/ μ L in CSP $\alpha^{+/+}$ mice (p value 0.0080), which was also significant in CSP $\alpha^{+/-}$ mice (p value 0.0337). When examined further, we found a decrease in the lymphocyte population in CSP $\alpha^{-/-}$ mice 3.65 ± 2.00 K/ μ L vs. 9.21 ± 1.99 K/ μ L in CSP $\alpha^{+/+}$ mice (p value 0.0054). A similar reduction was noted in CSP $\alpha^{+/-}$ mice (p value 0.0142). The monocyte population was also reduced in CSP $\alpha^{-/-}$ mice 0.052 ± 0.0249 vs. the CSP $\alpha^{+/-}$ mice 0.197 ± 0.139 (p value 0.0089) or wild-type. These differences in erythrocyte volume and lymphocyte and monocyte populations were not pursued in this manuscript, but CSP α is abundant in those cells so its deletion could affect their biogenesis or function.

4.2.2 Loss of CSP α does not affect the platelet secretion machinery levels

We first confirmed that CSP α protein was absent from platelets in CSP $\alpha^{-/-}$ mice via western blotting (Figure 4.1). Western blotting was used to probe for other proteins of the platelet secretory machinery and expression of v-SNARE, VAMP-8 and the t-SNAREs Syntaxin-11 and SNAP-23 were found to be unaffected. α -Synuclein, a CSP α interactor, was also unaffected as was the vesicle monoamine transporter (VMAT). Given that brain SNAP-25 levels were decreased in CSP $\alpha^{-/-}$ mouse brain, we were surprised to find that SNAP-23 levels were unchanged in platelets [199, 261, 263]. We confirmed this in CSP $\alpha^{-/-}$ brain and further showed that brain SNAP-23 was also reduced (Figure 4.2). In conclusion, we confirmed that the deletion of CSP α does result in a reduced SNAP-23 and SNAP-25 levels in the brain but not in platelets.

4.2.3 CSP $\alpha^{-/-}$ platelets have defective dense and α -granule secretion

The low amounts of blood recovered from and the small size of the CSP $\alpha^{-/-}$ mice limited the assays available to assess platelet secretion and activation. We used cytometry and assessed the surface exposure of P-selectin and LAMP-1 as metrics of α -granule and lysosome secretion. $\alpha_{IIb}\beta_3$ integrin surface expression and activation (Jon/A binding) were also measured (Figure 4.3). Platelets were stimulated with either 0.1 U/mL thrombin (Figure 4.3 A, B, C, D) or 100 ng/mL convulxin (Figure 4.3 E, F, G, H) for 2 min. In response to thrombin, there was significant reduction in P-selectin exposure in the CSP $\alpha^{-/-}$ platelets compared to CSP $\alpha^{+/+}$ (p value 0.0175) and to CSP $\alpha^{+/-}$ platelets (p value 0.0327) (Figure 4.3A). LAMP-1 exposure, Jon/A binding, and CD41/61 exposure were similar in CSP $\alpha^{+/+}$ and CSP $\alpha^{-/-}$ platelets in response to thrombin (Figure 4.3 B, C, D). In response

100 ng/mL convulxin, there was a significant reduction in P-selectin exposure in the CSP $\alpha^{-/-}$ platelets compared to CSP $\alpha^{+/+}$ platelets (p value 0.0427) (Figure 4.3E). We also saw a significant reduction in integrin activation (Jon/A binding) in the CSP $\alpha^{-/-}$ platelets compared to CSP $\alpha^{+/+}$ platelets (p value 0.0400) (Figure 4.3G). Consistently, the deletion of CSP α did not affect spreading on fibrinogen-coated surfaces (Figure 4.4). LAMP-1 exposure and CD41/61 levels were unaffected in response to convulxin (Figure 3F, H). To further examine the expression of other platelet proteins, we probed for GPVI and PECAM. PECAM surface levels were unaffected (Figure 4.5A), but there was a significant reduction of GPVI on CSP $\alpha^{-/-}$ platelets compared to CSP $\alpha^{+/+}$ platelets (p value 0.0400) (Figure 4.5B). Interestingly, GPVI levels were normal in CSP $\alpha^{+/-}$ platelets (Figure 4.5B). These data suggest that CSP α has a significant role in α granule secretion but not lysosome release. The size of the CSP $\alpha^{-/-}$ mice size limited our ability to assess the role of CSP α in dense granule secretion, so we used an ATP release assay using a modified luciferin/luciferase system (Figure 4.6). Platelets were either stimulated with 0.05 U/mL thrombin or 100 ng/mL convulxin over a ten-minute period to measure ATP release. Release in response to either thrombin or convulxin in the CSP $\alpha^{-/-}$ platelets was defective and was statistically significant at the 6-, 8-, and 10-minute time points (Figure 4.6 A and B). These data indicate that CSP α plays a significant role in platelet secretion, and it may play have a greater role in ITAM signaling pathways compared to G-protein coupled receptor signaling pathways.

4.2.4 Deletion of CSP α results in severely defective thrombosis

We next evaluated whether the defective secretion in the CSP $\alpha^{-/-}$ platelets was sufficient to affect hemostasis and thrombosis using two assays: *in vivo* tail-bleeding and *ex vivo* Bioflux microfluidics (Figure 4.7 and 4.8). The average tail bleeding times for the

CSP $\alpha^{+/+}$ mice 206 ± 121 sec (n=27) and CSP $\alpha^{+/-}$ mice 286 ± 185 sec (n=83) showed a slight but, statistically significant difference. However, the CSP $\alpha^{-/-}$ mice has a robustly increased bleeding time with bleeding from no animals (n=9) stopping prior to 10 minutes (p value <0.0001). Given the reduced size of the CSP $\alpha^{-/-}$ mice, we were unable to perform other *in vivo* thrombosis assays (*i.e.*, jugular vein puncture or FeCl₃ carotid injury). We therefore assessed thrombosis using a Bioflux microfluidics system coated with collagen and whole blood (Figure 4.8). As a comparator, we used blood from Munc13-4^{Jinx} mice, which have a robust dense granule secretion defect and are defective for all four parameters [47]. For all four parameters measured at low shear, the CSP $\alpha^{-/-}$ platelets were less responsive than CSP $\alpha^{+/+}$ platelets (Figure 4.8 A-E).

4.2.5 Sub-platelet Distribution of CSP α

To determine if CSP α is associated with granules in platelets, we used 3-Dimensional Structured Illumination Microscopy (3D-SIM) to examine immunofluorescence staining (Figure 4.9 A and B). The staining pattern of CSP α was punctate, suggesting a granular membrane distribution in platelets. To evaluate whether CSP α is on a granule, we performed colocalization studies with both LAMP-1 (membrane marker for lysosomes) and P-selectin (membrane marker for α -granules). In resting platelets, there was some overlap between LAMP-1 and CSP α (Figure 4.9A; Pearson correlation coefficient: 0.533 and Mander's overlap: 0.896). Similarly, there was some overlap between P-selectin and CSP α (Figure 4.9B; Pearson coefficient: 0.534 and Mander's overlap: 0.930). Absence of non-specific antibody staining was confirmed (Figure 4.10). To address if the deletion of CSP α affected dense granules, we evaluated the dense granules by vital staining with mepacrine [292]. The average numbers of mepacrine-positive structures were similar in

CSP α ^{+/+} (4.91±1.87/platelet; n=11 platelets) vs. CSP α ^{-/-} (4.36±1.12/platelet; n = 11 platelets) platelets. CSP α localization was examined to assess its association with platelet membranes in either a resting or activated state (Figure 4.9C). We disrupted the platelets using freeze-thaw cycles to generate cytosolic and membrane fractions by ultracentrifugation. In resting and activated platelets, CSP α is present mostly in the Triton X-100 soluble fractions. In resting platelets, CSP α is present 83.2% in the Triton X-100 soluble fraction and 16.7% in the Triton X-100 insoluble fraction. The distribution of CSP α changes modestly after activation with 0.1 U/mL thrombin, with greater amount being present in the Triton X-100 soluble fraction at 89.6% vs 10.4% present in the Triton X-insoluble fraction. Since CSP α was present in the Triton X-100 insoluble fractions, we further fractionated that using sucrose density gradient fractionation to assess if CSP α is in lipid rafts (Figure 4.11). We did not see CSP α migrating into the lipid raft fractions (9-11) compared to Syntaxin-11 where you see a visual shift in fraction 9. These data indicate that CSP α is associated with platelet membranes, but it doesn't shift to lipid rafts upon activation.

4.3 Discussion

In this chapter, we built on previous work and examined the function of CSP α in hemostasis using CSP α ^{-/-} mice. We confirmed the absence of CSP α in platelets, but this did not affect the levels of any of the SNARE proteins examined. Colocalization studies found that CSP α is located on both α and lysosomal granules and secretion from CSP α ^{-/-} platelets was defective from both dense and α granules. Consistent with the secretion defect, hemostasis in the CSP α ^{-/-} mice was affected significantly in both our tail-bleeding model

and low-shear Bioflux microfluidics model. These data imply that CSP α plays a significant role in platelet function and contributes to thrombosis and hemostasis.

Data from CSP $\alpha^{-/-}$ mice is consistent with previous studies have showed the importance of dense granule secretion for proper hemostatic function. The importance of the different v-SNAREs (VAMP-2, -3, -4, -5, -7, -8 and Ykt6) and t-SNAREs (SNAP-23 and Syntaxin-11) proteins have been assessed by either manipulating them in various transgenic mice strains or examining patient data [44, 45, 109, 110, 115-117]. VAMP-2, -3, -8 $^{-/-}$ mice and VAMP-2, -3, -7, -8 $^{-/-}$ mice (Joshi *et al.* in preparation) have been characterized by our lab and indicate that when dense granule secretion is affected it leads to hemostatic impairment which has been observed similarly in the CSP $\alpha^{-/-}$ mice via our tail-bleeding and low-shear Bioflux microfluidics model [115]. Because of limitations with the CSP $\alpha^{-/-}$ mice size and lifespan, we were not able to complete *ex vivo* granule secretion assays to fully characterize the secretion phenotypes from the dense, α , and lysosomal granules. To overcome these limitations, we set up a time-dependent ATP release assay which allowed us to characterize dense granule secretion [281]. From the ATP assay (Figure 4.6), we observed that CSP $\alpha^{-/-}$ platelets have a significant dense granule secretion defect which remained significantly lower compared to CSP $\alpha^{+/+}$ platelets over the 10-minute period. However, there are limitations to this assay because even though we see the defect in secretion, we do not know if is a true secretion defect or if granule cargo levels or trafficking could be affected in CSP $\alpha^{-/-}$ mice. Further studies are needed to not only examine the proteome of these mice, but also the morphology of CSP $\alpha^{-/-}$ platelets as well to evaluate granule numbers, size, and distribution. The data from CSP $\alpha^{-/-}$ mice suggests that loss of proteins outside of the VAMP isoforms can affect secretion efficiency. This

has been observed previously in the lab when characterizing $Unc13d^{Jinx}$ mice and to a milder degree in α -synuclein^{-/-} mice [47]. This reemphasizes the importance of dense granule release and highlights the importance of the different secondary agonists in dense granules that are important for platelet activation and recruitment.

SNARE regulation is critical, and the exact molecular function of CSP α has not been clearly defined. Studies in neurons have defined it as a part of a chaperone CSP α -Hsc70-SGT complex that functions to maintain SNAP-25 in the correct conformation for proper SNARE-complex assembly [261, 263]. Deletion of CSP α results in a decrease in SNAP-25 levels which leads to progressive neuron degeneration and a shorter lifespan in mice. This correlates to what have been found in patients with ANCL, where CSP α mutations disrupt SNAP-25 levels and lead to progressive neuronal dysfunction [136, 137, 269, 270]. Several studies suggest that the mutations in CSP α in ANCL lead to its oligomerization, which could lead to its mislocalization and disruption of its SNAP-25 co-chaperone activity [135, 274, 275]. A unique feature of all NCL diseases is the accumulation of ceroid, which suggests that something is being mis-trafficked or that endolysosomal function is disrupted because of the different mutations that causes this disease. Patients with ANCL have not clinically been diagnosed with bleeding diatheses, but their disruption in lysosomal function is of interest because of the many platelet related lysosomal organelle diseases like Hermansky-Pudlak, Chediak-Higashi, and Gray platelet syndrome [24, 34, 35, 51]. This led us to determine if CSP α has a physiological role in platelet function. Our data showed that loss of CSP α does affect platelet function and thrombosis. However, its deletion does not affect levels of any of the protein in the platelet SNARE-complex assembly. This suggests to us that CSP α may play a different role in

platelets, like protein trafficking, but the exact molecular mechanism is unclear. It would be of interest to do further analysis with ANCL patient samples to see if we would find a similar platelet phenotype like the $CSP\alpha^{-/-}$ platelets since there are limitations.

The importance of regulating the SNARE machinery has been exemplified by the relationship of Munc18b/Syntaxin-11 and how when either one is dysfunctional it causes Familial hemophagocytic lymphohistocytosis (FHL) [34, 44]. This has also been further shown by the relationship between $CSP\alpha$ /SNAP-25 in neurons, because $CSP\alpha$ dysfunction leads to Adult-onset ceroid neuronal lipofuscinosis [137, 261, 263, 270]. Studies in various mouse strains have shown the importance of the various v-SNARE and t-SNARE proteins and how they contribute individually or together in SNARE-complex assembly [109, 115]. In this study, we assessed the molecular role of $CSP\alpha$ in platelet secretion and function. The $CSP\alpha^{-/-}$ mice studies were limited because of their size and low survival rate of approximately 6-8 weeks. The deletion of $CSP\alpha$ had a significant effect on dense granule secretion and impaired GPVI integrin $\alpha IIb\beta 3$ activation. Overall, our data suggests that $CSP\alpha$ has a critical role in platelet function and thrombosis, but the exact molecular function of $CSP\alpha$ is unclear. Further investigations are therefore necessary to elucidate the exact molecular mechanisms.

Table 4.1 Hematological parameters for CSP α ^{-/-} mice

Parameter	CSP α ^{+/+}	CSP α ^{+/-}	CSP α ^{-/-}	CSP α ^{+/+} vs CSP α ^{-/-} p value	CSP α ^{+/-} vs CSP α ^{-/-} p value	CSP α ^{+/+} vs CSP α ^{+/-} p value
Erythrocytes						
Erythrocytes (M/ μ L)	8.12 \pm 0.460	7.70 \pm 0.579	8.66 \pm 1.68	0.7560	0.0768	0.5955
MCV (fL)	50.8 \pm 1.44	50.8 \pm 1.07	45.2 \pm 2.68	0.0118	0.0040	>0.9999
Hemoglobin (g/dL)	12.2 \pm 0.517	11.7 \pm 0.640	11.8 \pm 1.31	>0.9999	0.9798	0.5221
MCH (pg)	15.1 \pm 0.277	15.2 \pm 0.364	13.7 \pm 0.134	0.0163	0.0025	>0.9999
MCHC (g/dL)	29.8 \pm 0.663	30.0 \pm 0.825	30.1 \pm 0.288	>0.9999	>0.9999	>0.9999
Reticulocytes (K/ μ L)	335 \pm 36.2	378 \pm 174	470 \pm 110	0.0230	0.0841	>0.9999
Platelets						
Platelets (K/ μ L)	620 \pm 159	609 \pm 147	756 \pm 194	0.5530	0.1665	>0.9999
MPV (fL)	6.14 \pm 1.14	6.47 \pm 1.22	7.52 \pm 1.27	0.8328	0.8328	>0.9999
Leukocytes						
WBC (K/ μ L)	10.7 \pm 3.16	9.13 \pm 1.71	4.80 \pm 1.90	0.0080	0.0337	>0.9999
Neutrophils (K/ μ L)	1.21 \pm 1.26	0.618 \pm 0.326	0.904 \pm 0.296	>0.9999	0.5210	>0.9999
Lymphocytes (K/ μ L)	9.21 \pm 1.99	8.16 \pm 1.59	3.65 \pm 2.002	0.0054	0.0142	>0.9999
Monocytes (K/ μ L)	0.156 \pm 0.148	0.197 \pm 0.139	0.052 \pm 0.0249	0.1983	0.0089	0.5392
Eosinophils (K/ μ L)	0.149 \pm 0.0344	0.138 \pm 0.0640	0.188 \pm 0.118	>0.9999	0.5949	>0.9999
Basophils (K/ μ L)	0.0129 \pm 0.0125	0.010 \pm 0.010	0.004 \pm 0.00548	0.3596	0.7419	>0.9999

Abbreviations: MCV: mean corpuscular volume, MCH: mean corpuscular hemoglobin, MCHC: mean corpuscular hemoglobin concentrations, MPV: mean platelet volume, WBC: white blood cells.

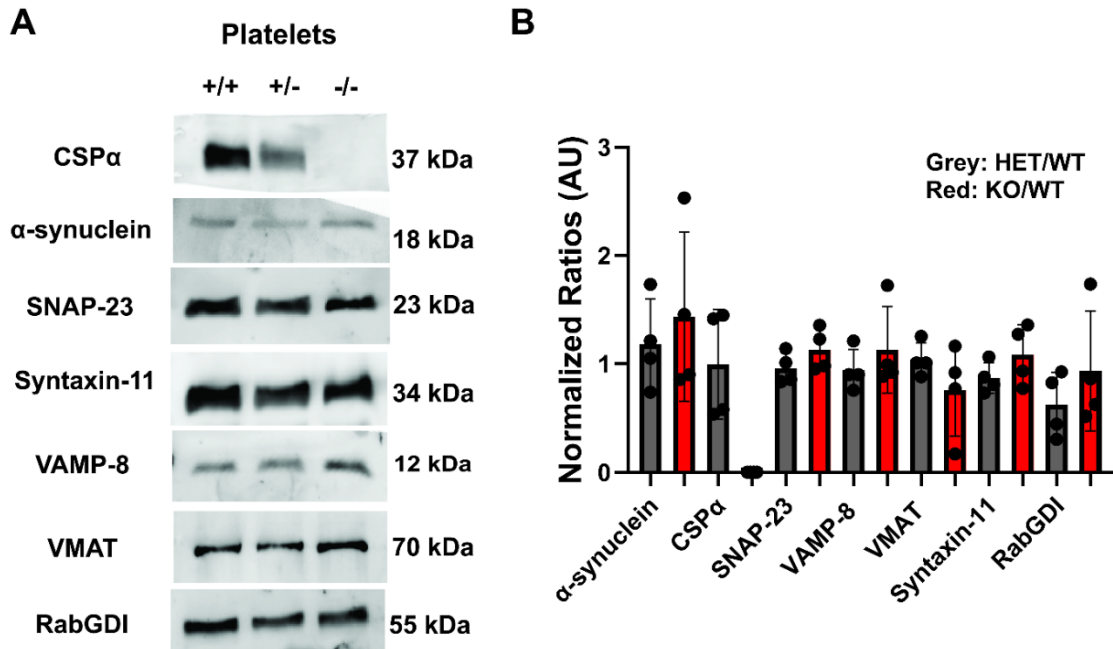


Figure 4.1 Platelet secretory machinery protein levels in CSP α ^{-/-} platelets are normal

(A) Washed platelets (5×10^7 platelets per lane) were prepared from CSP α ^{+/+}, CSP α ^{+/-}, and CSP α ^{-/-} mice (n=4) and the indicated proteins were probed by western blotting. Data are representative of four independent experiments. α -Synuclein, CSP α , SNAP-23, and VAMP-8 were normalized using RabGDI as a loading control. VMAT was normalized using Syntaxin-11 as a loading control. (B) Quantification of protein levels was performed using ImageLab and data was plotted as the ratio of CSP α ^{+/-} over CSP α ^{+/+} mice and CSP α ^{-/-} over CSP α ^{+/+} mice. Statistical analyses were done using individual values and performed using the Kruskal-Wallis multiple comparison test.

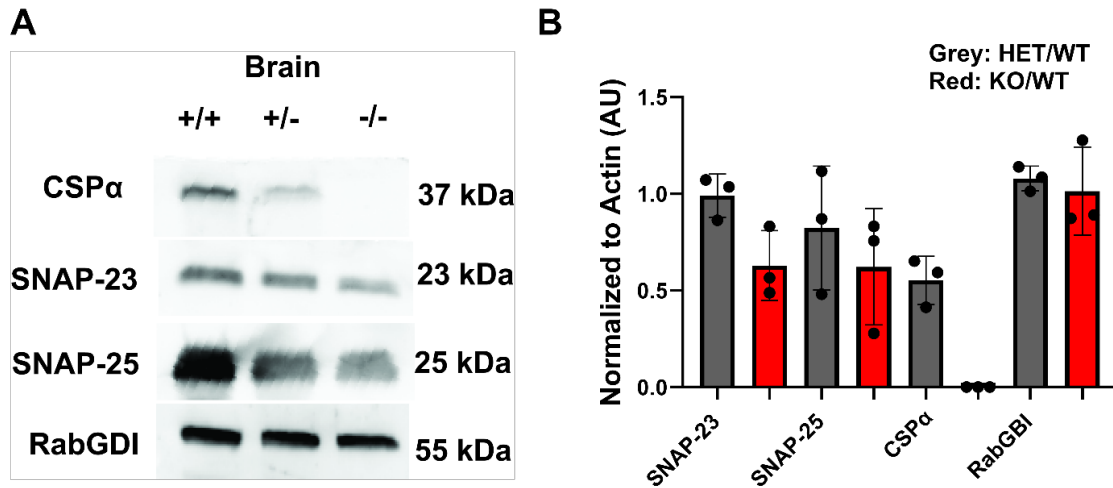


Figure 4.2 SNARE machinery protein levels in $CSP\alpha^{-/-}$ brain are defective

(A) Brain extracts ($50 \mu\text{g}/\mu\text{L}$) were prepared from $CSP\alpha^{+/+}$, $CSP\alpha^{+/-}$, and $CSP\alpha^{-/-}$ mice ($n=3$) and the indicated proteins were probed by western blotting. Data are representative of three independent experiments. SNAP-23, SNAP-25, and $CSP\alpha$ were normalized using RabGDI as a loading control. (B) Quantification of protein levels was performed using ImageLab and data was plotted as the ratio of $CSP\alpha^{+/-}$ over $CSP\alpha^{+/+}$ mice and $CSP\alpha^{-/-}$ over $CSP\alpha^{+/+}$ mice. Statistical analyses were done using individual values and performed using the Kruskal-Wallis multiple comparison test.

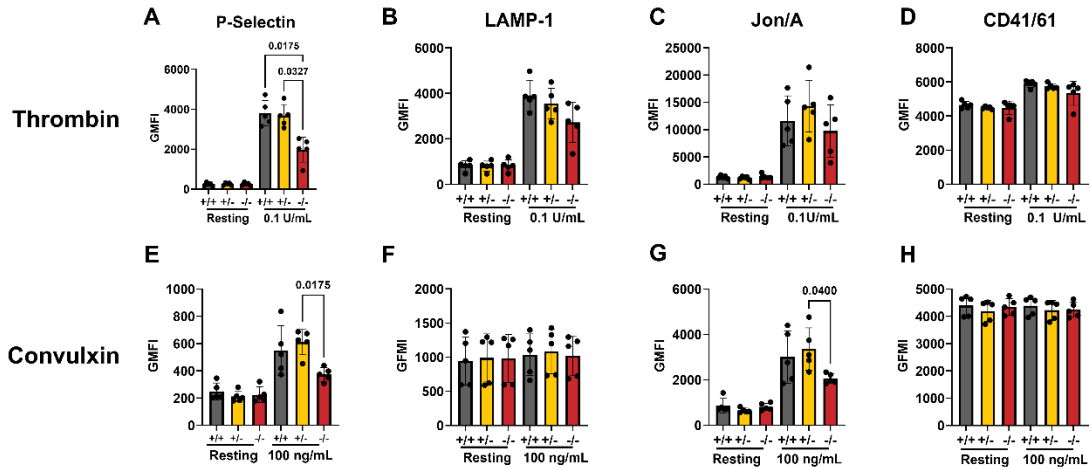


Figure 4.3 $CSP\alpha^{-/-}$ platelets have defective α -granule secretion and a negative effect on integrin activation

Washed platelets ($5 \times 10^7/\text{mL}$) from $CSP\alpha^{+/+}$, $CSP\alpha^{+/-}$, and $CSP\alpha^{-/-}$ mice were stimulated with 0.1 U/mL thrombin or 100 ng/mL convulxin for two minutes and then incubated with FITC anti-P-selectin (A, E), PE-conjugated LAMP-1 (B, F), PE-conjugated Jon/A (C, G), or FITC anti-CD41/61 (D, H) antibodies for 20 min at 37 °C. Fluorescent intensities were measured by flow cytometry. Shown are representative data and geometric mean fluorescent intensity (GMFI) (mean \pm standard error of mean) of ≥ 4 independent experiments. Statistical analyses were performed using the Kruskal-Wallis multiple comparison test

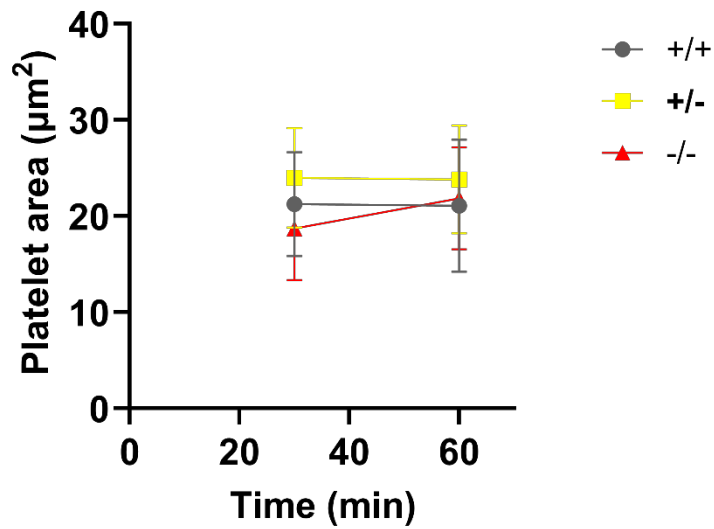


Figure 4.4 CSP $\alpha^{-/-}$ platelets do not have a spreading defect

Washed platelets ($1 \times 10^8/\text{mL}$) from CSP $\alpha^{+/+}$, CSP $\alpha^{+/-}$, and CSP $\alpha^{-/-}$ mice were allowed to adhere and spread on fibrinogen-coated coverslips. At the respective timepoints, the platelets were fixed and imaged for analysis. For each time point, >50 platelets were measured for quantification. Data are mean \pm standard error. Statistical analyses were done using two-way ANOVA multiple comparisons.

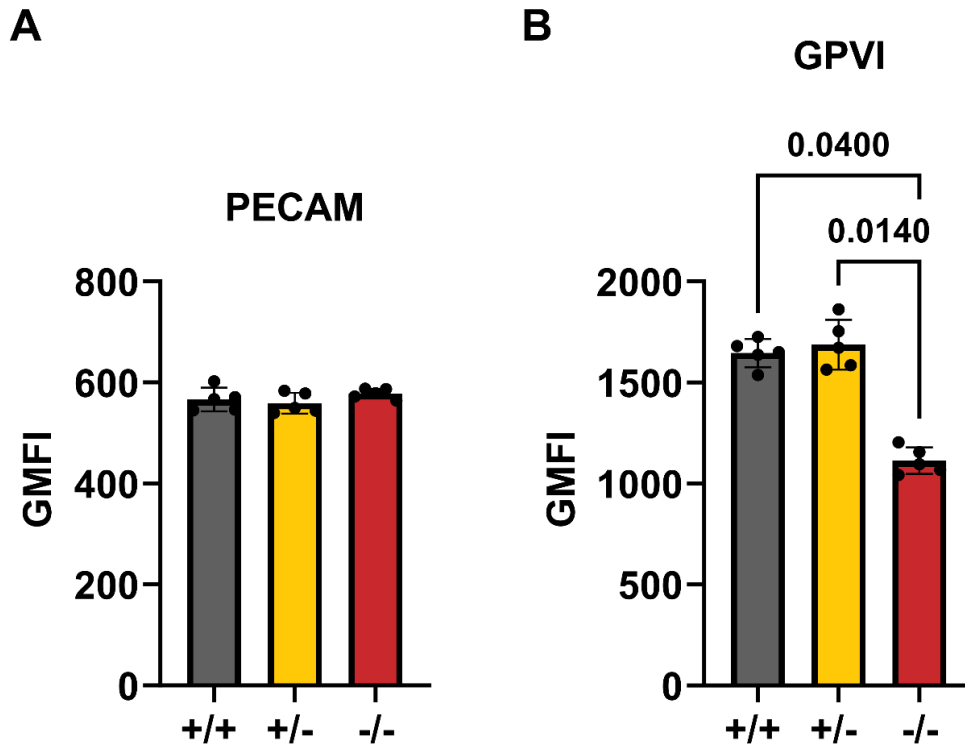


Figure 4.5 $CSP\alpha^{-/-}$ platelets have defective GPVI levels, but no defect in PECAM levels

Washed platelets ($5 \times 10^7/\text{mL}$) from $CSP\alpha^{+/+}$, $CSP\alpha^{+/-}$, and $CSP\alpha^{-/-}$ mice were resting and incubated with FITC-conjugated PECAM antibodies (A) or FITC-conjugated GPVI (B) antibodies for 20 min at 37 °C. Fluorescent intensities were measured by flow cytometry. Shown are representative data and geometric mean fluorescent intensity (GMFI) (mean \pm standard error of mean) of ≥ 4 independent experiments. Statistical analyses were performed using the Kruskal-Wallis multiple comparison test.

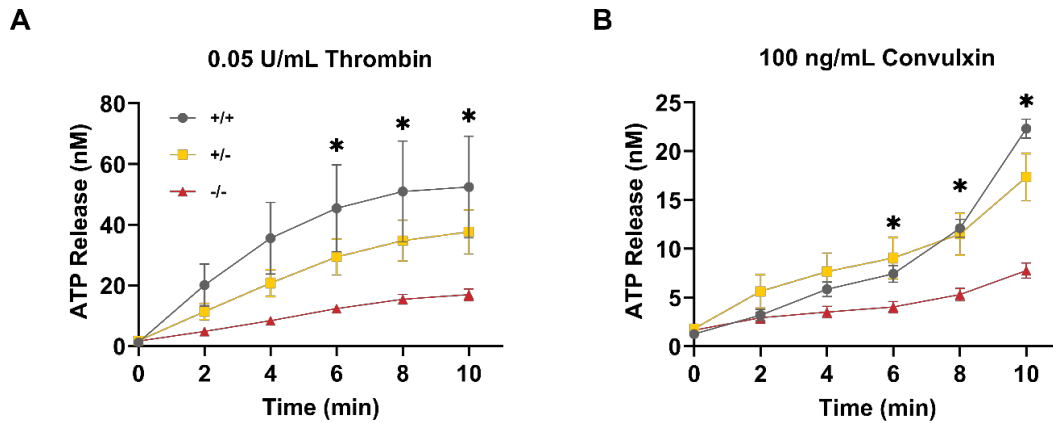


Figure 4.6 $CSP\alpha^{-/-}$ platelets have defective dense granule secretion

Platelet Rich Plasma (PRP) was isolated and adjusted to a concentration of 1×10^8 /mL from $CSP\alpha^{+/+}$, $CSP\alpha^{+/-}$, and $CSP\alpha^{-/-}$ mice. PRP was stimulated with 0.05 U/mL thrombin (A) or 100 ng/mL convulxin (B) over a ten-minute period at 37 °C for 2 min increments to measure ATP release from the platelets. Data are mean \pm standard error of the mean of triplicate measurements and are representative of 3 independent experiments. Statistical analyses were performed using two-way ANOVA multiple comparisons.

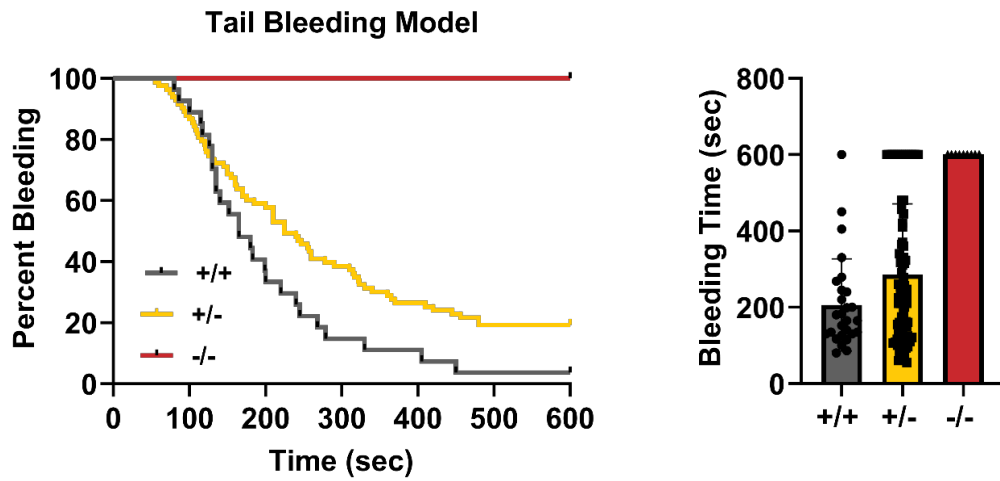


Figure 4.7 $CSP\alpha^{-/-}$ mice have a severe bleeding defect

Tail Bleeding assay was performed to analyze thrombus formation *in vivo*. $CSP\alpha^{+/+}$ (n=27), $CSP\alpha^{+/-}$ (n=83), and $CSP\alpha^{-/-}$ (n=9) mice were used to perform the experiment. Statistical analyses were performed using the Kaplan-Meier method using the log-rank comparison test.

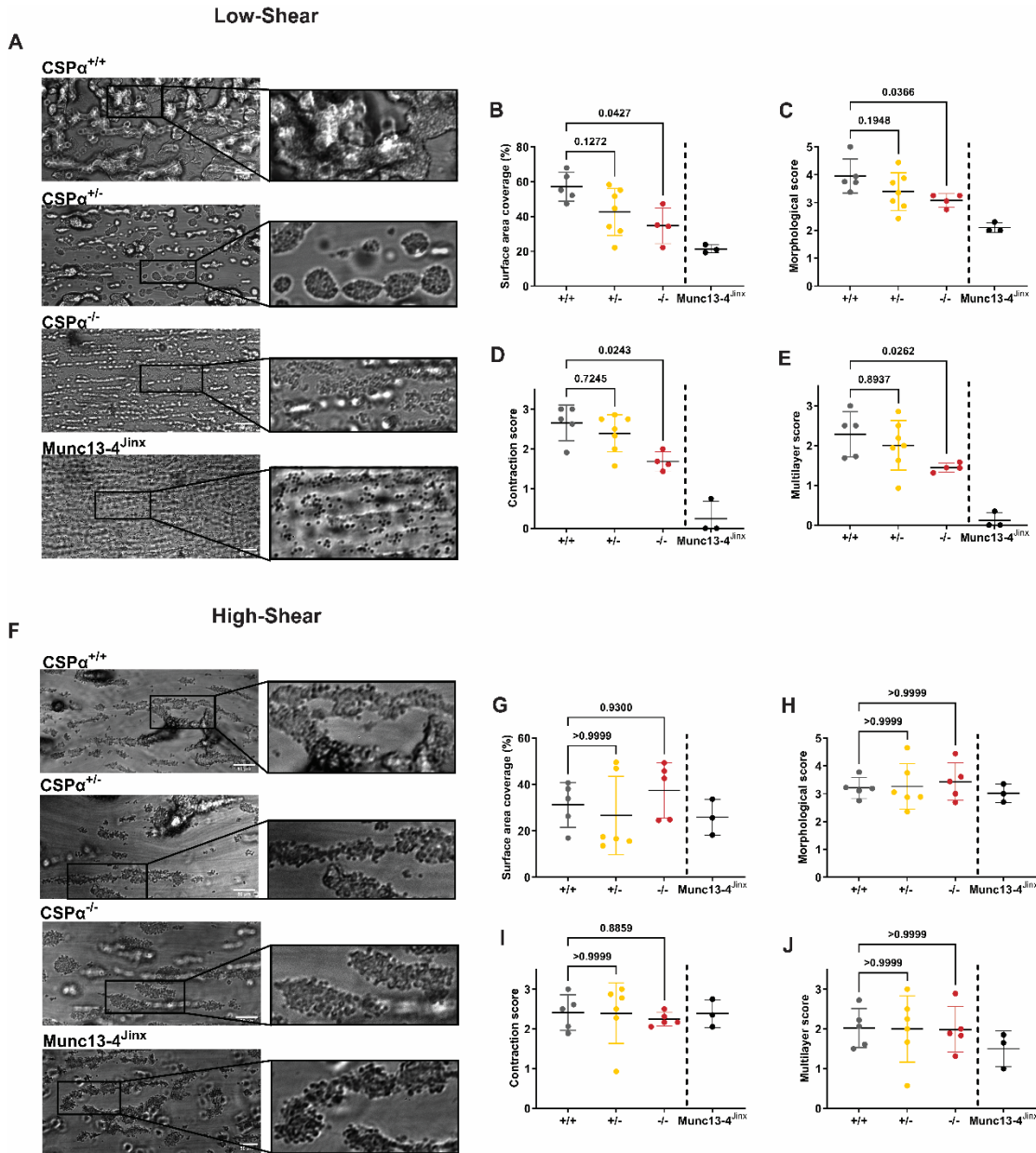


Figure 4.8 CSP α ^{-/-} mice have defective thrombosis under flow at low-shear rates

A Bioflux microfluidics system was used to examine thrombus formation at a low-shear rate of 10 dyn/cm² (A-E) or high-shear rate of 35 dyn/cm² (F-J) over immobilized collagen. (A) Representative images of thrombus formation were taken for CSP α ^{+/+}, CSP α ^{+/-}, and CSP α ^{-/-} mice at low-shear rates after post-perfusion washing. Quantitative analysis of platelet surface coverage area (B), morphological score (C), contraction score (D), and multilayer (E) were measured at the low-shear rate. (F) Representative images of thrombus formation were taken for CSP α ^{+/+}, CSP α ^{+/-}, and CSP α ^{-/-} mice at high-shear rates after post-perfusion washing. Quantitative analysis of platelet surface coverage area (B), morphological score (C), contraction score (D), and multilayer (E) were measured at the high-shear rate. Scale from 0: no thrombus formation to 5: fully formed contracted and multilayered thrombi.

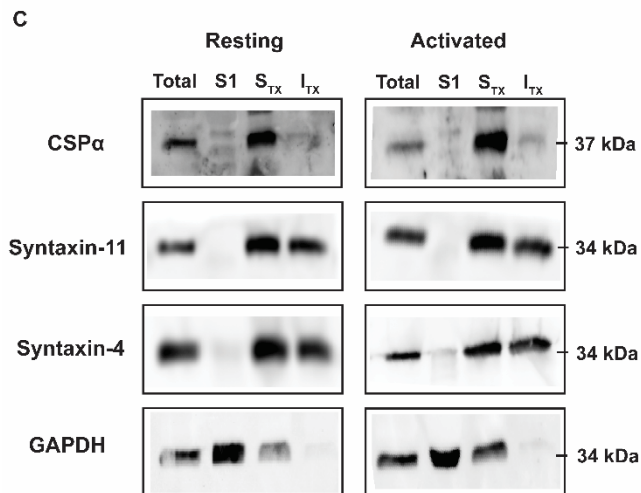
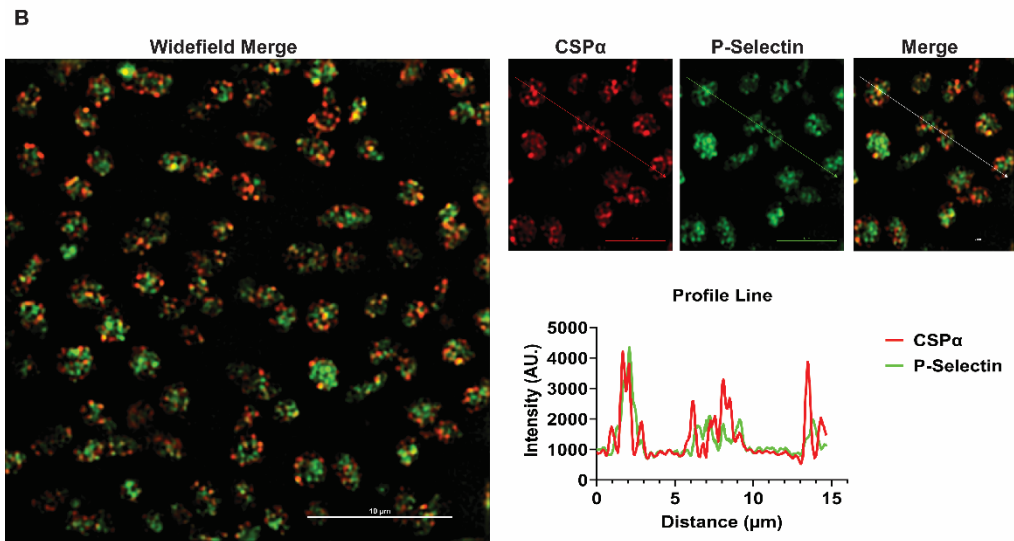
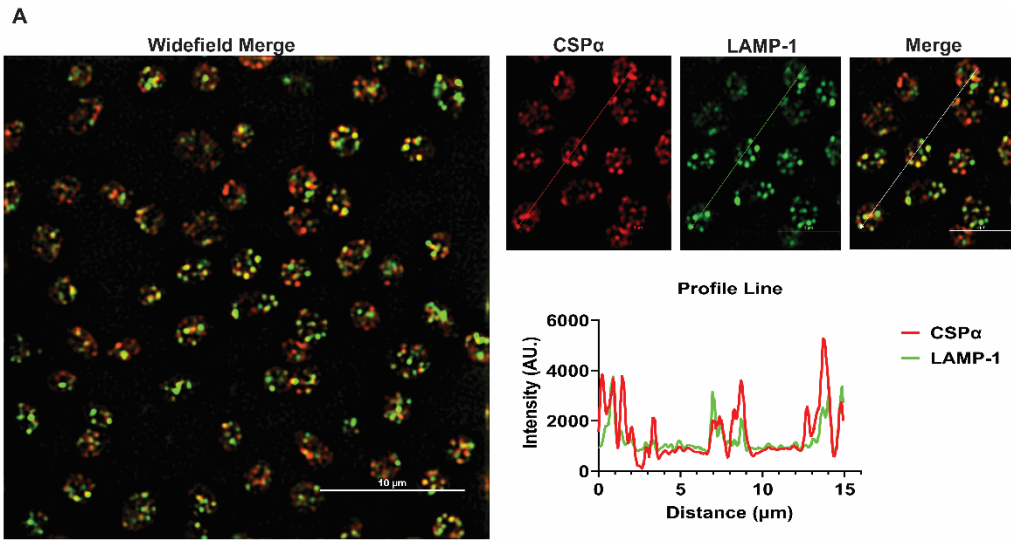


Figure 4.9 CSP α is membrane associated and is present on both lysosomes and α -granules

(A) WT platelets were immunostained for CSP α (red) and LAMP-1 (green) and imaged by using 3-Dimensional structured illumination microscopy (3D-SIM). The white lines in the merged images indicate where the profile line analyses were performed. Profile line analyses are shown below the images. (B) WT platelets were immunostained for CSP α (red) and P-selectin (green) and imaged by using 3-Dimensional structured illumination microscopy (3D-SIM). Scale bar: 10 μ m for widefield images; 5 μ m for cropped images. (C) Lysates were prepared from washed human platelets subjected to five freeze-thaw cycles and centrifuged to separate membrane and cytosol (S1) fractions. The membrane fraction was treated with 1% Triton X-100 to generate Triton X-100 soluble (S_{TX}) and Triton X-insoluble (I_{TX}) fractions which were separated by ultracentrifugation. The fractions were analyzed by SDS-PAGE and probed by Western blotting with the indicated antibodies. All data are representative of 2 independent experiments.

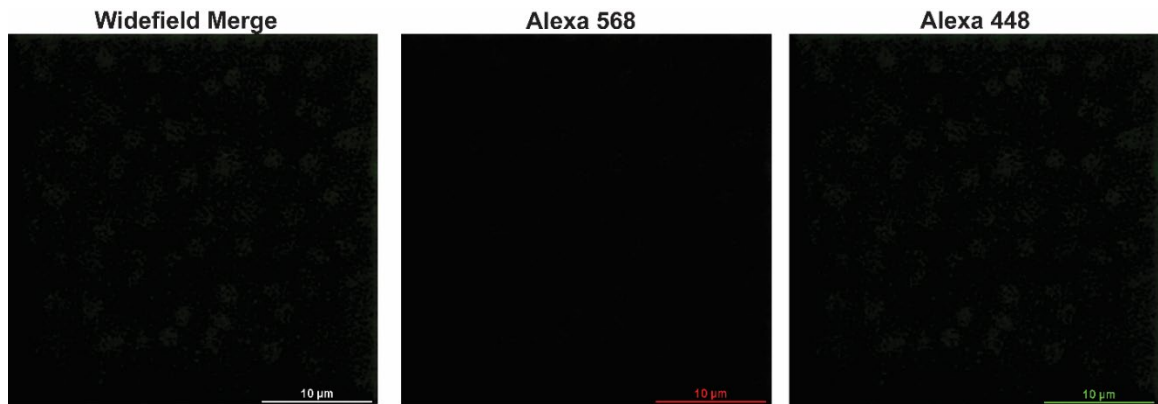


Figure 4.10 Control slides for immunofluorescence experiments

WT platelets were immunostained for Alexa 568 goat anti-rabbit secondary antibody (red) and Alexa 488 goat anti-rat secondary antibody (green) with no primary antibodies and imaged by super-resolution microscopy. These are representative control images from the CSP α (red) and LAMP-1/P-Selectin (green) experiment. Scale bar: 10 μ m.

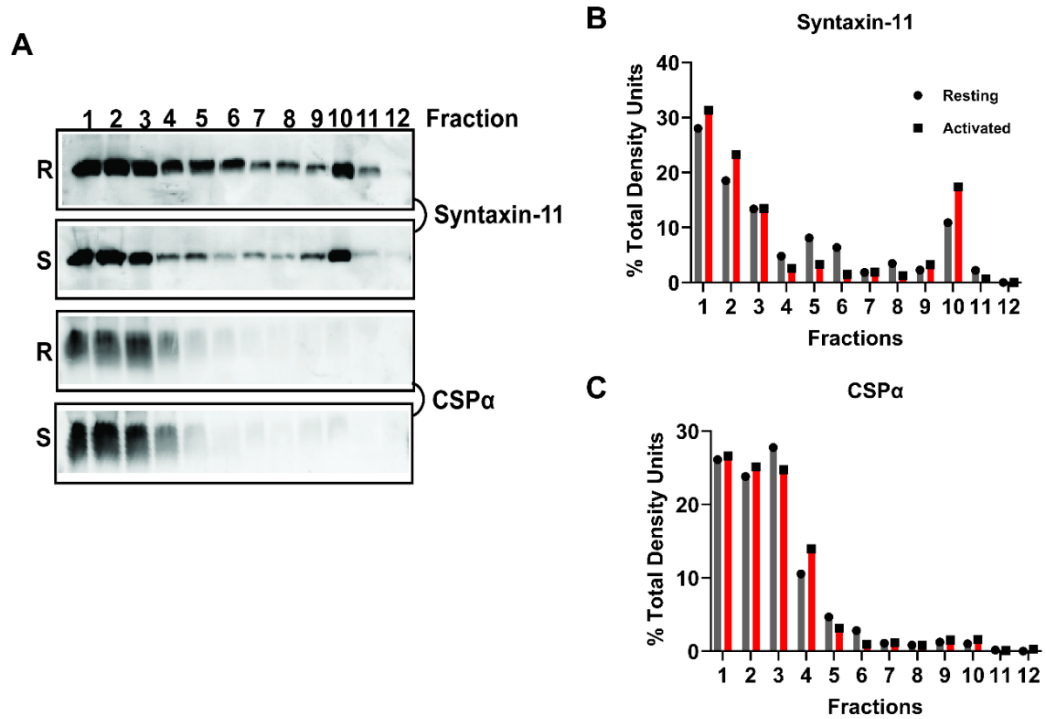


Figure 4.11 CSP α is not found in lipid rafts

(A) Resting or 0.1 U/mL thrombin stimulated platelets were lysed with 2X lysis buffer and layered under a sucrose gradient. The samples were centrifuged and after centrifugation they were collected in 1 mL fractions. The fractions were analyzed by SDS-PAGE and probed by western blotting for the indicated antibodies: Syntaxin-11 (B) and CSP α (C). All data are representative of three independent experiments.

CHAPTER 5. DISCUSSION

5.1 Overview

Overall, the work in this dissertation has focused on further understanding how the process of SNARE-mediated exocytosis is regulated in platelet secretion. Platelets are essential in maintaining the vascular microenvironment, so their dysfunction can be life-threatening, either by causing bleeding diatheses or occlusive cardiovascular events which account for 1 in 4 deaths worldwide [51, 280]. Current anti-thrombotic therapeutics, while effective, often cause bleeding underlining the need for new treatments. Therefore, it is essential to understand how platelets function and how their cargo release contribute to maintain vascular homeostasis to find novel anti-thrombotic targets.

Numerous proteins have been identified in the platelet secretory machinery over the last two decades, giving us a better understanding of how cargo release is mediated. The v-SNAREs (VAMP-2, -3, -4, -5, -7, -8 and Ykt6), t-SNAREs (Syntaxin-2, -4, -6, -7, -8, -11, -12, -16, -17, -18 and SNAP-23, -25, -29), chaperones (Munc18b and Tomosyn/STXBP5), and tethering/docking factors (Rab27 and Munc13-4) [100-102]. Studies have identified VAMP-8, Syntaxin-11, and SNAP-23 as key players. Deletion of these in platelets causes defective secretion from all three granules leading to bleeding defects and attenuated thrombus formation [44, 45, 115-117]. Recent studies focusing exclusively on the VAMP proteins (VAMP-2, -3, -7, and -8) in platelet secretion have identified how these proteins contribute individually or in combinations to platelet secretion suggesting that they are able to compensate for one another when they are deleted. An interesting observation in those studies is that only when VAMP-8 was deleted do you

see defects in dense granule secretion leading to hemostatic impairments [109, 115]. These effects are compounded when the other VAMPs are deleted, but defects were not observed when VAMP-2, -3, or -7 are knocked out individually or in combination. This further supports the role of VAMP-8 as the primary v-SNARE in platelets. Some of the key regulators in secretion have been identified like the chaperone Munc18b/STXBP2 for Syntaxin-11 and the tethering factor Munc13-4. Studies identified that these proteins are defective in Familial Hemophagocytic Lymphohistiocytosis type 3-5 (FHL Type 3-5) resulting in defective secretion from all three granules and bleeding defects [34, 41-45, 47]. Understanding the molecular roles of these various proteins has helped us gain insights into how SNARE-mediated exocytosis is regulated and the essential players in the process for maintaining hemostatic balance.

Platelet SNARE-mediated exocytosis is complex, and its mechanics have not been completely characterized. In this dissertation, we have identified two new regulatory elements, α -synuclein and its interacting protein, Cysteine String Protein- α (CSP α). In neurons, both are key players in neuronal SNARE-complex assembly and their dysfunction has been linked to several neurodegenerative diseases [188, 270, 295]. Studies have proposed that α -synuclein is a v-SNARE chaperone and has roles in SNARE-complex assembly, fusion pore opening, and docking [176, 196-207]. Studies examining CSP α have suggested it to be a chaperone for the SNAP-23/25 family of proteins with roles in chaperoning SNAP-25 and potentially trafficking [135, 261, 263, 278, 296]. Based on their roles in neurons, we asked whether these proteins are essential in platelet secretion and whether they regulate the function of any of the proteins in the platelet secretory machinery. To address these questions, we examined the respective platelet and hemostatic phenotypes

of α -synuclein^{-/-} mice (Chapter 3) and CSP α ^{-/-} mice (Chapter 4). My work demonstrated that α -synuclein has a limited role in platelet function and thrombosis; in contrast, CSP α is essential.

5.2 α -Synuclein's Limited Role in Platelet Secretion

α -Synuclein is well-known for its pathological role in Parkinson disease and several other neurodegenerative diseases. Its true molecular role is unclear, but studies proposed that it functions as a v-SNARE chaperone for VAMP-2 in neuronal SNARE complex assembly. Its deletion also reduces SNARE-complex assembly levels while overexpression enhances SNARE-complex assembly [198, 199]. We proposed that it plays a similar role in platelets, acting as a v-SNARE chaperone for any of the VAMP proteins, and chose to use platelets as a model to better understand α -synuclein's role in neurons as well. Platelet proteomic and western blotting data confirmed that α -synuclein is the only isoform present from the synuclein family and its highly abundant in platelets (Figure 3.10).

The data presented in this dissertation examining the platelet and hemostatic phenotype of α -synuclein^{-/-} mice suggests that α -synuclein plays a minimal role in platelet function and secretion. Analysis of the hematological parameters of α -synuclein^{-/-} mice established that platelet counts, and size were normal, so platelet biogenesis was unaffected by the deletion of α -synuclein. Western blotting analysis showed that the deletion of α -synuclein did not affect any of the proteins in platelet secretory machinery. Immunofluorescence studies revealed that α -synuclein is present in both the cytosol and on α and lysosomal granules. Levels of total surface and activated $\alpha_{IIb}\beta_3$ were unaffected

in resting and thrombin-stimulated platelets. Furthermore, surface exposure of P-selectin (α -granules) and LAMP-1 (lysosomal granules) were unaffected in thrombin-stimulated platelets. In response to that agonists convulxin, CRP, and U46619, P-selectin exposure and activated $\alpha_{IIb}\beta_3$ levels were reduced but this change was not statistically significant. Examining secretion from the three granules using secretion kinetic assays indicated that α -synuclein^{-/-} mice had a mild activation dependent dense granule secretion defect. Secretion from the other granules was minimally affected. We also examined serotonin uptake, PF4, and β -hexosaminidase and there were no defects in cargo levels. The mild defect in dense granule secretion in the α -synuclein^{-/-} mice does not affect aggregation (Lumi-aggregometry) or thrombus formation in the *in vivo* assays (FeCl₃ carotid artery injury model or jugular vein puncture model). This suggests that reducing dense granule secretion by approximately 10% is not enough to impact the hemostatic balance and cause thrombus formation defects. These results are generally like what has been observed in VAMP-7^{-/-} mice, which also have a mild reduction in dense granule secretion and only lysosomal granule secretion was significantly affected at high thrombin concentrations [107-109]. These defects observed in the VAMP-7^{-/-} mice were not sufficient to impact the hemostatic balance as well. The same effects were similarly observed in the global VAMP-3^{-/-}7^{-/-} mice and global and platelet specific VAMP-2^Δ3^Δ7^{-/-} mice where only α and lysosomal granule secretion were significantly affected but this did not disrupt the hemostatic balance as well [109]. Reduced secretion from the α and lysosomal granules is not sufficient to impair thrombus formation highlighting the need for the release of secondary agonists from the dense granules to ensure proper thrombus formation. It is only when VAMP-8 is knocked out that there are disruptions in the hemostatic balance because

of defective secretion from the dense granules. This has been observed in both global VAMP-8^{-/-} mice and global and platelet specific VAMP-2^{Δ3}Δ8^{-/-} mice, which have defective secretion from all three granules resulting in hemostatic impairments [110, 115]. Similar unpublished data from our lab examining the platelet and hemostatic phenotype of global VAMP-7^{-/-}8^{-/-} and platelet specific and global VAMP-2^{Δ3}Δ7^{-/-}8^{-/-} mice exhibit the same results (Joshi *et. al*, in preparation). This data suggests that VAMPs may be able to compensate for each other's functions when they have been genetically manipulated, but they cannot recover when the main v-SNARE, VAMP-8, is absent. The usage of multiple v-SNARE proteins could help explain why we see minimal effects when α -synuclein is deleted. If it is a v-SNARE chaperone for any of the VAMP proteins, they may be able to compensate by using a different VAMP protein that does not require the chaperone activity of α -synuclein. This is unclear because the deletion of α -synuclein did not affect any of the VAMP protein levels. This leads to the question of whether the effects of deleting α -synuclein would be more deleterious in combination with any of the VAMP knockout strains? Would it exacerbate the mild dense granule secretion phenotype observed in VAMP7^{-/-} mice or further disrupt the secretion phenotype seen in VAMP8^{-/-} mice? It is quite possible that the deletion of α -synuclein could further disrupt the phenotypes shown in those mice especially the VAMP-8^{-/-} mice. Future studies would need to be done to confirm this hypothesis. It would also be of interest in future studies to complete protein-binding experiments to determine which of the VAMP proteins interacts with α -synuclein or if it co-immunoprecipitates with the main SNARE complex proteins, VAMP8, Syntaxin-11, and SNAP-23. These experiments could give us a better understanding of α -synuclein's limited role in platelet function and secretion.

Our observation that α -synuclein plays a limited role in platelet secretion and function leads us to the question why are Parkinson disease patients at an increased risk for cerebral microbleeds? Our data suggests that Parkinson disease patients have increased cerebral microbleeds because of vascular defects rather than platelet dysfunction. Cerebral microbleeds are observed more in Parkinson disease patients that have dementia as well who are more likely to develop cerebral amyloid angiopathy, which weakens blood vessels causing cerebral microbleeds [220-225]. But this does lead to further questions since the deletion of α -synuclein does not affect platelet function. Would any of the missense or duplication mutations found to cause Parkinson disease affect platelet function making them either hypo- or hyper- functional? An early study using platelet samples from Parkinson disease patients did observe that platelet aggregation was reduced in response to the agonists ADP and epinephrine, but it was not clear if the patients had idiopathic Parkinson disease or one of the familial mutations [191, 219, 229, 237]. A study using healthy control platelet samples observed that the addition of exogenous full-length α -synuclein reduced α -granule secretion in response to the agonists ionomycin and thrombin [215]. In addition, a recent study observed comparable results when adding exogenous full-length α -synuclein they saw a reduction in platelet aggregation in response to thrombin as well [216]. These studies suggest that Parkinson disease patients could have hypofunctional platelets, which could contribute to the observed bleeding phenotype, along with vascular defects. Future studies would be needed to confirm this either using α -synuclein overexpressing mouse models or patient samples from Parkinson disease patients with the different familial mutations. Understanding the platelet phenotypes in Parkinson disease patients may still be of value since, outside of the increased risks of cerebral

microbleeds, no other bleeding diathesis has been recorded for these patients. It would also be of interest to examine if α -synuclein has a role in the endothelial cells of Parkinson disease patients. Its dysfunction in endothelial cells could contribute to impaired vascular integrity along with cerebral amyloid angiopathy as well. This may clarify the reason for cerebral microbleeds in Parkinson disease patients and suggest they are caused by vascular defects and platelet dysfunction.

5.3 Identification of CSP α 's Essential Role in Platelet Secretion

CSP α has been linked to several neurodegenerative diseases, but it is most well-known for its pathological role in adult-onset neuronal ceroid lipofuscinosis (ANCL) [136, 137, 269-272]. Its true molecular function remains unclear, but studies have shown that it is a critical chaperone for SNAP-25 in neurons [199, 261, 263]. Current literature also shows that it has a unique relationship with α -synuclein, and that α -synuclein overexpression can rescue the neurodegenerative phenotype in CSP α ^{-/-} mice [199]. Recent studies suggest that this may play roles in maintaining lysosomal homeostasis and protein trafficking [135, 136, 274, 275, 278, 296]. Based on its role in neurons, we believe CSP α plays a similar role in platelets and have used platelets as model to better understand its overall function. Proteome and western blotting data confirmed the presence of CSP α in platelets (Figure 4.1).

The data presented in Chapter 4 of this dissertation builds on the work in Chapter 3, examining the molecular role of α -synuclein but focused on the role of CSP α . We evaluated the platelet and hemostatic phenotype of CSP α ^{-/-} mice and our data suggests that CSP α has an essential role in platelet function and secretion. CSP α ^{-/-} mice are significantly

smaller and have a shorter lifespan compared to their wild-type and heterozygous littermates, so we were limited in some of the characterization assays we could perform. Deletion of CSP α did not affect platelet counts and sizes but did drastically affect other hematological parameters. There was a significant reduction in RBC size and mean corpuscular hemoglobin concentration along with an increase in the number of reticulocytes which is indicative of there being a high turnover of RBCs potentially because of their reduced size and mean corpuscular hemoglobin concentration. Another parameter that was drastically affected was the lymphocyte counts in the CSP $\alpha^{-/-}$ mice they were reduced by over 86.5% in comparison to CSP $\alpha^{+/+}$ mice. This drastic reduction is indicative that CSP α may play a role in the biogenesis of RBCs and lymphocytes. This result was not pursued in this manuscript, but it would be of interest to see if there are similar reductions in ANCL patients because it is not known if their immune cells and RBCs are also dysfunctional. Western blotting confirmed the reduction of SNAP-23 and SNAP-25 levels in the brain, but in platelets loss of CSP α did not affect any of the proteins in the platelet secretory machinery. Data also showed that CSP α is membrane associated and present on both α and lysosomal granules. Interestingly, CSP α was not found in lipid rafts after platelet activation. This could indicate that CSP α may play a role in ensuring proper SNARE-complex assembly with proteins outside of the key players, VAMP-8, Syntaxin-11, and SNAP-23. Total surface and activated $\alpha_{IIb}\beta_3$ levels were unaffected in thrombin-stimulated platelets. GPVI resting levels were reduced in CSP $\alpha^{-/-}$ mice. In convulxin-stimulated platelets, activated $\alpha_{IIb}\beta_3$ levels were reduced but not statistically significant. The reduction in GPVI levels could correlate to the reduction seen in activated $\alpha_{IIb}\beta_3$ levels because inside-out signaling is reduced when convulxin is used leading to less of $\alpha_{IIb}\beta_3$ switching

to its activated state. This indicates that CSP α could play a role in the ITAM signaling/trafficking pathway, but further studies would need to be done for confirmation. P-selectin exposure was affected in both thrombin and convulxin stimulated platelets. Generation of an ATP secretion assay allowed us to analyze ATP secretion from dense granules. ATP secretion was significantly reduced in response to both thrombin and convulxin stimulation, but lysosomal granule secretion was unaffected in the CSP $\alpha^{-/-}$ mice. These defects in α and dense granule secretion correlated with the tail bleeding defect and attenuated thrombus formation at low-shear rates observed in the CSP $\alpha^{-/-}$ mice. The smaller RBC size observed in CSP $\alpha^{-/-}$ mice may contribute to the reduction observed in thrombus formation as well. Smaller RBCs may not be effective at increasing blood viscosity and promoting platelet adhesion and activation leading to reduction in thrombus formation especially at lower shear rates where they play a more significant role [297]. The defect in thrombus formation in the CSP $\alpha^{-/-}$ mice was not observed at high shear rates where RBCs play less of a role, suggesting that high-shear rates are enough to overcome the defects observed in platelet secretion.

The defects observed in the CSP $\alpha^{-/-}$ mice are indicative of CSP α playing a critical role in the lysosomal-related organelles in platelets, dense and α granules. The phenotypes seen in these mice is similar to that observed in other lysosome-related organelle diseases such as, Familial hemophagocytic lymphohistocytosis (FHL) [34]. FHL Type 3 affects the Munc13-4/Unc13d gene, FHL Type 4 affects Syntaxin-11 gene, and FHL Type 5 affects Munc18b gene. In FHL Types 4 and 5 patients you see defective secretion from all three granules resulting in severe bleeding and attenuated thrombus formation [44, 45]. In the Unc13d^{J^{inx}} mice model, defective secretion from all three granules and attenuated thrombus

formation occurs [47]. It has not been observed if FHL Type 3 patients have a bleeding phenotype, but the mouse model is suggestive of it [43]. Bleeding phenotypes have not been observed in ANCL patients, but our current data suggests that they could experience bleeding. It would be interesting to reevaluate patient data to determine if they suffer from bleeding, as we found in the FHL patients.

It is clear that CSP α plays a role in maintaining hemostatic balance, but its exact molecular role in platelets remains unclear. Our data suggest that CSP α may not chaperone SNAP-23/25 proteins in platelets as is seen in neurons. SNAP-23 was unaffected by the deletion of CSP α . The deletion of CSP α also did not affect the levels of α -synuclein, our data and others suggest that CSP α potentially functions upstream of α -synuclein. A future study could examine the effects of α -synuclein overexpression to determine if it reverses the platelet phenotype of CSP $\alpha^{-/-}$ mice as it does neuronal function. Defining how these two proteins are mechanistically linked could be a key to understanding their roles in platelets and neurons. Recent data suggest that CSP α could play a role in lysosomal homeostasis and trafficking which may be the pathological cause of ANCL [135, 278, 296, 298]. Further studies investigating different signaling pathways like AKT could give us a clue if dysfunctional where exactly CSP α functions in platelets. It would also be of interest to examine the dense and alpha granule morphology and cargo contents to ensure that the deletion of CSP α did not affect granule biogenesis. We could not examine granule cargo contents using data from our secretion kinetic experiments because of limited sample sizes. Electron micrographs, proteome, and array data would give us an idea if the granules were formed and packaged correctly, giving us an insight if the secretion defect, we see is true and not because of incorrect granule formation and packaging. However, there are still

limitations to completing some of these future studies because of the reduced size and lifespan of $CSP\alpha^{-/-}$ mice. One possible way to navigate this could be the bone marrow transplantation to see if we could recapitulate the same defects in secretion seen in $CSP\alpha^{-/-}$ mice by grafting their bone marrow cells into WT mice and vice versa. Would grafting WT bone marrow cells into $CSP\alpha^{-/-}$ mice rescue the platelet secretion phenotype observed? It is quite possible that the WT bone marrow graft would rescue the platelet secretion phenotype seen in the $CSP\alpha^{-/-}$ platelets, but a potential limitation of this experiment is the $CSP\alpha^{-/-}$ mice survival rate after the surgery. When performing the tail bleeding assay several mice died from too much anesthesia because of their small size, and some also died the same day or overnight because their bleeding could not be manually stopped. Our limited studies with the global $CSP\alpha^{-/-}$ mice does indicate a critical role for $CSP\alpha$, but in the future, generating a platelet-specific knockout model may be the key to navigate the limitations of experiments allowing us to perform the *ex vivo* secretion kinetic experiments and *in vivo* assays like the $FeCl_3$ carotid artery injury model and the jugular vein puncture model to give us an more in depth look into the role of $CSP\alpha$ without the neurodegenerative phenotype affecting the lifespan and size.

5.4 $CSP\alpha$ and α -Synuclein's Potential Role in Platelet Signaling

$CSP\alpha$ and α -synuclein are both known to cause lysosomal-storage related neurodegenerative diseases. Their true molecular roles are unknown, but is believed that when these proteins form aggregates, they cause the mistrafficking of proteins which disrupts lysosomal homeostasis leading to neuronal death [135, 136, 208, 235, 238-240, 274, 275, 278, 296]. Our data in platelets suggest that these proteins may not act as

chaperones in platelet SNARE-complex assembly, but that they could possibly play a role in platelet signaling.

We found when examining GPVI levels there was a significant reduction in CSP α ^{-/-} mice compared to their wild-type and heterozygous littermates. In α -synuclein^{-/-} mice we saw a trending reduction in GPVI levels, but it did not reach significance. This is of interest because when using the GPVI specific agonist convulxin we saw a significant reduction in α _{IIb} β ₃ activation in the CSP α ^{-/-} mice as well as a trending reduction in the α -synuclein^{-/-} mice even though it did not reach significance. This reduction in integrin activation led to defects in dense granule secretion which was significantly affected in the CSP α ^{-/-} mice causing a severe bleeding defect. The reduction in GPVI levels could be why α _{IIb} β ₃ activation is affected but that remains unclear. This, however, contradicts previous data in the literature when examining GPVI^{-/-} mice. They were only shown to have a mild bleeding defect while with the CSP α ^{-/-} mice we observed a significant bleeding defect [299-301]. A possible explanation is that the deletion of these proteins causes mistrafficking of proteins that results in the defective platelet function and secretion. GPVI is known to be trafficked inside and out of platelets and that it can also shed during platelet activation or thrombotic states [302-305]. Future studies examining GPVI levels would be of interest whether looking at total levels in platelets or examining soluble GPVI levels to see if there is increase shedding in the both the CSP α ^{-/-} and α -synuclein^{-/-} mice. This could give insights into why GPVI levels are affected and α _{IIb} β ₃ activation is reduced when using the GPVI specific agonist convulxin compared to thrombin. Recent data in the literature also suggests that mTOR signaling may play a role in GPVI-mediated platelet activation but that remains unclear [306]. It would also be of interest to investigate different signaling pathways

specifically ITAM, AKT, and mTOR to see if there is a difference in any of those pathways that could possibly affect platelet activation as well. This suggests that CSP α and α -synuclein may be functionally linked with the deletion CSP α being more deleterious to platelet function and signaling. These future studies could give insight into how these two proteins play a role in platelet function and secretion.

5.5 CSP α 's Potential Role in Hematopoiesis

CSP α is expressed in numerous cell types that specialized in exocytosis. We found when examining the hematological parameters in the CSP $\alpha^{-/-}$ mice that they had a significant reduction in WBC count specifically in the lymphocyte and monocyte population. This suggests that there might possibly be defects in the hematopoietic stem cell niche affecting the production of immune cells since there were no overt changes observed in erythrocyte or platelet numbers. Future studies looking in the stem-cell populations in the CSP $\alpha^{-/-}$ mice would be of interest to see if CSP α plays a role in maintaining the hematopoietic stem cell niche. This could give insight if maintenance of the stem cell population groups is being skewed to one population over another. Another study of interest is further looking into spleen progenitor cells as well as the spleen histology in CSP $\alpha^{-/-}$ mice. Spleen size was severely reduced in the CSP $\alpha^{-/-}$ mice, but it correlated with the reduction in body weight and size observed. It would be of interest to further examine the histology of the spleen to get a closer look at the spleen morphology and germinal center numbers to see if those are possibly affected in the CSP $\alpha^{-/-}$ mice and could explain the reduction in lymphocyte and monocyte numbers.

Even though platelet biogenesis appears to be unaffected in the $CSP\alpha^{-/-}$ mice it remains unclear whether megakaryopoiesis or even granule biogenesis is affected. It would be of interest to complete future studies looking into both megakaryocyte and megakaryocyte progenitor numbers in the bone marrow. This would give insight into whether those numbers are affected which is unlikely based on the hematological parameters, but it would be a way to assess that megakaryocytes are being produced and differentiate from immature megakaryocytes into mature megakaryocytes. Another experiment to do would be to examine the bone histology of the $CSP\alpha^{-/-}$ mice as well. This will allow us to assess the number and size of megakaryocytes as well as laminin deposition which could give insights into if the hematopoietic stem cell niche is affected. Furthermore, experiments looking into if granule biogenesis in the megakaryocytes is affected is essential as well because this could possibly explain the defects seen in both dense and alpha granule secretion. Some ways to do that are looking into cargo levels of different proteins in the $CSP\alpha^{-/-}$ mice like PF4, vWF, and fibrinogen that can give insight if the synthesis or packaging of cargo molecules into alpha granules is affected. Thin-section electron microscopy could also be used to get further insight into granule numbers, size and distribution as well to see if those are possibility affected as well in the $CSP\alpha^{-/-}$ mice but it may not be possible because of limited sample size. These various experiments could give insights into the possible roles of $CSP\alpha$ in both megakaryopoiesis and hematopoietic stem cell maintenance. It also suggests that we should further investigate ANCL patients as well to see if they could have possible bleeding defects or defects in hematopoiesis. These patients do suffer from deleterious side effects on the neuronal side which could result in any potential bleeding disorders being overlooked, so it would be of utmost

importance to further look into ANCL patients to see if they have a similar bleeding phenotype like FHL patients.

5.6 Summary

The work presented in this dissertation offers valuable insights in understanding how the overall process of platelet secretion is regulated. We used platelets as a model to characterize the molecular roles of both α -synuclein and CSP α . We showed that while α -synuclein has a limited role in platelet function and secretion; its interacting partner, CSP α , has an essential role. Loss of α -synuclein causes a mild defect in dense granule secretion which did not affect overall thrombosis and hemostasis. While on the other hand, loss of CSP α causes a severe defect in both α and dense granule secretion leading to both defective bleeding and thrombus formation. These results further demonstrate the importance of dense granule secretion in maintaining hemostatic balance and how its severe dysfunction leads to various hemostatic impairments. Further understanding of the key players in the regulation of platelet secretion will be important in the development of novel anti-thrombotic therapeutics.

REFERENCES

1. Golebiewska, E.M. and A.W. Poole, *Platelet secretion: From haemostasis to wound healing and beyond*. Blood Rev, 2015. **29**(3): p. 153-62.
2. Smyth, S.S., et al., *Platelet functions beyond hemostasis*. J Thromb Haemost, 2009. **7**(11): p. 1759-66.
3. Tesfamariam, B., *Involvement of platelets in tumor cell metastasis*. Pharmacol Ther, 2016. **157**: p. 112-9.
4. Koupenova, M., et al., *Circulating Platelets as Mediators of Immunity, Inflammation, and Thrombosis*. Circ Res, 2018. **122**(2): p. 337-351.
5. Manning, K.L., et al., *Successful determination of platelet lifespan in C3H mice by in vivo biotinylation*. Lab Anim Sci, 1996. **46**(5): p. 545-8.
6. Harker, L.A., et al., *Effects of megakaryocyte growth and development factor on platelet production, platelet life span, and platelet function in healthy human volunteers*. Blood, 2000. **95**(8): p. 2514-22.
7. Schmitt, A., et al., *Of mice and men: comparison of the ultrastructure of megakaryocytes and platelets*. Exp Hematol, 2001. **29**(11): p. 1295-302.
8. Machlus, K.R. and J.E. Italiano, Jr., *The incredible journey: From megakaryocyte development to platelet formation*. J Cell Biol, 2013. **201**(6): p. 785-96.
9. Bluteau, D., et al., *Regulation of megakaryocyte maturation and platelet formation*. J Thromb Haemost, 2009. **7 Suppl 1**: p. 227-34.
10. Italiano, J.E., Jr., et al., *Blood platelets are assembled principally at the ends of proplatelet processes produced by differentiated megakaryocytes*. J Cell Biol, 1999. **147**(6): p. 1299-312.
11. Italiano, J.E., Jr., S. Patel-Hett, and J.H. Hartwig, *Mechanics of proplatelet elaboration*. J Thromb Haemost, 2007. **5 Suppl 1**: p. 18-23.
12. Lefrancais, E., et al., *The lung is a site of platelet biogenesis and a reservoir for haematopoietic progenitors*. Nature, 2017. **544**(7648): p. 105-109.
13. Hartwig, J. and J. Italiano, Jr., *The birth of the platelet*. J Thromb Haemost, 2003. **1**(7): p. 1580-6.
14. Eckly, A., et al., *Respective contributions of single and compound granule fusion to secretion by activated platelets*. Blood, 2016. **128**(21): p. 2538-2549.
15. Shin, E.K., et al., *Platelet Shape Changes and Cytoskeleton Dynamics as Novel Therapeutic Targets for Anti-Thrombotic Drugs*. Biomol Ther (Seoul), 2017. **25**(3): p. 223-230.
16. Sharda, A. and R. Flaumenhaft, *The life cycle of platelet granules*. F1000Res, 2018. **7**: p. 236.
17. Heijnen, H. and P. van der Sluijs, *Platelet secretory behaviour: as diverse as the granules ... or not?* J Thromb Haemost, 2015. **13**(12): p. 2141-51.
18. Fitch-Tewfik, J.L. and R. Flaumenhaft, *Platelet granule exocytosis: a comparison with chromaffin cells*. Front Endocrinol (Lausanne), 2013. **4**: p. 77.
19. King, S.M. and G.L. Reed, *Development of platelet secretory granules*. Semin Cell Dev Biol, 2002. **13**(4): p. 293-302.
20. Koseoglu, S. and R. Flaumenhaft, *Advances in platelet granule biology*. Curr Opin Hematol, 2013. **20**(5): p. 464-71.

21. Chen, Y., Y. Yuan, and W. Li, *Sorting machineries: how platelet-dense granules differ from alpha-granules*. *Biosci Rep*, 2018. **38**(5).
22. Blair, P. and R. Flaumenhaft, *Platelet alpha-granules: basic biology and clinical correlates*. *Blood Rev*, 2009. **23**(4): p. 177-89.
23. Handagama, P., et al., *Endocytosis of fibrinogen into megakaryocyte and platelet alpha-granules is mediated by alpha IIb beta 3 (glycoprotein IIb-IIIa)*. *Blood*, 1993. **82**(1): p. 135-8.
24. Ambrosio, A.L. and S.M. Di Pietro, *Storage pool diseases illuminate platelet dense granule biogenesis*. *Platelets*, 2017. **28**(2): p. 138-146.
25. Holmsen, H. and H.J. Weiss, *Secretable storage pools in platelets*. *Annu Rev Med*, 1979. **30**: p. 119-34.
26. McNicol, A. and S.J. Israels, *Platelet dense granules: structure, function and implications for haemostasis*. *Thromb Res*, 1999. **95**(1): p. 1-18.
27. Hiasa, M., et al., *Essential role of vesicular nucleotide transporter in vesicular storage and release of nucleotides in platelets*. *Physiol Rep*, 2014. **2**(6).
28. Fukami, M.H., H. Holmsen, and K. Ugurbil, *Histamine uptake in pig platelets and isolated dense granules*. *Biochem Pharmacol*, 1984. **33**(23): p. 3869-74.
29. Borgognone, A. and F.M. Pulcinelli, *Reduction of cAMP and cGMP inhibitory effects in human platelets by MRP4-mediated transport*. *Thromb Haemost*, 2012. **108**(5): p. 955-62.
30. Decouture, B., et al., *Impaired platelet activation and cAMP homeostasis in MRP4-deficient mice*. *Blood*, 2015. **126**(15): p. 1823-30.
31. Jedlitschky, G., et al., *The nucleotide transporter MRP4 (ABCC4) is highly expressed in human platelets and present in dense granules, indicating a role in mediator storage*. *Blood*, 2004. **104**(12): p. 3603-10.
32. Bentfeld-Barker, M.E. and D.F. Bainton, *Identification of primary lysosomes in human megakaryocytes and platelets*. *Blood*, 1982. **59**(3): p. 472-81.
33. Dell'Angelica, E.C., et al., *Lysosome-related organelles*. *FASEB J*, 2000. **14**(10): p. 1265-78.
34. Bowman, S.L., et al., *The road to lysosome-related organelles: Insights from Hermansky-Pudlak syndrome and other rare diseases*. *Traffic*, 2019. **20**(6): p. 404-435.
35. Banushi, B. and F. Simpson, *Overlapping Machinery in Lysosome-Related Organelle Trafficking: A Lesson from Rare Multisystem Disorders*. *Cells*, 2022. **11**(22).
36. Meng, R., et al., *Defective release of alpha granule and lysosome contents from platelets in mouse Hermansky-Pudlak syndrome models*. *Blood*, 2015. **125**(10): p. 1623-32.
37. Barbosa, M.D., et al., *Identification of the homologous beige and Chediak-Higashi syndrome genes*. *Nature*, 1996. **382**(6588): p. 262-5.
38. Buchanan, G.R. and R.I. Handin, *Platelet function in the Chediak-Higashi syndrome*. *Blood*, 1976. **47**(6): p. 941-8.
39. Nagle, D.L., et al., *Identification and mutation analysis of the complete gene for Chediak-Higashi syndrome*. *Nat Genet*, 1996. **14**(3): p. 307-11.
40. Sepulveda, F.E., et al., *LYST controls the biogenesis of the endosomal compartment required for secretory lysosome function*. *Traffic*, 2015. **16**(2): p. 191-203.

41. Bryceson, Y.T., et al., *Defective cytotoxic lymphocyte degranulation in syntaxin-11 deficient familial hemophagocytic lymphohistiocytosis 4 (FHL4) patients*. Blood, 2007. **110**(6): p. 1906-15.
42. zur Stadt, U., et al., *Familial hemophagocytic lymphohistiocytosis type 5 (FHL-5) is caused by mutations in Munc18-2 and impaired binding to syntaxin 11*. Am J Hum Genet, 2009. **85**(4): p. 482-92.
43. Feldmann, J., et al., *Munc13-4 is essential for cytolytic granules fusion and is mutated in a form of familial hemophagocytic lymphohistiocytosis (FHL3)*. Cell, 2003. **115**(4): p. 461-73.
44. Al Hawas, R., et al., *Munc18b/STXBP2 is required for platelet secretion*. Blood, 2012. **120**(12): p. 2493-500.
45. Ye, S., et al., *Syntaxin-11, but not syntaxin-2 or syntaxin-4, is required for platelet secretion*. Blood, 2012. **120**(12): p. 2484-92.
46. Nakamura, L., et al., *First characterization of platelet secretion defect in patients with familial hemophagocytic lymphohistiocytosis type 3 (FHL-3)*. Blood, 2015. **125**(2): p. 412-4.
47. Ren, Q., et al., *Munc13-4 is a limiting factor in the pathway required for platelet granule release and hemostasis*. Blood, 2010. **116**(6): p. 869-77.
48. Chicka, M.C., et al., *Role of Munc13-4 as a Ca²⁺-dependent tether during platelet secretion*. Biochem J, 2016. **473**(5): p. 627-39.
49. Chen, C.H., et al., *alpha-granule biogenesis: from disease to discovery*. Platelets, 2017. **28**(2): p. 147-154.
50. Hayward, C.P., *Inherited disorders of platelet alpha-granules*. Platelets, 1997. **8**(4): p. 197-209.
51. Nurden, A. and P. Nurden, *Advances in our understanding of the molecular basis of disorders of platelet function*. J Thromb Haemost, 2011. **9 Suppl 1**: p. 76-91.
52. Nurden, A.T. and P. Nurden, *The gray platelet syndrome: clinical spectrum of the disease*. Blood Rev, 2007. **21**(1): p. 21-36.
53. Bem, D., et al., *VPS33B regulates protein sorting into and maturation of alpha-granule progenitor organelles in mouse megakaryocytes*. Blood, 2015. **126**(2): p. 133-43.
54. Kahr, W.H., et al., *Abnormal megakaryocyte development and platelet function in Nbeal2(-/-) mice*. Blood, 2013. **122**(19): p. 3349-58.
55. Albers, C.A., et al., *Exome sequencing identifies NBEAL2 as the causative gene for gray platelet syndrome*. Nat Genet, 2011. **43**(8): p. 735-7.
56. Gunay-Aygun, M., et al., *NBEAL2 is mutated in gray platelet syndrome and is required for biogenesis of platelet alpha-granules*. Nat Genet, 2011. **43**(8): p. 732-4.
57. Rivera, J., et al., *Platelet receptors and signaling in the dynamics of thrombus formation*. Haematologica, 2009. **94**(5): p. 700-11.
58. Bye, A.P., A.J. Unsworth, and J.M. Gibbins, *Platelet signaling: a complex interplay between inhibitory and activatory networks*. J Thromb Haemost, 2016. **14**(5): p. 918-30.
59. Stalker, T.J., et al., *Platelet signaling*. Handb Exp Pharmacol, 2012(210): p. 59-85.

60. Radomski, M.W., R.M. Palmer, and S. Moncada, *The role of nitric oxide and cGMP in platelet adhesion to vascular endothelium*. *Biochem Biophys Res Commun*, 1987. **148**(3): p. 1482-9.
61. Enjyoji, K., et al., *Targeted disruption of cd39/ATP diphosphohydrolase results in disordered hemostasis and thromboregulation*. *Nat Med*, 1999. **5**(9): p. 1010-7.
62. Marcus, A.J., et al., *The endothelial cell ecto-ADPase responsible for inhibition of platelet function is CD39*. *J Clin Invest*, 1997. **99**(6): p. 1351-60.
63. Woodfin, A., M.B. Voisin, and S. Nourshargh, *PECAM-1: a multi-functional molecule in inflammation and vascular biology*. *Arterioscler Thromb Vasc Biol*, 2007. **27**(12): p. 2514-23.
64. Jonnalagadda, D., L.T. Izu, and S.W. Whiteheart, *Platelet secretion is kinetically heterogeneous in an agonist-responsive manner*. *Blood*, 2012. **120**(26): p. 5209-16.
65. Estevez, B. and X. Du, *New Concepts and Mechanisms of Platelet Activation Signaling*. *Physiology (Bethesda)*, 2017. **32**(2): p. 162-177.
66. Gremmel, T., A.L. Frelinger, 3rd, and A.D. Michelson, *Platelet Physiology*. *Semin Thromb Hemost*, 2016. **42**(3): p. 191-204.
67. Andrews, R.K. and M.C. Berndt, *Platelet physiology and thrombosis*. *Thromb Res*, 2004. **114**(5-6): p. 447-53.
68. Moroi, M. and S.M. Jung, *Platelet glycoprotein VI: its structure and function*. *Thromb Res*, 2004. **114**(4): p. 221-33.
69. Bergmeier, W. and L. Stefanini, *Platelet ITAM signaling*. *Curr Opin Hematol*, 2013. **20**(5): p. 445-50.
70. Asselin, J., et al., *A collagen-like peptide stimulates tyrosine phosphorylation of syk and phospholipase C gamma2 in platelets independent of the integrin alpha2beta1*. *Blood*, 1997. **89**(4): p. 1235-42.
71. Polgar, J., et al., *Platelet activation and signal transduction by convulxin, a C-type lectin from *Crotalus durissus terrificus* (tropical rattlesnake) venom via the p62/GPVI collagen receptor*. *J Biol Chem*, 1997. **272**(21): p. 13576-83.
72. Cruz, M.A., et al., *The platelet glycoprotein Ib-von Willebrand factor interaction activates the collagen receptor alpha2beta1 to bind collagen: activation-dependent conformational change of the alpha2-I domain*. *Blood*, 2005. **105**(5): p. 1986-91.
73. Chen, H. and M.L. Kahn, *Reciprocal signaling by integrin and nonintegrin receptors during collagen activation of platelets*. *Mol Cell Biol*, 2003. **23**(14): p. 4764-77.
74. Dorsam, R.T. and S.P. Kunapuli, *Central role of the P2Y12 receptor in platelet activation*. *J Clin Invest*, 2004. **113**(3): p. 340-5.
75. Leon, C., et al., *Differential involvement of the P2Y1 and P2Y12 receptors in platelet procoagulant activity*. *Arterioscler Thromb Vasc Biol*, 2003. **23**(10): p. 1941-7.
76. Leon, C., et al., *Defective platelet aggregation and increased resistance to thrombosis in purinergic P2Y(1) receptor-null mice*. *J Clin Invest*, 1999. **104**(12): p. 1731-7.
77. Gachet, C., *Regulation of platelet functions by P2 receptors*. *Annu Rev Pharmacol Toxicol*, 2006. **46**: p. 277-300.

78. Hechler, B., M. Cattaneo, and C. Gachet, *The P2 receptors in platelet function*. Semin Thromb Hemost, 2005. **31**(2): p. 150-61.
79. FitzGerald, G.A., *Mechanisms of platelet activation: thromboxane A2 as an amplifying signal for other agonists*. Am J Cardiol, 1991. **68**(7): p. 11B-15B.
80. Hamberg, M., J. Svensson, and B. Samuelsson, *Thromboxanes: a new group of biologically active compounds derived from prostaglandin endoperoxides*. Proc Natl Acad Sci U S A, 1975. **72**(8): p. 2994-8.
81. Paul, B.Z., J. Jin, and S.P. Kunapuli, *Molecular mechanism of thromboxane A(2)-induced platelet aggregation. Essential role for p2t(ac) and alpha(2a) receptors*. J Biol Chem, 1999. **274**(41): p. 29108-14.
82. Crawley, J.T., et al., *The central role of thrombin in hemostasis*. J Thromb Haemost, 2007. **5 Suppl 1**: p. 95-101.
83. Mann, K.G., *Thrombin formation*. Chest, 2003. **124**(3 Suppl): p. 4S-10S.
84. Jackson, S.P., W.S. Nesbitt, and S. Kulkarni, *Signaling events underlying thrombus formation*. J Thromb Haemost, 2003. **1**(7): p. 1602-12.
85. Coughlin, S.R., *Protease-activated receptors in hemostasis, thrombosis and vascular biology*. J Thromb Haemost, 2005. **3**(8): p. 1800-14.
86. Kahn, M.L., et al., *Protease-activated receptors 1 and 4 mediate activation of human platelets by thrombin*. J Clin Invest, 1999. **103**(6): p. 879-87.
87. Sambrano, G.R., et al., *Role of thrombin signalling in platelets in haemostasis and thrombosis*. Nature, 2001. **413**(6851): p. 74-8.
88. Weiss, E.J., et al., *Protection against thrombosis in mice lacking PAR3*. Blood, 2002. **100**(9): p. 3240-4.
89. Kahn, M.L., et al., *A dual thrombin receptor system for platelet activation*. Nature, 1998. **394**(6694): p. 690-4.
90. Durrant, T.N., M.T. van den Bosch, and I. Hers, *Integrin alpha(IIb)beta(3) outside-in signaling*. Blood, 2017. **130**(14): p. 1607-1619.
91. Nesbitt, W.S., et al., *Distinct glycoprotein Ib/V/IX and integrin alpha IIbbeta 3-dependent calcium signals cooperatively regulate platelet adhesion under flow*. J Biol Chem, 2002. **277**(4): p. 2965-72.
92. Shattil, S.J., *Signaling through platelet integrin alpha IIb beta 3: inside-out, outside-in, and sideways*. Thromb Haemost, 1999. **82**(2): p. 318-25.
93. Watson, S.P., et al., *GPVI and integrin alphaIIb beta3 signaling in platelets*. J Thromb Haemost, 2005. **3**(8): p. 1752-62.
94. Kloepper, T.H., C.N. Kienle, and D. Fasshauer, *An elaborate classification of SNARE proteins sheds light on the conservation of the eukaryotic endomembrane system*. Mol Biol Cell, 2007. **18**(9): p. 3463-71.
95. Jahn, R. and R.H. Scheller, *SNAREs--engines for membrane fusion*. Nat Rev Mol Cell Biol, 2006. **7**(9): p. 631-43.
96. Sudhof, T.C. and J. Rizo, *Synaptic vesicle exocytosis*. Cold Spring Harb Perspect Biol, 2011. **3**(12).
97. Mollinedo, F., et al., *Combinatorial SNARE complexes modulate the secretion of cytoplasmic granules in human neutrophils*. J Immunol, 2006. **177**(5): p. 2831-41.
98. Chen, Y.A. and R.H. Scheller, *SNARE-mediated membrane fusion*. Nat Rev Mol Cell Biol, 2001. **2**(2): p. 98-106.

99. Fasshauer, D., et al., *Conserved structural features of the synaptic fusion complex: SNARE proteins reclassified as Q- and R-SNAREs*. Proc Natl Acad Sci U S A, 1998. **95**(26): p. 15781-6.
100. Burkhardt, J.M., et al., *The first comprehensive and quantitative analysis of human platelet protein composition allows the comparative analysis of structural and functional pathways*. Blood, 2012. **120**(15): p. e73-82.
101. Zeiler, M., M. Moser, and M. Mann, *Copy number analysis of the murine platelet proteome spanning the complete abundance range*. Mol Cell Proteomics, 2014. **13**(12): p. 3435-45.
102. Joshi, S. and S.W. Whiteheart, *The nuts and bolts of the platelet release reaction*. Platelets, 2017. **28**(2): p. 129-137.
103. Lemons, P.P., et al., *Regulated secretion in platelets: identification of elements of the platelet exocytosis machinery*. Blood, 1997. **90**(4): p. 1490-500.
104. Schoch, S., et al., *SNARE function analyzed in synaptobrevin/VAMP knockout mice*. Science, 2001. **294**(5544): p. 1117-22.
105. Banerjee, M., et al., *Cellubrevin/vesicle-associated membrane protein-3-mediated endocytosis and trafficking regulate platelet functions*. Blood, 2017. **130**(26): p. 2872-2883.
106. Schraw, T.D., et al., *Granule stores from cellubrevin/VAMP-3 null mouse platelets exhibit normal stimulus-induced release*. Blood, 2003. **102**(5): p. 1716-22.
107. Koseoglu, S., et al., *VAMP-7 links granule exocytosis to actin reorganization during platelet activation*. Blood, 2015. **126**(5): p. 651-60.
108. Peters, C.G., A.D. Michelson, and R. Flaumenhaft, *Granule exocytosis is required for platelet spreading: differential sorting of alpha-granules expressing VAMP-7*. Blood, 2012. **120**(1): p. 199-206.
109. Joshi, S., et al., *The complementary roles of VAMP-2, -3, and -7 in platelet secretion and function*. Platelets, 2023. **34**(1): p. 2237114.
110. Ren, Q., et al., *Endobrevin/VAMP-8 is the primary v-SNARE for the platelet release reaction*. Mol Biol Cell, 2007. **18**(1): p. 24-33.
111. Graham, G.J., et al., *Endobrevin/VAMP-8-dependent dense granule release mediates thrombus formation in vivo*. Blood, 2009. **114**(5): p. 1083-90.
112. Kondkar, A.A., et al., *VAMP8/endobrevin is overexpressed in hyperreactive human platelets: suggested role for platelet microRNA*. J Thromb Haemost, 2010. **8**(2): p. 369-78.
113. Shiffman, D., et al., *Association of gene variants with incident myocardial infarction in the Cardiovascular Health Study*. Arterioscler Thromb Vasc Biol, 2008. **28**(1): p. 173-9.
114. Shiffman, D., et al., *Gene variants of VAMP8 and HNRPUL1 are associated with early-onset myocardial infarction*. Arterioscler Thromb Vasc Biol, 2006. **26**(7): p. 1613-8.
115. Joshi, S., et al., *Alterations in platelet secretion differentially affect thrombosis and hemostasis*. Blood Adv, 2018. **2**(17): p. 2187-2198.
116. Suh, Y.H., et al., *Deletion of SNAP-23 results in pre-implantation embryonic lethality in mice*. PLoS One, 2011. **6**(3): p. e18444.

117. Williams, C.M., et al., *Platelet-specific deletion of SNAP23 ablates granule secretion, substantially inhibiting arterial and venous thrombosis in mice*. *Blood Adv*, 2018. **2**(24): p. 3627-3636.
118. Chen, D., et al., *Molecular mechanisms of platelet exocytosis: role of SNAP-23 and syntaxin 2 in dense core granule release*. *Blood*, 2000. **95**(3): p. 921-9.
119. Chen, D., et al., *Molecular mechanisms of platelet exocytosis: role of SNAP-23 and syntaxin 2 and 4 in lysosome release*. *Blood*, 2000. **96**(5): p. 1782-8.
120. Zhang, J., et al., *Dynamic cycling of t-SNARE acylation regulates platelet exocytosis*. *J Biol Chem*, 2018. **293**(10): p. 3593-3606.
121. Tang, B.L., D.Y. Low, and W. Hong, *Syntaxin 11: a member of the syntaxin family without a carboxyl terminal transmembrane domain*. *Biochem Biophys Res Commun*, 1998. **245**(2): p. 627-32.
122. Salaun, C., G.W. Gould, and L.H. Chamberlain, *Lipid raft association of SNARE proteins regulates exocytosis in PC12 cells*. *J Biol Chem*, 2005. **280**(20): p. 19449-53.
123. Greaves, J., et al., *Palmitoylation of the SNAP25 protein family: specificity and regulation by DHHC palmitoyl transferases*. *J Biol Chem*, 2010. **285**(32): p. 24629-38.
124. Bodin, S., H. Tronchere, and B. Payrastre, *Lipid rafts are critical membrane domains in blood platelet activation processes*. *Biochim Biophys Acta*, 2003. **1610**(2): p. 247-57.
125. Munday, A.D. and J.A. Lopez, *Posttranslational protein palmitoylation: promoting platelet purpose*. *Arterioscler Thromb Vasc Biol*, 2007. **27**(7): p. 1496-9.
126. Sim, D.S., J.R. Dilks, and R. Flaumenhaft, *Platelets possess and require an active protein palmitoylation pathway for agonist-mediated activation and in vivo thrombus formation*. *Arterioscler Thromb Vasc Biol*, 2007. **27**(6): p. 1478-85.
127. De Vos, M.L., D.S. Lawrence, and C.D. Smith, *Cellular pharmacology of cerulenin analogs that inhibit protein palmitoylation*. *Biochem Pharmacol*, 2001. **62**(8): p. 985-95.
128. Lawrence, D.S., J.T. Zilfou, and C.D. Smith, *Structure-activity studies of cerulenin analogues as protein palmitoylation inhibitors*. *J Med Chem*, 1999. **42**(24): p. 4932-41.
129. Dowal, L., et al., *Proteomic analysis of palmitoylated platelet proteins*. *Blood*, 2011. **118**(13): p. e62-73.
130. Gundersen, C.B., *Cysteine string proteins*. *Prog Neurobiol*, 2020. **188**: p. 101758.
131. Arnold, C., et al., *Structure-function analysis of the cysteine string protein in Drosophila: cysteine string, linker and C terminus*. *J Exp Biol*, 2004. **207**(Pt 8): p. 1323-34.
132. Gundersen, C.B., et al., *Extensive lipidation of a Torpedo cysteine string protein*. *J Biol Chem*, 1994. **269**(30): p. 19197-9.
133. Chamberlain, L.H. and R.D. Burgoyne, *The cysteine-string domain of the secretory vesicle cysteine-string protein is required for membrane targeting*. *Biochem J*, 1998. **335** (Pt 2)(Pt 2): p. 205-9.
134. Greaves, J. and L.H. Chamberlain, *Dual role of the cysteine-string domain in membrane binding and palmitoylation-dependent sorting of the molecular chaperone cysteine-string protein*. *Mol Biol Cell*, 2006. **17**(11): p. 4748-59.

135. Henderson, M.X., et al., *Neuronal ceroid lipofuscinosis with DNAJC5/CSPalpha mutation has PPT1 pathology and exhibit aberrant protein palmitoylation*. Acta Neuropathol, 2016. **131**(4): p. 621-37.
136. Naseri, N., M. Sharma, and M. Velinov, *Autosomal dominant neuronal ceroid lipofuscinosis: Clinical features and molecular basis*. Clin Genet, 2021. **99**(1): p. 111-118.
137. Mukherjee, A.B., et al., *Emerging new roles of the lysosome and neuronal ceroid lipofuscinoses*. Mol Neurodegener, 2019. **14**(1): p. 4.
138. Cardenas, E.I., et al., *Munc18-2, but not Munc18-1 or Munc18-3, regulates platelet exocytosis, hemostasis, and thrombosis*. J Biol Chem, 2019. **294**(13): p. 4784-4792.
139. Hough, A., J. Polgar, and G.L. Reed, *Munc18-syntaxin complexes and exocytosis in human platelets*. J Biol Chem, 2003. **278**(22): p. 19627-33.
140. Sudhof, T.C. and J.E. Rothman, *Membrane fusion: grappling with SNARE and SM proteins*. Science, 2009. **323**(5913): p. 474-7.
141. Schraw, T.D., et al., *Platelets from Munc18c heterozygous mice exhibit normal stimulus-induced release*. Thromb Haemost, 2004. **92**(4): p. 829-37.
142. Ashery, U., et al., *Friends and foes in synaptic transmission: the role of tomosyn in vesicle priming*. Trends Neurosci, 2009. **32**(5): p. 275-82.
143. Sakisaka, T., et al., *Dual inhibition of SNARE complex formation by tomosyn ensures controlled neurotransmitter release*. J Cell Biol, 2008. **183**(2): p. 323-37.
144. Ye, S., et al., *Platelet secretion and hemostasis require syntaxin-binding protein STXBP5*. J Clin Invest, 2014. **124**(10): p. 4517-28.
145. Zhu, Q., et al., *Syntaxin-binding protein STXBP5 inhibits endothelial exocytosis and promotes platelet secretion*. J Clin Invest, 2014. **124**(10): p. 4503-16.
146. Zhu, Q.M., et al., *Novel Thrombotic Function of a Human SNP in STXBP5 Revealed by CRISPR/Cas9 Gene Editing in Mice*. Arterioscler Thromb Vasc Biol, 2017. **37**(2): p. 264-270.
147. van Loon, J.E., et al., *Effect of genetic variations in syntaxin-binding protein-5 and syntaxin-2 on von Willebrand factor concentration and cardiovascular risk*. Circ Cardiovasc Genet, 2010. **3**(6): p. 507-12.
148. van Loon, J.E., et al., *Effect of genetic variation in STXBP5 and STX2 on von Willebrand factor and bleeding phenotype in type 1 von Willebrand disease patients*. PLoS One, 2012. **7**(7): p. e40624.
149. Stenmark, H., *Rab GTPases as coordinators of vesicle traffic*. Nat Rev Mol Cell Biol, 2009. **10**(8): p. 513-25.
150. Shirakawa, R., et al., *Munc13-4 is a GTP-Rab27-binding protein regulating dense core granule secretion in platelets*. J Biol Chem, 2004. **279**(11): p. 10730-7.
151. Neef, M., et al., *Munc13-4 is an effector of rab27a and controls secretion of lysosomes in hematopoietic cells*. Mol Biol Cell, 2005. **16**(2): p. 731-41.
152. Elstak, E.D., et al., *The munc13-4-rab27 complex is specifically required for tethering secretory lysosomes at the plasma membrane*. Blood, 2011. **118**(6): p. 1570-8.
153. Menasche, G., et al., *Mutations in RAB27A cause Griscelli syndrome associated with haemophagocytic syndrome*. Nat Genet, 2000. **25**(2): p. 173-6.
154. Tolmachova, T., et al., *Rab27b regulates number and secretion of platelet dense granules*. Proc Natl Acad Sci U S A, 2007. **104**(14): p. 5872-7.

155. Koch, H., K. Hofmann, and N. Brose, *Definition of Munc13-homology-domains and characterization of a novel ubiquitously expressed Munc13 isoform*. *Biochem J*, 2000. **349**(Pt 1): p. 247-53.
156. Sudhof, T.C., *The presynaptic active zone*. *Neuron*, 2012. **75**(1): p. 11-25.
157. Polgar, J. and G.L. Reed, *A critical role for N-ethylmaleimide-sensitive fusion protein (NSF) in platelet granule secretion*. *Blood*, 1999. **94**(4): p. 1313-8.
158. Zhao, C., J.T. Slevin, and S.W. Whiteheart, *Cellular functions of NSF: not just SNAPs and SNAREs*. *FEBS Lett*, 2007. **581**(11): p. 2140-9.
159. Barnard, R.J., A. Morgan, and R.D. Burgoyne, *Stimulation of NSF ATPase activity by alpha-SNAP is required for SNARE complex disassembly and exocytosis*. *J Cell Biol*, 1997. **139**(4): p. 875-83.
160. Hanson, P.I. and S.W. Whiteheart, *AAA+ proteins: have engine, will work*. *Nat Rev Mol Cell Biol*, 2005. **6**(7): p. 519-29.
161. Baker, R.W. and F.M. Hughson, *Chaperoning SNARE assembly and disassembly*. *Nat Rev Mol Cell Biol*, 2016. **17**(8): p. 465-79.
162. Matveeva, E.A., P. He, and S.W. Whiteheart, *N-Ethylmaleimide-sensitive fusion protein contains high and low affinity ATP-binding sites that are functionally distinct*. *J Biol Chem*, 1997. **272**(42): p. 26413-8.
163. Morrell, C.N., et al., *Regulation of platelet granule exocytosis by S-nitrosylation*. *Proc Natl Acad Sci U S A*, 2005. **102**(10): p. 3782-7.
164. Greene, T.K., et al., *Towards a standardization of the murine tail bleeding model*. *J Thromb Haemost*, 2010. **8**(12): p. 2820-2.
165. Mohammed, B.M., D.M. Monroe, and D. Gailani, *Mouse models of hemostasis*. *Platelets*, 2020. **31**(4): p. 417-422.
166. Kurz, K.D., B.W. Main, and G.E. Sandusky, *Rat model of arterial thrombosis induced by ferric chloride*. *Thromb Res*, 1990. **60**(4): p. 269-80.
167. Grover, S.P. and N. Mackman, *How useful are ferric chloride models of arterial thrombosis?* *Platelets*, 2020. **31**(4): p. 432-438.
168. Eckly, A., et al., *Mechanisms underlying FeCl3-induced arterial thrombosis*. *J Thromb Haemost*, 2011. **9**(4): p. 779-89.
169. Barr, J.D., et al., *Red blood cells mediate the onset of thrombosis in the ferric chloride murine model*. *Blood*, 2013. **121**(18): p. 3733-41.
170. Rhee, S.W., et al., *Venous puncture wound hemostasis results in a vaulted thrombus structured by locally nucleated platelet aggregates*. *Commun Biol*, 2021. **4**(1): p. 1090.
171. Tomaiuolo, M., et al., *Interrelationships between structure and function during the hemostatic response to injury*. *Proc Natl Acad Sci U S A*, 2019. **116**(6): p. 2243-2252.
172. Tomaiuolo, M., L.F. Brass, and T.J. Stalker, *Regulation of Platelet Activation and Coagulation and Its Role in Vascular Injury and Arterial Thrombosis*. *Interv Cardiol Clin*, 2017. **6**(1): p. 1-12.
173. Coenen, D.M., T.G. Mastenbroek, and J. Cosemans, *Platelet interaction with activated endothelium: mechanistic insights from microfluidics*. *Blood*, 2017. **130**(26): p. 2819-2828.
174. Herbig, B.A., X. Yu, and S.L. Diamond, *Using microfluidic devices to study thrombosis in pathological blood flows*. *Biomicrofluidics*, 2018. **12**(4): p. 042201.

175. Prakhya, K.S., et al., *Platelet glycogenolysis is important for energy production and function*. Platelets, 2023. **34**(1): p. 2222184.
176. Maroteaux, L., J.T. Campanelli, and R.H. Scheller, *Synuclein: a neuron-specific protein localized to the nucleus and presynaptic nerve terminal*. J Neurosci, 1988. **8**(8): p. 2804-15.
177. Burre, J., M. Sharma, and T.C. Sudhof, *Cell Biology and Pathophysiology of alpha-Synuclein*. Cold Spring Harb Perspect Med, 2018. **8**(3).
178. Maroteaux, L. and R.H. Scheller, *The rat brain synucleins; family of proteins transiently associated with neuronal membrane*. Brain Res Mol Brain Res, 1991. **11**(3-4): p. 335-43.
179. Bruening, W., et al., *Synucleins are expressed in the majority of breast and ovarian carcinomas and in preneoplastic lesions of the ovary*. Cancer, 2000. **88**(9): p. 2154-63.
180. George, J.M., *The synucleins*. Genome Biol, 2002. **3**(1): p. REVIEWS3002.
181. Jakes, R., M.G. Spillantini, and M. Goedert, *Identification of two distinct synucleins from human brain*. FEBS Lett, 1994. **345**(1): p. 27-32.
182. Lavedan, C., et al., *Identification, localization and characterization of the human gamma-synuclein gene*. Hum Genet, 1998. **103**(1): p. 106-12.
183. Ltic, S., et al., *Alpha-synuclein is expressed in different tissues during human fetal development*. J Mol Neurosci, 2004. **22**(3): p. 199-204.
184. Pei, Y. and R.W. Maitta, *Alpha synuclein in hematopoiesis and immunity*. Heliyon, 2019. **5**(10): p. e02590.
185. Ueda, K., T. Saitoh, and H. Mori, *Tissue-dependent alternative splicing of mRNA for NACP, the precursor of non-A beta component of Alzheimer's disease amyloid*. Biochem Biophys Res Commun, 1994. **205**(2): p. 1366-72.
186. Smith, A.N., et al., *alpha-Synuclein is the major platelet isoform but is dispensable for activation, secretion, and thrombosis*. Platelets, 2023. **34**(1): p. 2267147.
187. Runwal, G. and R.H. Edwards, *The Membrane Interactions of Synuclein: Physiology and Pathology*. Annu Rev Pathol, 2021. **16**: p. 465-485.
188. Goedert, M., *Alpha-synuclein and neurodegenerative diseases*. Nat Rev Neurosci, 2001. **2**(7): p. 492-501.
189. Galvin, J.E., V.M. Lee, and J.Q. Trojanowski, *Synucleinopathies: clinical and pathological implications*. Arch Neurol, 2001. **58**(2): p. 186-90.
190. Melland, H., E.M. Carr, and S.L. Gordon, *Disorders of synaptic vesicle fusion machinery*. J Neurochem, 2021. **157**(2): p. 130-164.
191. Stefanis, L., *alpha-Synuclein in Parkinson's disease*. Cold Spring Harb Perspect Med, 2012. **2**(2): p. a009399.
192. Varkey, J., et al., *Membrane curvature induction and tubulation are common features of synucleins and apolipoproteins*. J Biol Chem, 2010. **285**(42): p. 32486-93.
193. Chandra, S., et al., *A broken alpha -helix in folded alpha -Synuclein*. J Biol Chem, 2003. **278**(17): p. 15313-8.
194. Hoyer, W., et al., *Impact of the acidic C-terminal region comprising amino acids 109-140 on alpha-synuclein aggregation in vitro*. Biochemistry, 2004. **43**(51): p. 16233-42.

195. Farzadfard, A., et al., *The C-terminal tail of alpha-synuclein protects against aggregate replication but is critical for oligomerization*. Commun Biol, 2022. **5**(1): p. 123.
196. Burre, J., *The Synaptic Function of alpha-Synuclein*. J Parkinsons Dis, 2015. **5**(4): p. 699-713.
197. Burre, J., M. Sharma, and T.C. Sudhof, *alpha-Synuclein assembles into higher-order multimers upon membrane binding to promote SNARE complex formation*. Proc Natl Acad Sci U S A, 2014. **111**(40): p. E4274-83.
198. Burre, J., et al., *Alpha-synuclein promotes SNARE-complex assembly in vivo and in vitro*. Science, 2010. **329**(5999): p. 1663-7.
199. Chandra, S., et al., *Alpha-synuclein cooperates with CSPalpha in preventing neurodegeneration*. Cell, 2005. **123**(3): p. 383-96.
200. Hawk, B.J.D., R. Khounlo, and Y.K. Shin, *Alpha-Synuclein Continues to Enhance SNARE-Dependent Vesicle Docking at Exorbitant Concentrations*. Front Neurosci, 2019. **13**: p. 216.
201. Diao, J., et al., *Native alpha-synuclein induces clustering of synaptic-vesicle mimics via binding to phospholipids and synaptobrevin-2/VAMP2*. Elife, 2013. **2**: p. e00592.
202. Khounlo, R., et al., *Membrane Binding of alpha-Synuclein Stimulates Expansion of SNARE-Dependent Fusion Pore*. Front Cell Dev Biol, 2021. **9**: p. 663431.
203. Lai, Y., et al., *Nonaggregated alpha-synuclein influences SNARE-dependent vesicle docking via membrane binding*. Biochemistry, 2014. **53**(24): p. 3889-96.
204. Logan, T., et al., *alpha-Synuclein promotes dilation of the exocytotic fusion pore*. Nat Neurosci, 2017. **20**(5): p. 681-689.
205. Nellikka, R.K., et al., *alpha-Synuclein kinetically regulates the nascent fusion pore dynamics*. Proc Natl Acad Sci U S A, 2021. **118**(34).
206. Yoo, G., Y.K. Shin, and N.K. Lee, *The Role of alpha-Synuclein in SNARE-mediated Synaptic Vesicle Fusion*. J Mol Biol, 2022: p. 167775.
207. Zhao, X., et al., *SNARE Proteins Mediate alpha-Synuclein Secretion via Multiple Vesicular Pathways*. Mol Neurobiol, 2022. **59**(1): p. 405-419.
208. Abeliovich, A., et al., *Mice lacking alpha-synuclein display functional deficits in the nigrostriatal dopamine system*. Neuron, 2000. **25**(1): p. 239-52.
209. Chandra, S., et al., *Double-knockout mice for alpha- and beta-synucleins: effect on synaptic functions*. Proc Natl Acad Sci U S A, 2004. **101**(41): p. 14966-71.
210. Al-Wandi, A., et al., *Absence of alpha-synuclein affects dopamine metabolism and synaptic markers in the striatum of aging mice*. Neurobiol Aging, 2010. **31**(5): p. 796-804.
211. Anwar, S., et al., *Functional alterations to the nigrostriatal system in mice lacking all three members of the synuclein family*. J Neurosci, 2011. **31**(20): p. 7264-74.
212. Greten-Harrison, B., et al., *Alphabeta-gamma-Synuclein triple knockout mice reveal age-dependent neuronal dysfunction*. Proc Natl Acad Sci U S A, 2010. **107**(45): p. 19573-8.
213. Reheman, A., et al., *Mice with deleted multimerin 1 and alpha-synuclein genes have impaired platelet adhesion and impaired thrombus formation that is corrected by multimerin 1*. Thromb Res, 2010. **125**(5): p. e177-83.

214. Kim, K.S., et al., *Regulation of Weibel-Palade body exocytosis by alpha-synuclein in endothelial cells*. J Biol Chem, 2010. **285**(28): p. 21416-25.
215. Park, S.M., et al., *Evidence that alpha-synuclein functions as a negative regulator of Ca(++)-dependent alpha-granule release from human platelets*. Blood, 2002. **100**(7): p. 2506-14.
216. Acquasaliente, L., et al., *Exogenous human alpha-Synuclein acts in vitro as a mild platelet antiaggregant inhibiting alpha-thrombin-induced platelet activation*. Sci Rep, 2022. **12**(1): p. 9880.
217. Spillantini, M.G., et al., *Alpha-synuclein in Lewy bodies*. Nature, 1997. **388**(6645): p. 839-40.
218. Parkinson, J., *An essay on the shaking palsy. 1817*. J Neuropsychiatry Clin Neurosci, 2002. **14**(2): p. 223-36; discussion 222.
219. Poewe, W., et al., *Parkinson disease*. Nat Rev Dis Primers, 2017. **3**: p. 17013.
220. Daida, K., et al., *The presence of cerebral microbleeds is associated with cognitive impairment in Parkinson's disease*. J Neurol Sci, 2018. **393**: p. 39-44.
221. Ham, J.H., et al., *Cerebral microbleeds in patients with Parkinson's disease*. J Neurol, 2014. **261**(8): p. 1628-35.
222. Kim, J.H., et al., *Characterization of cerebral microbleeds in idiopathic Parkinson's disease*. Eur J Neurol, 2015. **22**(2): p. 377-83.
223. Tsai, H.H., et al., *Amyloid related cerebral microbleed and plasma Abeta40 are associated with cognitive decline in Parkinson's disease*. Sci Rep, 2021. **11**(1): p. 7115.
224. Yamashiro, K., et al., *The prevalence and risk factors of cerebral microbleeds in patients with Parkinson's disease*. Parkinsonism Relat Disord, 2015. **21**(9): p. 1076-81.
225. Jellinger, K.A. and J. Attems, *Cerebral amyloid angiopathy in Lewy body disease*. J Neural Transm (Vienna), 2008. **115**(3): p. 473-82.
226. Stefaniuk, C.M., et al., *alpha-Synuclein concentration increases over time in plasma supernatant of single donor platelets*. Eur J Haematol, 2018.
227. Tian, C., et al., *Erythrocytic alpha-Synuclein as a potential biomarker for Parkinson's disease*. Transl Neurodegener, 2019. **8**: p. 15.
228. Kasuga, K., M. Nishizawa, and T. Ikeuchi, *alpha-Synuclein as CSF and Blood Biomarker of Dementia with Lewy Bodies*. Int J Alzheimers Dis, 2012. **2012**: p. 437025.
229. Funayama, M., et al., *Molecular genetics of Parkinson's disease: Contributions and global trends*. J Hum Genet, 2023. **68**(3): p. 125-130.
230. Sulzer, D. and R.H. Edwards, *The physiological role of alpha-synuclein and its relationship to Parkinson's Disease*. J Neurochem, 2019. **150**(5): p. 475-486.
231. Tang, F.L., et al., *VPS35 in Dopamine Neurons Is Required for Endosome-to-Golgi Retrieval of Lamp2a, a Receptor of Chaperone-Mediated Autophagy That Is Critical for alpha-Synuclein Degradation and Prevention of Pathogenesis of Parkinson's Disease*. J Neurosci, 2015. **35**(29): p. 10613-28.
232. Meade, R.M., D.P. Fairlie, and J.M. Mason, *Alpha-synuclein structure and Parkinson's disease - lessons and emerging principles*. Mol Neurodegener, 2019. **14**(1): p. 29.

233. Martin, I., et al., *LRRK2 pathobiology in Parkinson's disease*. J Neurochem, 2014. **131**(5): p. 554-65.
234. Lin, X., et al., *Leucine-rich repeat kinase 2 regulates the progression of neuropathology induced by Parkinson's-disease-related mutant alpha-synuclein*. Neuron, 2009. **64**(6): p. 807-27.
235. Hunn, B.H., et al., *Impaired intracellular trafficking defines early Parkinson's disease*. Trends Neurosci, 2015. **38**(3): p. 178-88.
236. Dhungel, N., et al., *Parkinson's Disease Genes VPS35 and EIF4G1 Interact Genetically and Converge on alpha-Synuclein*. Neuron, 2023. **111**(1): p. 138.
237. Pouloupoulos, M., O.A. Levy, and R.N. Alcalay, *The neuropathology of genetic Parkinson's disease*. Mov Disord, 2012. **27**(7): p. 831-42.
238. Cuervo, A.M., et al., *Impaired degradation of mutant alpha-synuclein by chaperone-mediated autophagy*. Science, 2004. **305**(5688): p. 1292-5.
239. Martinez-Vicente, M., et al., *Dopamine-modified alpha-synuclein blocks chaperone-mediated autophagy*. J Clin Invest, 2008. **118**(2): p. 777-88.
240. Mazzulli, J.R., et al., *alpha-Synuclein-induced lysosomal dysfunction occurs through disruptions in protein trafficking in human midbrain synucleinopathy models*. Proc Natl Acad Sci U S A, 2016. **113**(7): p. 1931-6.
241. Zinsmaier, K.E., et al., *A cysteine-string protein is expressed in retina and brain of Drosophila*. J Neurogenet, 1990. **7**(1): p. 15-29.
242. Gundersen, C.B. and J.A. Umbach, *Suppression cloning of the cDNA for a candidate subunit of a presynaptic calcium channel*. Neuron, 1992. **9**(3): p. 527-37.
243. Braun, J.E. and R.H. Scheller, *Cysteine string protein, a DnaJ family member, is present on diverse secretory vesicles*. Neuropharmacology, 1995. **34**(11): p. 1361-9.
244. Buchner, E. and C.B. Gundersen, *The DnaJ-like cysteine string protein and exocytotic neurotransmitter release*. Trends Neurosci, 1997. **20**(5): p. 223-7.
245. Chamberlain, L.H. and R.D. Burgoyne, *Identification of a novel cysteine string protein variant and expression of cysteine string proteins in non-neuronal cells*. J Biol Chem, 1996. **271**(13): p. 7320-3.
246. Coppola, T. and C. Gundersen, *Widespread expression of human cysteine string proteins*. FEBS Lett, 1996. **391**(3): p. 269-72.
247. Chamberlain, L.H. and R.D. Burgoyne, *Cysteine-string protein: the chaperone at the synapse*. J Neurochem, 2000. **74**(5): p. 1781-9.
248. Evans, G.J., A. Morgan, and R.D. Burgoyne, *Tying everything together: the multiple roles of cysteine string protein (CSP) in regulated exocytosis*. Traffic, 2003. **4**(10): p. 653-9.
249. Zinsmaier, K.E., *Cysteine-string protein's neuroprotective role*. J Neurogenet, 2010. **24**(3): p. 120-32.
250. Chamberlain, L.H. and R.D. Burgoyne, *Cysteine string protein functions directly in regulated exocytosis*. Mol Biol Cell, 1998. **9**(8): p. 2259-67.
251. Brown, H., et al., *Cysteine string protein (CSP) is an insulin secretory granule-associated protein regulating beta-cell exocytosis*. EMBO J, 1998. **17**(17): p. 5048-58.

252. Schmitz, F., et al., *CSPalpha-deficiency causes massive and rapid photoreceptor degeneration*. Proc Natl Acad Sci U S A, 2006. **103**(8): p. 2926-31.
253. Gundersen, C.B., et al., *Cysteine string protein beta is prominently associated with nerve terminals and secretory organelles in mouse brain*. Brain Res, 2010. **1332**: p. 1-11.
254. Koscielny, G., et al., *The International Mouse Phenotyping Consortium Web Portal, a unified point of access for knockout mice and related phenotyping data*. Nucleic Acids Res, 2014. **42**(Database issue): p. D802-9.
255. Li, J., X. Qian, and B. Sha, *Heat shock protein 40: structural studies and their functional implications*. Protein Pept Lett, 2009. **16**(6): p. 606-12.
256. Stahl, B., S. Tobaben, and T.C. Sudhof, *Two distinct domains in hsc70 are essential for the interaction with the synaptic vesicle cysteine string protein*. Eur J Cell Biol, 1999. **78**(6): p. 375-81.
257. Braun, J.E., S.M. Wilbanks, and R.H. Scheller, *The cysteine string secretory vesicle protein activates Hsc70 ATPase*. J Biol Chem, 1996. **271**(42): p. 25989-93.
258. Chamberlain, L.H. and R.D. Burgoyne, *Activation of the ATPase activity of heat-shock proteins Hsc70/Hsp70 by cysteine-string protein*. Biochem J, 1997. **322** (Pt 3)(Pt 3): p. 853-8.
259. Boal, F., et al., *The variable C-terminus of cysteine string proteins modulates exocytosis and protein-protein interactions*. Biochemistry, 2004. **43**(51): p. 16212-23.
260. Tobaben, S., et al., *A trimeric protein complex functions as a synaptic chaperone machine*. Neuron, 2001. **31**(6): p. 987-99.
261. Sharma, M., J. Burre, and T.C. Sudhof, *CSPalpha promotes SNARE-complex assembly by chaperoning SNAP-25 during synaptic activity*. Nat Cell Biol, 2011. **13**(1): p. 30-9.
262. Zinsmaier, K.E., et al., *Paralysis and early death in cysteine string protein mutants of Drosophila*. Science, 1994. **263**(5149): p. 977-80.
263. Sharma, M., et al., *CSPalpha knockout causes neurodegeneration by impairing SNAP-25 function*. EMBO J, 2012. **31**(4): p. 829-41.
264. Ruiz, R., et al., *Cysteine string protein-alpha is essential for the high calcium sensitivity of exocytosis in a vertebrate synapse*. Eur J Neurosci, 2008. **27**(12): p. 3118-31.
265. Fernandez-Chacon, R., et al., *The synaptic vesicle protein CSP alpha prevents presynaptic degeneration*. Neuron, 2004. **42**(2): p. 237-51.
266. Calo, L., et al., *CSPalpha reduces aggregates and rescues striatal dopamine release in alpha-synuclein transgenic mice*. Brain, 2021. **144**(6): p. 1661-1669.
267. Graham, M.E. and R.D. Burgoyne, *Comparison of cysteine string protein (Csp) and mutant alpha-SNAP overexpression reveals a role for csp in late steps of membrane fusion in dense-core granule exocytosis in adrenal chromaffin cells*. J Neurosci, 2000. **20**(4): p. 1281-9.
268. Zhang, H., et al., *Cysteine-string proteins regulate exocytosis of insulin independent from transmembrane ion fluxes*. FEBS Lett, 1998. **437**(3): p. 267-72.
269. Noskova, L., et al., *Mutations in DNAJC5, encoding cysteine-string protein alpha, cause autosomal-dominant adult-onset neuronal ceroid lipofuscinosis*. Am J Hum Genet, 2011. **89**(2): p. 241-52.

270. Huang, L. and Z. Zhang, *CSPalpha in neurodegenerative diseases*. Front Aging Neurosci, 2022. **14**: p. 1043384.
271. Cadieux-Dion, M., et al., *Recurrent mutations in DNAJC5 cause autosomal dominant Kufs disease*. Clin Genet, 2013. **83**(6): p. 571-5.
272. Benitez, B.A., et al., *Exome-sequencing confirms DNAJC5 mutations as cause of adult neuronal ceroid-lipofuscinosis*. PLoS One, 2011. **6**(11): p. e26741.
273. Diez-Ardanuy, C., et al., *A cluster of palmitoylated cysteines are essential for aggregation of cysteine-string protein mutants that cause neuronal ceroid lipofuscinosis*. Sci Rep, 2017. **7**(1): p. 10.
274. Greaves, J., et al., *Palmitoylation-induced aggregation of cysteine-string protein mutants that cause neuronal ceroid lipofuscinosis*. J Biol Chem, 2012. **287**(44): p. 37330-9.
275. Zhang, Y.Q. and S.S. Chandra, *Oligomerization of Cysteine String Protein alpha mutants causing adult neuronal ceroid lipofuscinosis*. Biochim Biophys Acta, 2014. **1842**(11): p. 2136-46.
276. Jedlickova, I., et al., *Autosomal-dominant adult neuronal ceroid lipofuscinosis caused by duplication in DNAJC5 initially missed by Sanger and whole-exome sequencing*. Eur J Hum Genet, 2020. **28**(6): p. 783-789.
277. Huber, R.J., *Recent insights into the networking of CLN genes and proteins in mammalian cells*. J Neurochem, 2023. **165**(5): p. 643-659.
278. Lee, J., Y. Xu, and Y. Ye, *Safeguarding Lysosomal Homeostasis by DNAJC5/CSPalpha-Mediated Unconventional Protein Secretion and Endosomal Microautophagy*. Front Cell Dev Biol, 2022. **10**: p. 906453.
279. Benitez, B.A., et al., *Clinically early-stage CSPalpha mutation carrier exhibits remarkable terminal stage neuronal pathology with minimal evidence of synaptic loss*. Acta Neuropathol Commun, 2015. **3**: p. 73.
280. Wendelboe, A.M. and G.E. Raskob, *Global Burden of Thrombosis: Epidemiologic Aspects*. Circ Res, 2016. **118**(9): p. 1340-7.
281. VerPlank, L., et al., *Chemical Genetic Analysis of Platelet Granule Secretion-Probe 3*, in *Probe Reports from the NIH Molecular Libraries Program*. 2010: Bethesda (MD).
282. Holly, S.P., et al., *Ether lipid metabolism by AADACL1 regulates platelet function and thrombosis*. Blood Adv, 2019. **3**(22): p. 3818-3828.
283. Joshi, S., et al., *Ferric Chloride-Induced Arterial Thrombosis and Sample Collection for 3D Electron Microscopy Analysis*. J Vis Exp, 2023(193).
284. Chanzu, H., et al., *Platelet alpha-granule cargo packaging and release are affected by the luminal proteoglycan, serglycin*. J Thromb Haemost, 2021. **19**(4): p. 1082-1095.
285. Walsh, T.G., et al., *Loss of the exocyst complex component EXOC3 promotes hemostasis and accelerates arterial thrombosis*. Blood Adv, 2021. **5**(3): p. 674-686.
286. Sudhof, T.C., *The synaptic vesicle cycle*. Annu Rev Neurosci, 2004. **27**: p. 509-47.
287. Bendor, J.T., T.P. Logan, and R.H. Edwards, *The function of alpha-synuclein*. Neuron, 2013. **79**(6): p. 1044-66.

288. Bogale, T.A., et al., *Alpha-Synuclein in the Regulation of Brain Endothelial and Perivascular Cells: Gaps and Future Perspectives*. Front Immunol, 2021. **12**: p. 611761.
289. Barbour, R., et al., *Red blood cells are the major source of alpha-synuclein in blood*. Neurodegener Dis, 2008. **5**(2): p. 55-9.
290. Xiao, W., et al., *Late stages of hematopoiesis and B cell lymphopoiesis are regulated by alpha-synuclein, a key player in Parkinson's disease*. Immunobiology, 2014. **219**(11): p. 836-44.
291. Hashimoto, M., et al., *NACP, a synaptic protein involved in Alzheimer's disease, is differentially regulated during megakaryocyte differentiation*. Biochem Biophys Res Commun, 1997. **237**(3): p. 611-6.
292. Skaer, R.J., R.J. Flemans, and S. McQuilkan, *Mepacrine stains the dense bodies of human platelets and not platelet lysosomes*. Br J Haematol, 1981. **49**(3): p. 435-8.
293. Tana, C., et al., *Molecular and Clinical Issues about the Risk of Venous Thromboembolism in Older Patients: A Focus on Parkinson's Disease and Parkinsonism*. Int J Mol Sci, 2018. **19**(5).
294. Burgoyne, R.D. and A. Morgan, *Cysteine string protein (CSP) and its role in preventing neurodegeneration*. Semin Cell Dev Biol, 2015. **40**: p. 153-9.
295. Calabresi, P., et al., *Alpha-synuclein in Parkinson's disease and other synucleinopathies: from overt neurodegeneration back to early synaptic dysfunction*. Cell Death Dis, 2023. **14**(3): p. 176.
296. Gorenberg, E.L. and S.S. Chandra, *The Role of Co-chaperones in Synaptic Proteostasis and Neurodegenerative Disease*. Front Neurosci, 2017. **11**: p. 248.
297. Gillespie, A.H. and A. Doctor, *Red Blood Cell Contribution to Hemostasis*. Front Pediatr, 2021. **9**: p. 629824.
298. Nieto-Gonzalez, J.L., et al., *Loss of postnatal quiescence of neural stem cells through mTOR activation upon genetic removal of cysteine string protein-alpha*. Proc Natl Acad Sci U S A, 2019. **116**(16): p. 8000-8009.
299. Lockyer, S., et al., *GPVI-deficient mice lack collagen responses and are protected against experimentally induced pulmonary thromboembolism*. Thromb Res, 2006. **118**(3): p. 371-80.
300. Kato, K., et al., *The contribution of glycoprotein VI to stable platelet adhesion and thrombus formation illustrated by targeted gene deletion*. Blood, 2003. **102**(5): p. 1701-7.
301. Nieswandt, B., et al., *Long-term antithrombotic protection by in vivo depletion of platelet glycoprotein VI in mice*. J Exp Med, 2001. **193**(4): p. 459-69.
302. Bender, M., et al., *Differentially regulated GPVI ectodomain shedding by multiple platelet-expressed proteinases*. Blood, 2010. **116**(17): p. 3347-55.
303. Chatterjee, M. and M. Gawaz, *Clinical significance of receptor shedding-platelet GPVI as an emerging diagnostic and therapeutic tool*. Platelets, 2017. **28**(4): p. 362-371.
304. Montague, S.J., et al., *Soluble GPVI is elevated in injured patients: shedding is mediated by fibrin activation of GPVI*. Blood Adv, 2018. **2**(3): p. 240-251.
305. Suzuki, H., et al., *Intracellular localization of glycoprotein VI in human platelets and its surface expression upon activation*. Br J Haematol, 2003. **121**(6): p. 904-12.

306. Wang, L., et al., *mTOR regulates GPVI-mediated platelet activation*. J Transl Med, 2021. **19**(1): p. 201.

VITA

Alexis N. Smith

Birthplace: Mississippi

Education

Ph.D. in Molecular and Cellular Biochemistry Expected 2024

University of Kentucky College of Medicine, Lexington, KY

B.S., Chemistry 2013-2017

University of Mississippi, University, MS

Awards/Fellowships/Honors

- 24th University of Kentucky Gill Heart and Vascular Institute Cardiovascular Research Day Travel Award. **Oct. 28, 2022.**
- Carl Storm Underrepresented Minority (CSURM) Fellowship recipient for 2022 Gordon Research Conference on Hemostasis. **July 31-Aug. 5, 2022.**
- International Society on Thrombosis and Haemostasis 2022 Congress Early Career Travel Award. **July 9-13, 2022.**
- 2020 National Science Foundation Kentucky-West Virginia Louis Stokes Alliance for Minority Participation Cohort 1 Bridge to Doctorate Fellowship at the University of Kentucky. **Aug. 2020- July 2022.**
- Lyman T. Johnson Torch Bearer Award, University of Kentucky College of Medicine. **Oct. 21, 2021.**
- International Society on Thrombosis and Haemostasis 2021 Congress Early Career Travel Award. **July 17-21, 2021.**
- ASBMB 2020 Annual Meeting Graduate/Postdoctoral Travel Award. **Apr. 4-7, 2020.** (Cancelled)

Publications

- **Smith, A.N.**, Joshi, S., Chanzu, H., Alfar, H., Prakhya S., Omali, L., and Whiteheart S.W. “ α -Synuclein is the Major Platelet Isoform but is Dispensable for Activation, Secretion, and Thrombosis” *Platelets*, 2023. **34**(1): p. 2267147.
- Joshi, S., Prakhya K.S., **Smith, A.N.**, Chanzu, H., Zhang, M., Whiteheart, S.W. “The Complementary Roles of VAMP-2,-3, and -7 in Platelet Secretion and Hemostasis” *Platelets*, 2023. **34**(1): p. 2237114.
- Joshi, S., **Smith, A.N.**, Prakhya, K.S., Alfar, H.R., Lykins J., Zhang, M., Pokrovskaya I., Aronova, M., Leapman R.D., Storrie, B., and Whiteheart S.W. “Ferric Chloride-

Induced Arterial Thrombosis and Sample Collection for 3D Electron Microscopy Analysis” *J. Vis. Exp.* 2023 (193).

Alexis N. Smith